A Reconnaissance Study of Water and Carbon Fluxes in Tropical Watersheds of Peninsular Malaysia: Stable Isotope Constraints

Muhammad Izzuddin Syakir Ishak

Thesis submitted to the
Faculty of Graduate Studies and Postdoctoral Studies
University of Ottawa

In partial fulfillment of degree requirement for a

Doctor of Philosophy (Ph.D.)
in Earth Sciences

uOttawa

L'Université canadienne
Canada's university

Contents

Glossary

ΔS	*changes in groundwater storage*
‰	*permil (part per thousand)*
DID	*Drainage and Irrigation Department of Malaysia*
E_d	*Physical evaporation from water bodies and land surfaces*
ENSO	*El Niño–Southern Oscillation*
ET	*Evapotranspiration*
GMWL	*Global Meteoric Water Line*
GSR	*Global Solar Radiation*
I_n	*Canopy evaporation/Interception*
ITCZ	*Inter-tropical convergence zone*
LEL	*Local Evaporation Line*
MMD	*Malaysian Meteorological Department*
NEM	*Northeast Monsoon*
NPP	*Net Primary Productivity*
P	*Precipitation*
PAR	*Photosynthetically Active Solar Radiation*
Q	*River discharge*
SSN	*Solar Sunspot Number*
SWM	*Southwest Monsoon*
T	*Transpiration*
TEMP	*Temperature*
WUE	*Water-use-efficiency*

List of Figures

List of Tables

Acknowledgement

I would like to express the deepest appreciation to my supervisor Professor Jan Veizer for his guidance, concern and patience. His mentorship was paramount in providing an academic experience consistent with my long-term career goals.

I would also like to thank my co-supervisor, Professor Ian Clark for his guidance through his book the Environmental Isotopes in Hydrogeology, which truly broadened my horizon in watershed science.

I am grateful for the friendship of all members in the Department of Earth Sciences, University of Ottawa, especially Hélène J. De Gouffe and Lisa-Robin Murphy of Earth Sciences Administrative Office, Paul Middlestead, Wendi Abdi and Patricia Wickham of G.G. Hatch Laboratory and Kern Lee, with whom I worked closely and puzzled over many of the same problems.

This project would not have been possible without the assistance of Ana Salwa Abd Razak and Mohd Zamri Hassan from Malaysia. Gratitude is also extended to the Drainage and Irrigation Department of Malaysia (DID), Department of Environment Malaysia (DOE) and Meteorological Department of Malaysia for their permission to access the data as a part of my thesis.

Financial supports for my research were provided by the Ministry of Higher Education of Malaysia, the Universiti Sains Malaysia and the Natural Sciences and Engineering Research Council of Canada (NSERC).

Finally, I would like to thank my wife Norhasimah Md Dzinan. Her support and patience are the testament of love for the past eight years of our marriage. My children, Wafa Qistina, Qisth Afeef and Qisth Yusuf, are my soul. I thank my parents, Ishak Ahmad and Zahariah Ismail for their encouragement and allowing me to be as ambitious as I wanted to be. My parents- in-law, Md Dzinan Ibrahim and Siti Aminah Yahya and all family members for their support, I am forever grateful.

Une étude de Reconnaissance des Flux D'eau et de Carbone dans les Bassins Versants Tropicaux de la Malaisie Péninsulaire : Contraintes des Isotopes Stables

Résumé

L'évapotranspiration est un lien pour les cycles de l'énergie et de carbone planétaires, encore mal connue. Ici, j'ai utilisé des isotopes stables de l'oxygène et de l'hydrogène pour partitionner flux d'eau due à la transpiration des plantes à partir du flux d'évaporation directe des sols, plans d'eau et des plantes. Les zones d'étude, les bassins versants Langat et Kelantan représentent des exemples de domaines dominés par les moussons du sud-ouest et du nord-est respectifs sur les deux côtés de la barrière orographique principal (chaîne de montagnes Titiwangsa). Pluviométrie annuelle pour le bassin versant Langat, obtenu à partir de 30 années de données hydrologiques dire, est 2145 ± 237 mm. Provisoirement, 48 % de ces précipitations retourne dans l'atmosphère par la transpiration (*T*), avec 33 % divisé en décharge (*Q*), 8 % dans l'interception (I_n), et 11 % en évaporation (E_d). Dans le bassin versant de Kelantan, la moyenne annuelle des précipitations, également basé sur les données hydrologiques de 30 ans, est 2383 ± 120 mm. Semblable à Langat, le T représente 43 % des précipitations (*P*), 45 % sont déversées dans la mer de Chine du Sud (*Q*), 12 % partitionné en interception (I_n) et provisoirement 0 % pour l'évaporation (E_d). E_d pour le bassin versant Langat ne représente qu'une petite proportion en termes d'importance volumétrique, à près de ~ 11% avec une forte incidence sur les empreintes digitales isotopiques des eaux liées à la mousson sud-ouest de l'été (SWM). Notez, cependant, que E_d négligeable pour le bassin versant de Kelantan peut être un artefact de la pluie et de la rivière des échantillons d'eau à seule partie côtière en aval du bassin versant. L'humidité élevée (80 %) a également été enregistré pour le bassin versant de la péninsule malaisienne.

T s'approprie environ la moitié de toute l'énergie solaire absorbée par les continents, ici ~ 1000 * 10^3 g H_2O m^{-2} an^{-1} similaire à d'autres régions tropicales au 900-1200 * 10^3 g H_2O m^{-2} an^{-1}. Les flux de carbone associés sont ~ 1300 g C m^{-2} an^{-1}, indépendant de réponses *P*. Végétation à l'irradiance solaire, via la photosynthèse *T* et reflète l' importance de la régulation stomatique des flux d'eau et de carbone. Afin de maintenir un niveau élevé de transpiration dans la région tropicale, «constante» l'approvisionnement en eau est nécessaire pour le pompage continu de l'eau qui fournit des nutriments à la plante, ce qui suggère que l'eau et le cycle du carbone sont co-piloté par l'énergie du soleil. L'existence de la courroie de transport de l'eau peut être préalable à la livraison des éléments nutritifs, par conséquent, le fonctionnement du cycle du carbone. Potentiellement, cela pourrait changer notre point de vue sur le rôle que joue la biologie dans le cycle de l'eau. Dans cette perspective, le cycle de l'eau est le moyen qui redistribue l'énergie solaire incidente à travers la planète, et les structures anatomiques de plantes alors aider à optimiser la boucle de transfer d'énergie par évaporation et les précipitations dans le cycle hydrologique .

Les principales caractéristiques de la géochimie aquatique des rivières Langat et Kelantan déduites de l'analyse en composantes principales sont contrôlées par trois composantes qui expliquent 80 % et 82 % de la variance totale. Ces composants reflétent le facteur géogénique la pollution superposé, ce dernier particulièrement prononcé dans les sections urbaines de la rivière Langat et dominante en aval de la rivière Kelantan. Il n'existe aucune corrélation entre les variations saisonnières dans les grandes variables de la chimie des ions et environnementaux tels que les précipitations, le débit, la température ou l'activité solaire.

A Reconnaissance Study of Water and Carbon Fluxes in Tropical Watersheds of Peninsular Malaysia: Stable Isotope Constraints

Abstract

Evapotranspiration is a nexus for planetary energy and carbon cycles, as yet poorly constrained. Here I use stable isotopes of oxygen and hydrogen to partition flux of water due to plant transpiration from the direct evaporative flux from soils, water bodies and plant. The study areas, Langat and Kelantan watersheds represent examples of domains dominated by the respective Southwest and Northeast monsoons on the two sides of the main orographic barrier (Titiwangsa mountain range). Mean annual rainfall for the Langat watershed, obtained from 30 years of hydrological data, is 2145 ± 237 mm. Tentatively, 48% of this precipitation returns to the atmosphere via transpiration (*T*), with 33% partitioned into discharge (*Q*), 8% into interception (I_n), and 11% into evaporation (E_d). In the Kelantan watershed, the mean annual rainfall, also based on the 30 year hydrological data, is 2383 ± 120 mm. Similar to Langat, the *T* accounts for 43% of precipitation (*P*), 45% is discharged into South China Sea (*Q*), 12% partitioned into interception (I_n) and tentatively 0% for evaporation (E_d). E_d for the Langat watershed represents only a small proportion in terms of volumetric significance, up to almost ~11% with strong effect on the isotopic fingerprints of waters associated with the summer Southwest Monsoon (SWM). Note, however, that insignificant E_d for the Kelantan watershed may be an artefact of rain and river water sampling at only coastal downstream portion of the watershed. High humidity (80%) also was recorded for the Malaysian Peninsula watershed.

T appropriates about half of all solar energy absorbed by the continents, here ~1000*10^3 g H_2O m^{-2} yr^{-1} similar to other tropical regions at 900-1200*10^3 g H_2O m^{-2} yr^{-1}. The associated carbon fluxes are ~ 1300 g C $m^{-2}yr^{-1}$, independent of *P*. Vegetation responses to solar irradiance, via *T* and photosynthesis reflects the importance of stomatal regulation of the water and carbon fluxes. In order to maintain high transpiration in the tropical region, "constant" water supply is required for continuous pumping of water that delivers nutrients to the plant, suggesting that water and carbon cycle are co-driven by the energy of the sun. The existence of the water conveyor belt may be precondition for nutrient delivery, hence operation of the carbon cycle. Potentially, this may change our perspective on the role that biology plays in the water cycle. In such perspective, the global water cycle is the medium that redistributes the incoming solar energy across the planet, and the anatomical structures of plants then help to optimize the loop of energy transfer via evaporation and precipitation in the hydrologic cycle.

The main features of aquatic geochemistry of the Langat and Kelantan rivers inferred from the Principal Component Analysis are controlled by three components that explain 80% and 82% of total variances. These components are reflecting of the geogenic factor with superimposed pollution, the latter particularly pronounced in urbanized sections of the Langat river and dominant in downstream of the Kelantan river. There is no correlation between seasonal variations in major ion chemistry and environmental variables such as precipitation, discharge, temperature or solar activity.

Chapter 1: Introduction

Globally, continental precipitation (*P*) accounts for 110,000 km^3/year and evapotranspiration (*ET*) for about 65,000 km^3/yr, with the balance of 45,000 km^3/year eventually flowing downstream through rivers and aquifers to the ocean [*Oki and Kanae, 2006*]. Evapotranspiration is a major pathway of water vapor to the atmosphere driven by sun, the main energy source to water cycle. The amount of solar radiation that is absorbed by the earth decreases with latitude, from equator to the poles. It is this variation in surface heating that drives the circulation of the ocean and atmosphere and, thus, much of the hydrologic cycle [*Berner and Berner, 1996*].

Tropics receive high solar radiation and serve as the dominant source of moisture to higher latitudes. In response to global warming, climate models predict a more humid world, where the movement of water in the hydrologic cycle through evaporation and precipitation is intensified [*Schlesinger, 1991*]. This should become greater as the tropics warm, and therefore will drive a faster water cycle [*Bowen, 2011*]. Moreover, changes in the hydrologic cycle through geologic time, associated with changes in global temperature, imply that atmospheric water vapour acts as the most prominent greenhouse gas (GHG) that potentially nearly triples the effects of greenhouse warming caused by other GHGs [*Schlesinger, 1991*: *Chahine, 1992*].

From the energy balance perspective (Figure 1), incoming solar radiation (left hand side) and outgoing radiation (right hand side) must be balanced, resulting in 235 Wm^{-2} of energy reradiated back to the space. The outgoing radiation from the earth mostly occurs at higher altitude with effective emission temperature of -19°C. This allows GHGs to absorb the infrared radiation emitted by the earth surface and atmosphere, resulting in a warming effect. Clouds, an integral part of water cycle, play an important role in the natural GHGs effect, both scattering and absorbing the radiation. Satellite data for the last decade show a small decline in the global cloud albedo, enough to enhance the intensity of short-wave solar energy input into the system, by about 2 to 6 Wm^{-2} [*Palle et al., 2005*], but overall impact of clouds on climate is complex and still open to debate. By reflecting the incoming solar radiation they reduce the direct solar energy input to environment. At the same time, by trapping the long-wave energy emitted by the earth, they reduced the net outflow of heat energy from the environment into space. The solar radiation reflected by clouds and the atmosphere accounts for approximately 77 Wm^{-2}, similar to evapotranspiration and precipitation fluxes, each accounting for ~78 Wm^{-2} [*Baede et al., 2001; Stocker et al., 2001*]. If the clouds have higher water content, their albedo will be higher and reflect more solar radiation, thereby cooling the climate [*Baede et al, 2001*]. At this stage, the overall interactions among water vapour, clouds and radiation are believed to constitute a positive feedback, and water vapour is therefore an amplifier that enhances the greenhouse effect [*Chahine, 1992*], significantly altering the earth's energy balance. Note, nevertheless that the potential influence of clouds and their cooling albedo effect on the hydrologic cycle via radiative heating remains a mystery [*Stevens and Bony, 2013*]

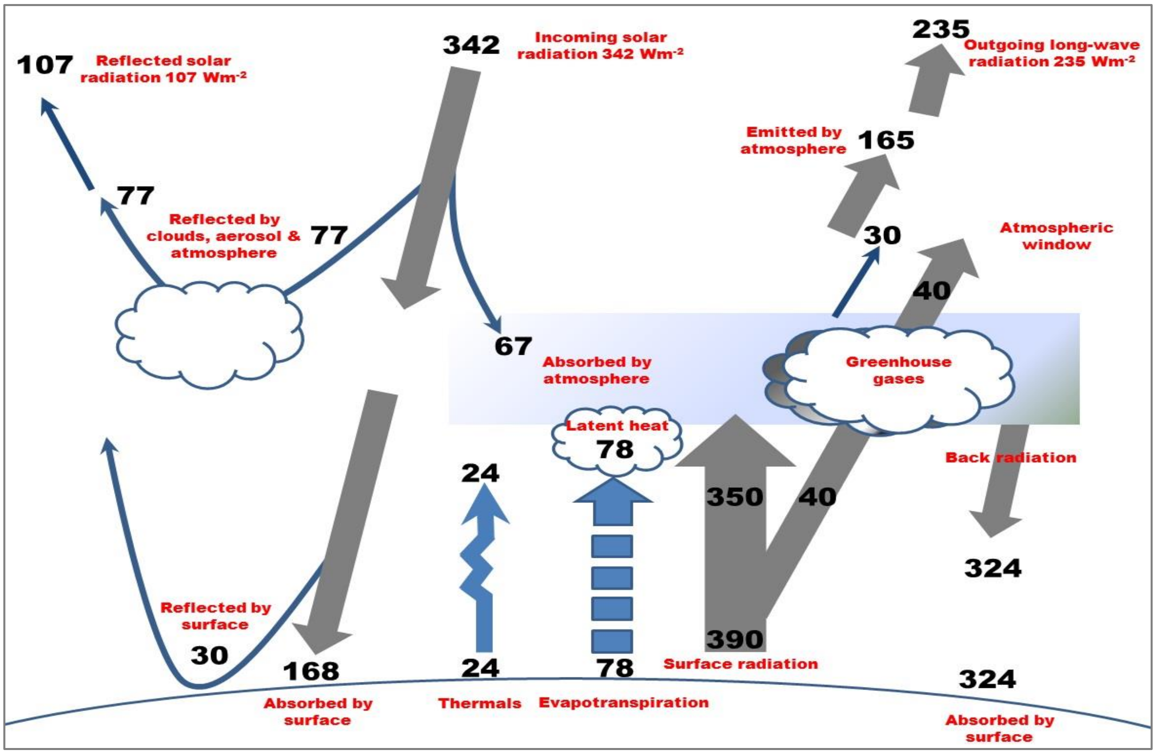

Figure 1: The role of clouds in the earth's energy balance (Wm^{-2}) from [*Baede et al., 2001*]

Global climate change can affect precipitation, temperature, surface radiation and evapotranspiration (*ET*), impacting the renewable fresh water resources [*Mu et al, 2011*]. Moreover, growing population, greater food and energy productions also have had tremendous impacts on land cover changes, water and nutrient cycling and the chemistry of the atmosphere degrading the water quality, hence stressing the fresh water resources. It is estimated that about 2.7 billion people live in high risk of a violent conflict. A further 1.2 billion people are at high risk from political instability [*Ki-moon, 2012*] often due to climate and water-related crises (i.e. pollution).

As population escalates, development and prosperity increase per capita food intake [*Fereres et al, 2011; Immerzeel and Biekens, 2012*], placing additional concerns on food security at times of water scarcity. Generally, the global fresh water consumption is almost 6000 km^3 yr^{-1}, of which 70% goes to agriculture, mostly in Asia [*Kabat, 2012*]. In addition, expansion of the cities requires a huge amount of energy and its delivery impacts the environmental quality of air, soil and water. Advancing urbanization alters these natural systems affecting the fate and transport of chemical elements. Given that the water cycle permeates the entire biosphere, any pollutant that is introduced into water cycle ultimately results in deterioration of water quality. The outcome is less abundant clean water resource for human consumption. Considering the population density in Southeast Asia and the role of local agriculture for human wellbeing, understanding the hydrologic balance of the watersheds in the region, and the impact that humanity impose on the regional ecosystems and water balance becomes one of important research priorities.

Food production (agriculture) is closely coupled to water consumption, the relationship subsumed in the biological term of plant *transpiration*. The mechanism involves absorption of soil water by plant roots, translocation of liquid through the vascular system of the leaf to stomata, and its subsequent evaporation to the atmosphere [*Dingman, 2008*]. As the water evaporates, plants absorb carbon dioxide (CO_2) and exchange H_2O between the plant and the atmosphere [*Nobel, 2005*]. Transpiration is a physical process, which is driven by the potential-energy gradients that originate with the movement of water vapor into the air through the stomata in response to vapor pressure difference. As the water vapour escapes to atmosphere via stomata, potential energy decreases, inducing the flow of water through the vascular system. This creates a water content gradient between the root and the soil, resulting in movement of soil water into the root. Absorption at the root surface decreases water content in the adjacent soil creating a hydraulic gradient that follows Darcy Law [*Dingsman, 2008*].

Water uptakes by plant through the root system is regulated by stomata with an ultimate goal maximizing carbon gain per unit water loss [*Frank and Beerling, 2009*; *Katul et al. 2010*; *de Boer et al., 2011*]. The stomata may open or close in order to control the diffusion of moisture from the leaf and the intake of atmospheric carbon dioxide into the leaf. This causes a steady flow of water from the root system to the leaves during photosynthesis resulting in conversion of carbon dioxide into organic matter [*Farquhar et al., 1989; Sellers et al., 1997; Heldt*, *2010*]. Note that the potential uptake of CO_2 diminishes as stomatal conductance decreases [*Cox et al., 2000*]. Less open stomata as a response to elevated CO_2 reduces transpiration [*Gedney et al., 2006; Betts et al., 2007*], resulting in increased runoff.

Plants generally grow more rapidly with abundant water and sunlight. Interplay of these principal factors (temperature, water and solar radiation) [*Nemani et al 2002*] set the Net Primary Productivity (*NPP*) equilibrium state that is characteristic of the ambient environmental and climatic conditions. Moreover, plants that grow under conditions of water stress generally utilize additional moisture more effectively. Other things being equal, addition of water usually translates to proportionally higher *NPP* [*Huxman et al., 2004*].

In the *mid-latitudes and poleward*, the feedback between temperature and plant growth (*NPP*) is generally positive, with warmer temperatures resulting in enhanced vegetation. For semi-arid regions, the feedback is negative (increased vegetation, more evaporation, cooler temperatures). Note that higher temperatures co-vary also with precipitation (*P*) over most areas of the planet [*Delire et al., 2011*], with *NPP* (g $Cm^{-2}yr^{-1}$) [*Knapp and Smith, 2001: Zheng et al., 2001: Zheng et al., 2003*] usually accounting for about 0.05% of *P* in term of mass [*Ferguson and Veizer, 2007*] (Figure 2). Regression of *P-NPP* therefore reflects the proportion of *P* that is available to plant transpiration (*T*) [*Lee and Veizer, 2003*]. In contrast, for *equatorial regions* with *P* beyond approximately 1500 mm, the *NPP* reaches a plateau because the biological system operates at its optimal capacity with respect to energy input by sun. Solar radiation thus appears to be the limiting factor.

The theoretical upper limit for biological transformation of solar light energy (photons) to chemical energy is 11%, but natural ecosystems operate mostly with 3-6% efficiency [*Miyamoto, 1997*]. Studies of 15 large watersheds (Figure 2) in North and South America, Africa, Australia and New Guinea are consistent with the proposition that the optimal rate of plant growth in the tropics is independent of additional water input [see also *Nemani et al, 2002*]. While the ecosystems strive to optimize their efficiency towards the theoretical plateau, the level of the plateau itself is set by the incident solar radiation. Enhanced photosynthetically active solar radiation (PAR) will result in elevation of the *NPP* plateau, in invigoration of global evaporation and precipitation, and in enhanced transfer of moisture towards the higher latitudes. A decline in PAR results in an opposite shift. The coupled water - carbon system may thus oscillate with solar activity [*Ferguson and Veizer, 2007*].

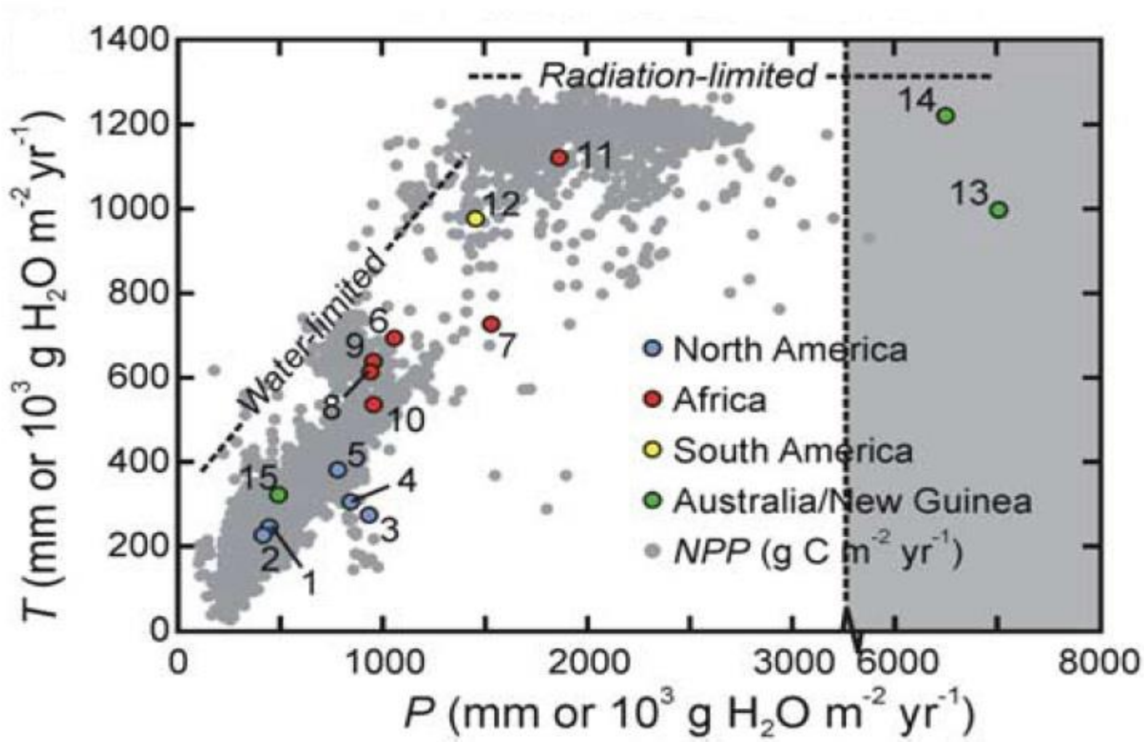

Figure 2: The relationship between *P* and *T* for watersheds in North America, South America, Africa, Australia, and New Guinea (shaded region represents P > 5500 mm). 1, North Saskatchewan River; 2, South Saskatchewan River; 3, Ottawa River; 4, St. Lawrence River; 5, Mississippi River; 6, Bani River; 7, Upper Niger River; 8, Black Volta River; 9, White Volta River; 10, Oti River; 11, Nyong River; 12, Piracicaba River; 13, Ok Tedi; 14, Upper Fly River; 15, Murray-Darling River [*after Ferguson and Veizer*, *2007*]

Interaction between solar radiation, water vapour and clouds is believed to result in an overall positive feedback [*Susan*, *2007*] that, in turn, determines the climate. Irrespective of the details of this systematic, terrestrial water and carbon cycles are coupled via transpiration process, but because water is by far more abundant than carbon [*Veizer*, *2005*], water must play a significant role in modulation of the carbon cycle [*Ferguson and Veizer 2007*].

If interaction of solar radiation, water vapour and clouds and their interaction are the dominant influences on climate and vegetation, what would be the specific mechanisms that maintain the system? What are the implications of an anthropogenic factor for the terrestrial water cycle?

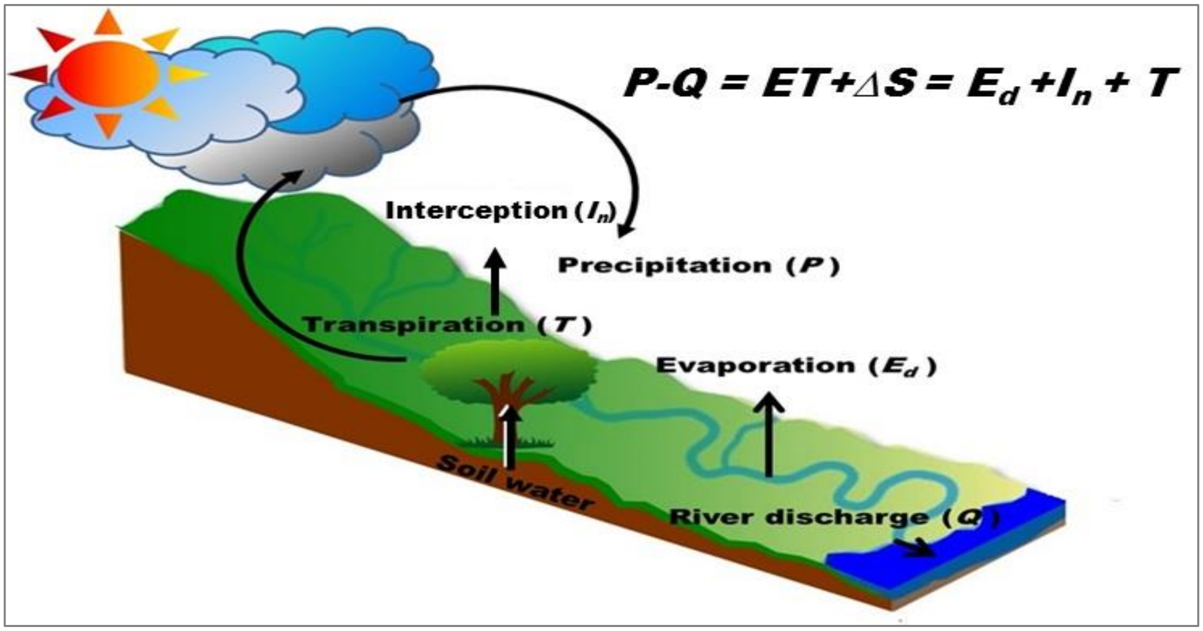

Figure 3: Schematic diagram of annual water balance of a closed watershed, described by the apportionment of annual water input, *P*.

1.1 Study objectives

The aim of this study is to better quantify the relationship between regional climate, hydrology and biology in the tropical environment of Peninsular Malaysia. The study concentrates on selected watersheds because these can be considered as quasi-closed entities with respect to the overall water cycle (Figure 3) and because basic hydrological data, such as precipitation and discharge are usually available from long term monitoring by official agencies. This information can be coupled with empirical chemical and isotopic data of water samples for quantification of natural water fluxes within the watershed and for elucidation of any potential superimposed anthropogenic impact. Moreover, the terrestrial water cycle plays the decisive role in nutrient delivery to vegetation and thus carbon intake by biological system within the watersheds. Because water and carbon cycles are coupled via the process of plant transpiration (photosynthesis) at a specific ratio, called water-use efficiency (WUE) [*Choudhury et al.,1998; Choudhury, 2000; Chen and Coughenour, 2004; Bery and Roderick, 2004; Kuchment et al., 2006*], this coupling enables conversion of the water transpiration flux into the related first-order estimate of the photosynthetic carbon flux [*Telmer and Veizer, 2000; Lee and Veizer, 2003; Ferguson and Veizer; 2007; Schulte et al, 2011; Jasechko et al., 2013*]. Considering the paucity of such data for tropical region of Southeast Asia, such first-order estimates can serves as the first reconnaissance contribution to understanding the regional water cycle.

While the publicly available hydrological data for watersheds usually list precipitation (P) and discharge variations (Q), understanding the regional water cycle requires knowledge of components that constitute evapotranspiration, such as physical evaporation from water bodies (E_d) and canopy (I_n) plus transpiration (T). Yet, relative contributions of evaporation and plant transpiration to the annual terrestrial water vapour flux at regional scales are poorly constrained. Partitioning evaporation and transpiration in the study areas can be done by using a stable isotope approach, a non-conventional hydrological technique. [*Gibson et al., 1993; Clark and Fritz, 1997; Ferreti et al., 2003; Henderson-Sellers and McGuffie, 2004; Fekete et al.,2006: Schulte et al., 2011*]. Evaporation consist of the abiotic fluxes of moisture from land surfaces and water bodies (E_d) and from the plant canopy (Interception, I_n), whereas plant transpiration (*T*) represents the biologically mediated transfer of moisture from soil to the atmosphere via the vascular system of plants. Collectively, E_d, I_n and *T* constitute the total evapotranspiration (*ET*) flux and define the conventional water balance equation for a closed hydrologic system;

$$P=Q+ET+\Delta S \qquad (1)$$

where *P* and *Q* represent area-standardized estimates of mean annual water input by precipitation and output by river discharge, respectively. ΔS represents the inter-annual changes in the proportion of *P* stored in the watershed. For multi-year (years to decades) measurements of *P* and *Q*, *S* is assumed to be a constant and therefore $\Delta S=0$, and the annual water input *P* is then balanced solely by outputs via *ET* and *Q*. Consequently, (*P*-*Q*) represents an approximation of *ET* (Figure 3). Previous study of large watersheds in North America [*Telmer and Veizer, 2000; Lee and Veizer, 2003; Karim et al, 2007; Ferguson et al., 2007*], Africa [*Freitag et al., 2008*], New Guinea [*Ferguson and Veizer, 2007*] and globally [*Jasechko et al., 2013*] have utilized the stable isotopes of water in order to partition *ET* into a fractioning water flux, E_d, and non-fractionating water fluxes (*T* and I_n). Fundamentally, the methodology that was developed for large watersheds globally [*Ferguson and Veizer, 2007*; *Jasechko et al, 2013*] is intended to offer first-order estimates of regional E_d and *T* that is applicable at a hierarchy of spatial and temporal watershed scales. Because of the tropical setting of Peninsular Malaysia it is expected that its *T/NPP* relationship will reflect the pattern of tropical, radiation limited, ecosystems (Figure 2) and temporal variability of *P* and *T* may potentially respond to any secular trends in solar flux. Pending the existence of pertinent datasets, the search for potential coupling of solar variability to regional climate and hydrology on annual to decadal time scale will also be the theme of the present study.

The objectives discussed above are summarized into three main aspects.

1. Establish the water balance for Langat and Kelantan watersheds
2. Partitioning evapotranspiration using the stable isotope approach
3. Using the estimated Transpiration amount as a proxy to understand the role of water cycle in terrestrial ecosystem

1.2 Contribution to new knowledge

Evapotranspiration, a nexus for planetary energy and carbon cycles, is as yet poorly constrained. Stable isotopes of oxygen and hydrogen enable partitioning of the flux of water into a component that is due to plant transpiration from that due to direct evaporative flux from soil and water bodies. The present reconnaissance study documents that plant transpiration is the dominant flux which optimizes the energy loop of the hydrologic cycle. In the Malaysian Peninsula, the transpiration fluxes in the Langat and Kelantan watersheds account for 48 and 43% of the annual water budget, respectively, and they appropriate about half of all solar energy absorbed by the region. This transpiration conveyor belt of water is the precondition for nutrient delivery and thus carbon intake by biological systems. Potentially, this may change our perspective on the role that transpiration plays in the water cycle.

This thesis is written in article format comprising Introduction (Chapter 1), Study Area (Chapter 2), Sample Collection and Analytical Procedures (Chapter 3), Water budget of the watersheds based on isotopic constraints (Chapter 4), Isotopes, Climate, and Hydrology: Temporal variations (Chapter 5), Implication for Carbon Cycle (Chapter 6) and Hydrology and river chemistry (Chapter 7). Part of the Chapter 4 was published in International Association of Hydrological Sciences Red Book series (IAHS) Publication 363, (2014):

Syakir, MI., K. Lee, I. D. Clark and J. Veizer “A Reconnaissance Study of Water and Carbon Fluxes in a Tropical Watershed of Peninsular Malaysia: Stable Isotope Constraints”. Hydrology in a Changing World: Environmental and Human Dimensions. Proceedings of FRIEND-Water 2014, Hanoi, Vietnam, IAHS Publication 363, (2014)

Chapter 2: Study Area

Peninsular Malaysia, located between 1^0 and 7^0 North and 99^0 to 105^0 East, comprises an area of 130 268 km^2, elongated approximately in NNW-SSE direction with a maximum length of 750 km and breadth of 330 km (Figure 4). Topographic features of Peninsular Malaysia can be generally observed based on differences in elevation. Low lying areas represent terrains with sediments of variable thicknesses, overlain by unconsolidated alluvial, costal and marine deposits. The landscapes of undulating to mountainous areas of Peninsula, mostly in inland locations, represent primarily denudational terrains of bedrock, resulting from weathering and erosional processes during the Cenozoic era.

The Peninsula is orographically characterized by the mountainous interior, with the highland forming the backbone that separates the eastern and western zones. The Main Range, Titiwangsa, the most prominent and continuous of the mountain ranges, is composed mostly of granite (Figure 5) with several enclaves of metasedimentary rocks. It extends southeast from southern Thailand for a distance of 480 km. These series of mountain ranges control the network pattern of streams and rivers that mostly serve as the state boundaries. Rivers dominate regionally the Peninsula drainage pattern [*Hutchison and Tan, 2009*].

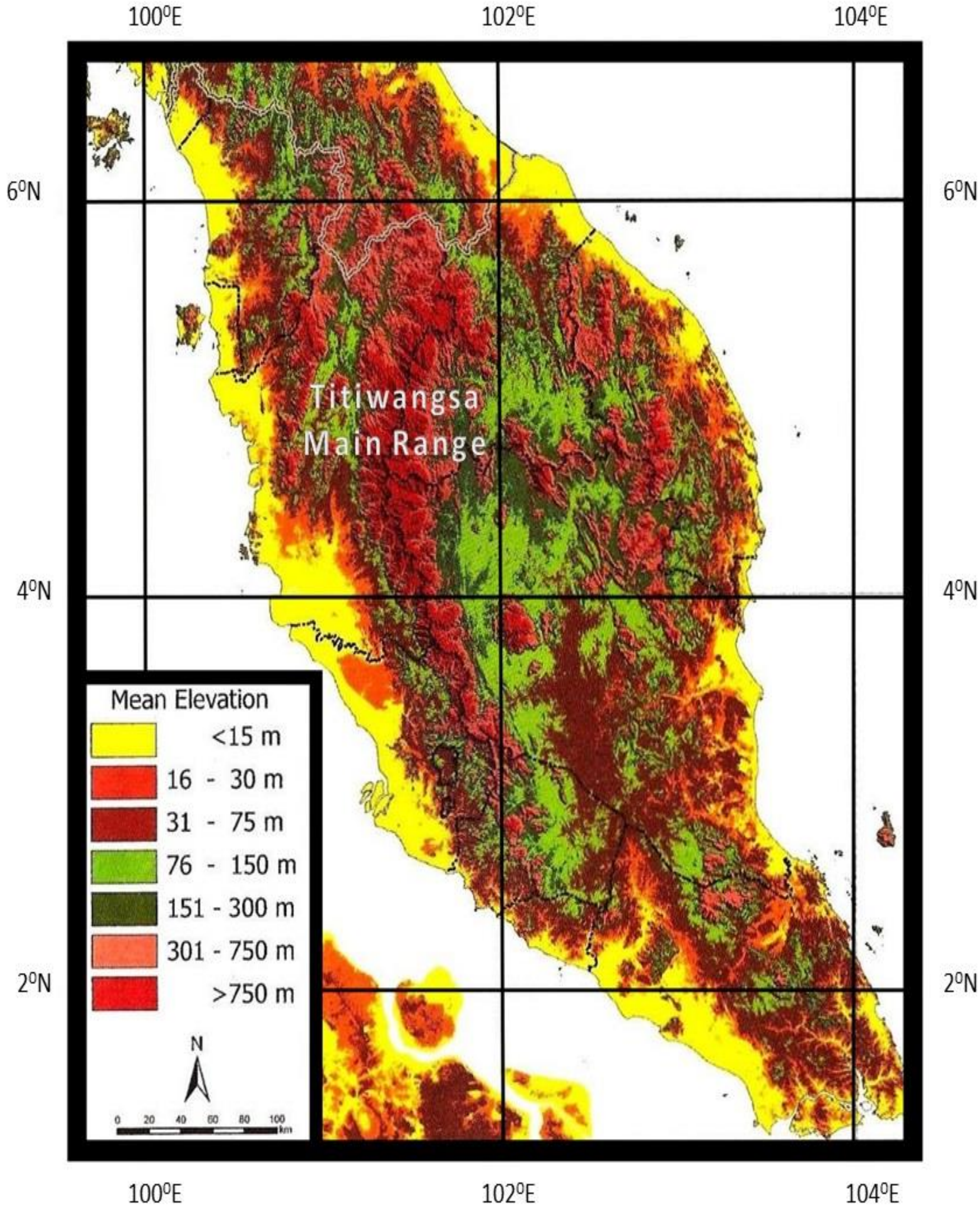

Figure 4: Mean elevations of terrain in Peninsular Malaysia (*Fatt after Hutchison and Tan, 2009*)

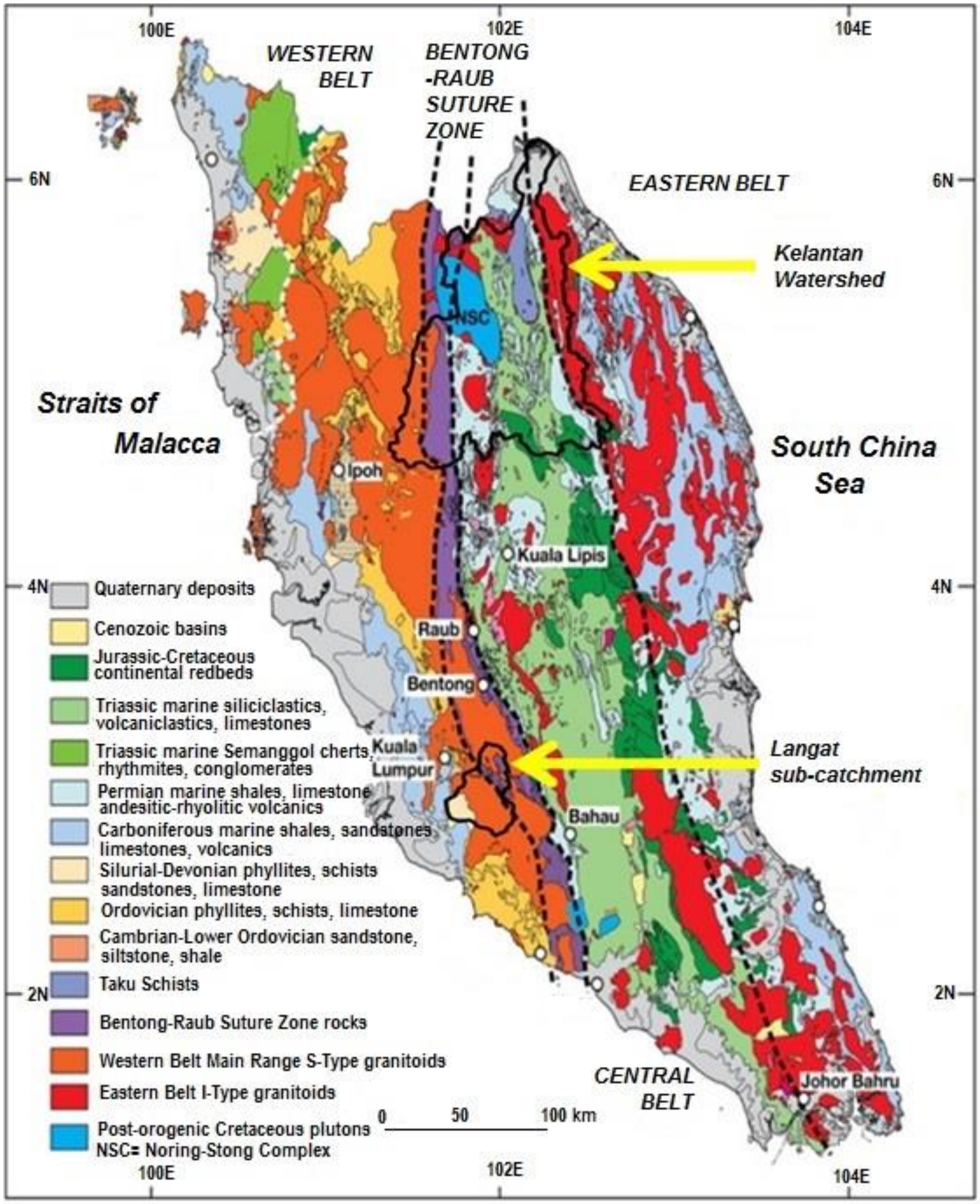

Figure 5: Geology of the study areas with outlines of the Langat sub-catchment and Kelantan watershed. The Geology Map of Peninsular Malaysia is modified from [*Metcalfe, 2013*].

The *climate* of Peninsular Malaysia is tropical and the humidity is high all year round, with temperatures ranging from 21^0C to 32^0C. The rainfall regime over the region is governed mainly by the monsoonal seasons, primarily modulated by the atmospheric pressure patterns in Southeast Asia that results from pressure difference between Asian continent and Australian land mass, termed the Inter-Tropical Convergence Zone (ITCZ). During the northern hemisphere winter (Figure 6), a combination of high pressure in China and low pressure over Australia, forces the ITCZ further south, bringing the northeast monsoon (NEM) (September to February) over Peninsular Malaysia. The circulation reverses during the northern hemisphere summer, with low pressure over Asia and high pressure over Australia, resulting in migration of the ITCZ northwards.

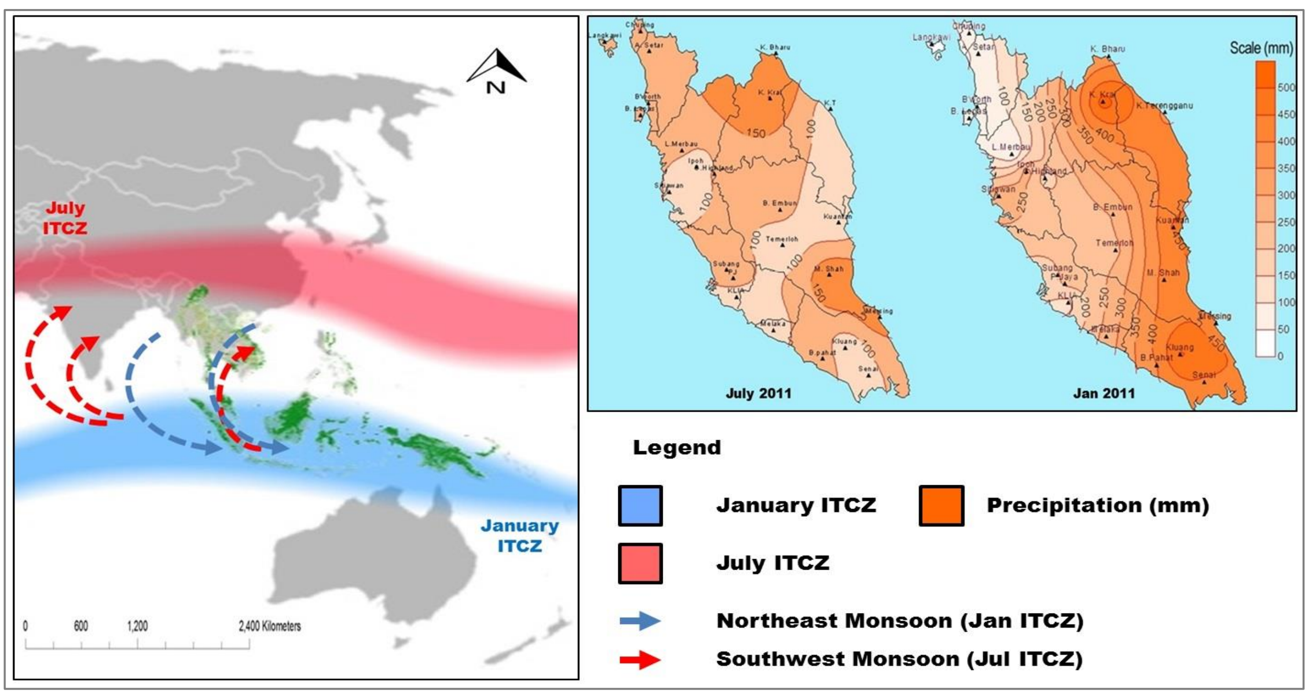

Figure 6: Climate regimes in Peninsular Malaysia. The regional map is a sketch based on the information provided by National Oceanic and Atmospheric Administration (NOAA) and the Precipitation map is obtained from the Meteorological Department of Malaysia.

At this time, Peninsular Malaysia is influenced by the southwest monsoon (SWM) (March to August) and the whole of Peninsular Malaysia experiences a relatively drier period [*Suhaila et al, 2010*]. Nevertheless, the Peninsular Malaysia does not have distinct dry and wet seasons [*Takanashi et al*, *2010*]. Heavy rainfall arises also from convective rain in between monsoon seasons [*Suhaila et al*, *2010*]. These two seasons, the SWM and NEM are the main factor that control rainfall events [*Camerlengo and Demmler*, *1997*] but the highest rainfall events are associated with the NEM periods. Overall, the rainfall is relatively evenly distributed throughout the year and the vegetation in Peninsular Malaysia is tropical evergreen [*Stibig et al*, *2007*]. The studied Langat and Kelantan watersheds represent examples of domains dominated by the respective Southwest and Northeast monsoons on the two sides of the main orographic barrier (Titiwangsa mountain range) (Figure 7).

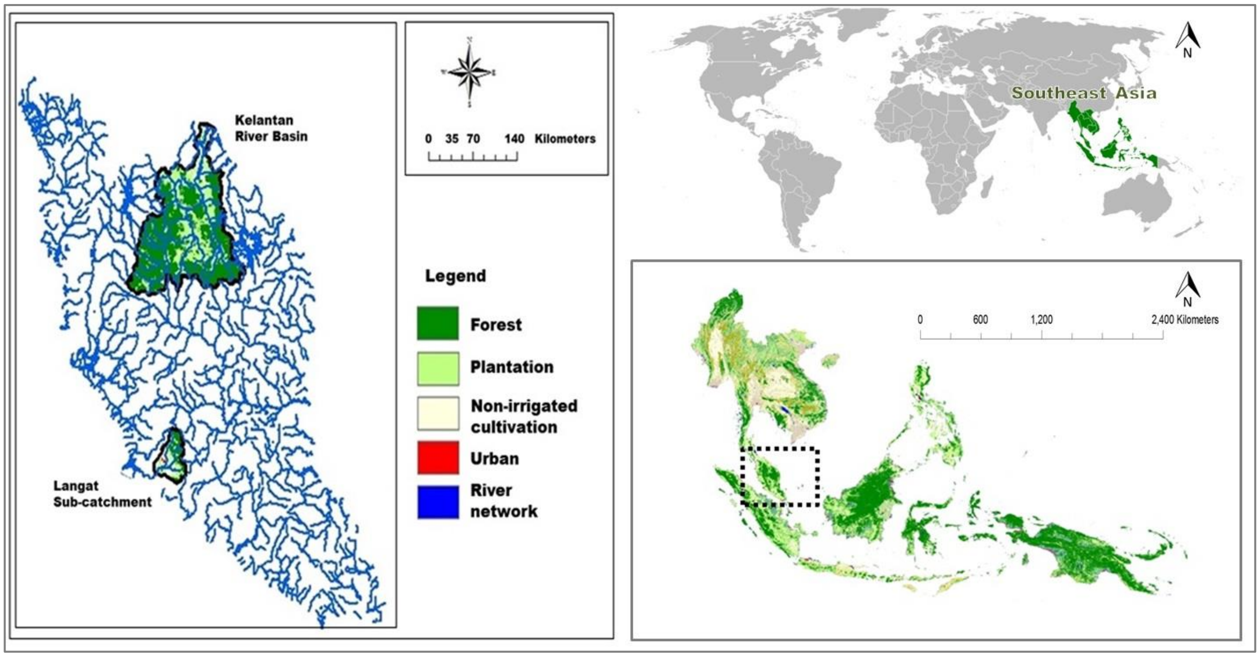

Figure 7: Drainage network and location of the Langat and Kelantan watersheds in Peninsular Malaysia. Inset map shows the location of Peninsular Malaysia relative to Southeast Asia.

2.1 Langat Basin

Langat Basin is located south of Kuala Lumpur, the capital city of Malaysia. The area is approximately 2940 km^2 and encompasses two reservoirs (Hulu Langat and Semenyih) that are critical for power and water supply for approximately 1.2 million people in the basin, particularly in urbanized areas such as Kajang, Bangi and Putrajaya. The Hulu Langat Reservoir with the catchment size of 54 km^2 was built in 1981 purposely for water and power supply at a moderate capacity. The Semenyih Reservoir with the catchment size of 41 km^2 was built in 1982 for domestic and industrial water supply. The main river is known as Langat River with the total length of 141 km, draining in south-southwest direction, from the

Main Range down to the Strait of Malacca. Langat basin contains several smaller tributaries, with Semenyih being the largest.

The Langat watershed is comprised of mountainous section upstream, hilly area (urban, residential and agriculture) and flat alluvial portion (mostly agriculture). Most of the mountainous area in the watershed is considered undisturbed. The hilly area, characterised by gentle slopes, spreads widely from north to east in the middle part of the basin, and in the lower part of the hills it extends to Dengkil. Flat alluvial plain is located in the southwest of Langat Basin. Most of the area is build up by clay and silt with abundant peat. In this study the flat alluvial zone is excluded from consideration because of invasion of marine saline wedges. Hence the study area is constrained to 1443 km^2 sub-catchment that encompasses only the upstream, Kajang (urban) and Dengkil (including Semenyih as the tributary) portions of the catchment.

2.1.1 Geology of Langat Sub-Catchment

The bedrock in the Main Range near the source of the river is granite, mostly of Permian age, and the surrounding hilly area is comprised of metamorphosed sandstone, shale, mudstone, and schist. The upper part of the bedrock was weathered. Jelebu Schist (JS) of Lower-Upper Ordovician within the Langat sub-catchment form a continuous schist domain (Bentong-Raub suture) along its western margin with enclaves of the Main Range granitoids (Figure 5). JS and other metasedimentary rocks, a belt from 1 km to 19 km wide and about 5300 m thick, contain chiastolite and graphitic schist, phyllite, quartzite, hornsfels and chert. Small localized exposures of intermediate to ultrabasic rocks are also associated with the metasedimentary rocks [*Khoo, 1998*]. Downstream area of the Langat sub-catchment is underlain by Kajang schist (KS) of Silurian-Devonian age. The formation is dark-grey to black carbonaceous quartz-muscovite schist interlayered with thin bands and lenses of orange to buff quartz muscovite schist and minor intercalations of marble and phyllite [*Yin, 1976; Raj 1995*]

2.1.2 Climate and Hydrology of Langat sub-catchment

The Langat sub-catchment is located in the west coastal region of Peninsular Malaysia where the elevation varies from approximately 20 m ASL near Dengkil to 1420 m ASL in the upper reaches of the watersheds. Generally, the sub-catchment is characterized by warm climate with uniform annual temperatures and humidity. The sub-catchment experiences two seasons; the wet season from April to November and a relatively dry spell that occurs from January to March. The regional weather is influenced mostly by the Southwest monsoon, a product of the July ITCZ belt. The mean annual rainfall in the watershed is 2145±237 mm for the area of 1443 km^2 and the mean annual river discharge is 35.38±4 m^3/s. The mean annual temperature at Langat is 26±0.3 ^oC with mean relative humidity of 82±1%.

2.1.3 Vegetation and land-use in Langat sub-catchment

Langat sub-catchment is typified by massive development, especially by agriculture which accounts for 52% of its areal extent. Oil palm (32%) is the most dominant plantation, with additional, non-irrigated crops, such as cassava and cocoa, accounting for 20%. Approximately 44% of the Langat sub-catchment is still covered by tropical rainforest, primarily a lowland dipterocarp type below 300 m ASL. Only 3% of the watershed is urbanized and no data exist for the balance of 1% (Figure 7a).

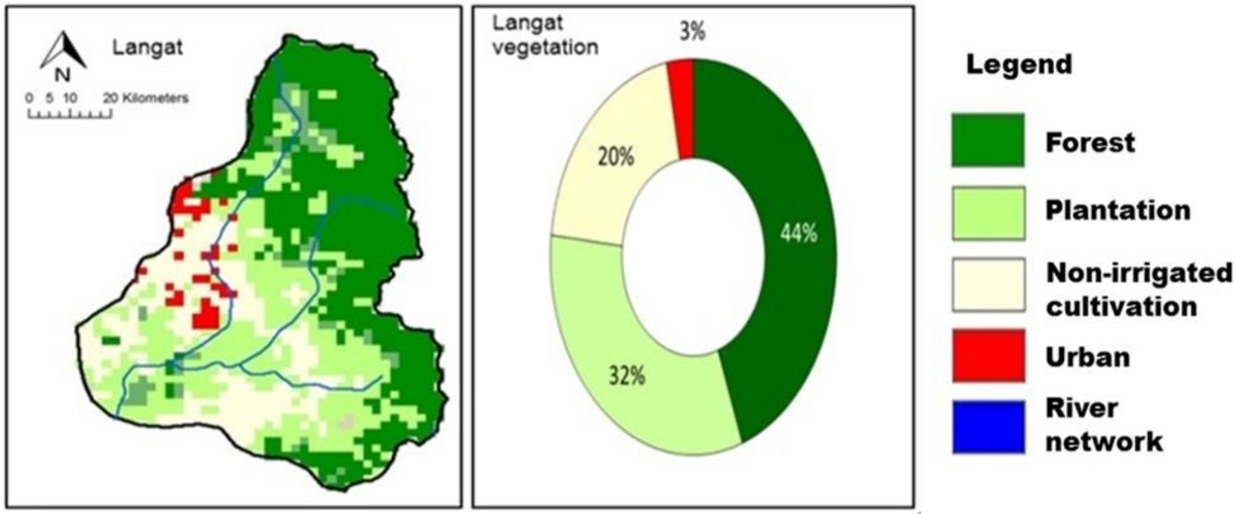

Figure 7a: Land cover map of Langat sub-catchment based on GLC 2000 data from [*Stibig et al, 2007*].

2.2 Kelantan Basin

The Kelantan River basin is located in the northeastern part of Peninsular Malaysia between latitudes 4° 40' and 6° 12' North, and longitudes 101° 20' and 102° 20' East. The river is about 355 km long [*Hutchison and Tan, 2009*] and drains an area of approximately 13,659 km^2, occupying around 85% of the State of Kelantan. The Kelantan River starts with the confluence of the Galas and Lebir Rivers upstream of Kuala Krai, only about 100 km above its river mouth. The Kelantan River then runs northward through Kuala Krai, Tanah Merah, Pasir Mas and the capital city Kota Bharu, discharging into the South China Sea. The eastern and western portions of the watershed, consisting of mountain ranges, have a soil cover of a mixture of fine to coarse sand and clay of granitic pedigree.

2.2.1 Geology of Kelantan Basin

The Kelantan watershed lies between the Noring-Stong Complex in the west and the Boundary Range of Eastern Belt plutons in the east. The central part of the catchment is underlain by the Permo-Triassic Taku Schist in the north. Due south the geology is dominated by Upper Permian-Triassic Gua Musang (GM) Formation and Upper Carboniferous-Triassic [*Foo, 1983*] Aring (Ar) Formation (Figure 5)

The Stong Complex of post-orogenic Cretaceous plutons consists mainly of Noring granite that crops out in the west of the watershed. It is composed of K-feldspar, plagioclase, quartz, biotite, hornblende, sphene, apatite, allanite, epidote, zircon, magnetite, pyrite and ilmenite. Taku Schists occur as a north-south elongated body, about 80 km long and 8 to 22 km wide, stretching approximately from Tanah Merah (first sampling station) to central east Kelantan. The lithology of Taku Schist is mainly pelitic, consisting of quartz-mica-schist, quartz-mica-garnet schist and garnet-mica-schist. Narrow bands of amphibolite schist and serpentinite are also present [*Khoo and Lim, 1983*]. Gua Musang Formation is predominantly calcareous and argillaceous, subjacent to Triassic sedimentary rocks of the Gunong Rabong Formation. The Aring Formation is mainly volcanic. Downstream areas of Kelantan Basin (Pasir Mas and River View) are characterized by clay, silt and gravel of Quaternary age.

2.2.2 Climate and Hydrology of Kelantan Basin

Monsoonal rains dominate the regional climate, with the Northeast Monsoon (NEM) bringing the bulk of the precipitation from November to January. The basin has an annual rainfall of about 2383±120 mm. The mean annual temperature at Kota Bharu is 27±0.1 ^{o}C with mean relative humidity of 81±0.5%. The mean annual flow of the Kelantan River measured at Tanah Merah is 483±43 m^3/s.

2.2.3 Vegetation and land-use in Kelantan watershed

Kelantan Basin is less urbanized. Tropical rainforest remains the major land cover, accounting for 68% of the total basin area. The remaining 32% are plantations, mostly oil palm (~28%) and minor (4%) non-irrigated cultivation, presumably cassava. Rice paddies planted in the lowlands area are relatively insignificant, ~ 0.21% (Figure 7b).

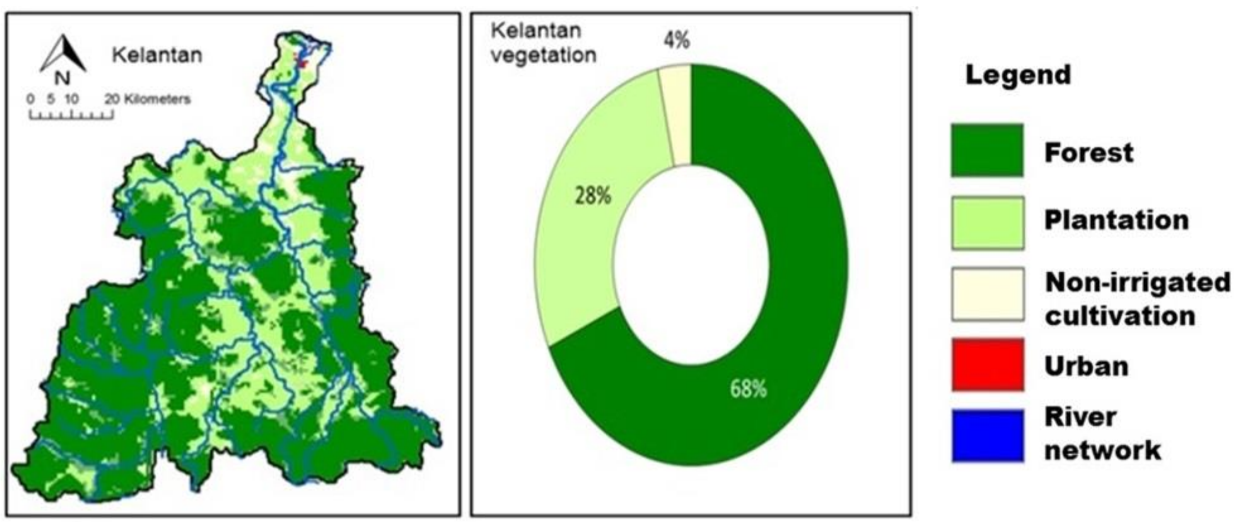

Figure 7b: Land cover map of Kelantan watershed based on GLC 2000 data from [*Stibig et al, 2007*].

Chapter 3: Sample Collection and Analytical Procedures

Sample collection was carried out for 18-month period, from May 2010 to December 2011. Sampling includes rainfall, river water and groundwater. Due to limitation in local support, *rainfall* samples were collected only two to eight times per month following the International Atomic Energy Agency (IAEA/World Meteorological Organization (WMO)) technical procedure [*IAEA/WMO, 2004*]. The samples were collected with a 1-L Nalgene™ bottle affixed to a pole in an area unobstructed by vegetation and then stored unfiltered in 30 mL Nalgene™ bottles.

3.1 Water sampling

Samples of *river waters* were collected approximately bi-weekly at the upstream, midstream and downstream of the watersheds in the western, Langat sub-catchment (Figure 8). In the eastern Kelantan Basin, the sampling stations covered only downstream area due to logistic constraints. Monthly river flow data for Langat and Kelantan rivers were available from gauges maintained and operated by the Drainage and Irrigation Department of Malaysia (DID). Sample collection for Kelantan River was not carried out during the month of December, peak of northeast monsoon, due to safety reason as the flow increased to 268% of the annual discharge average.

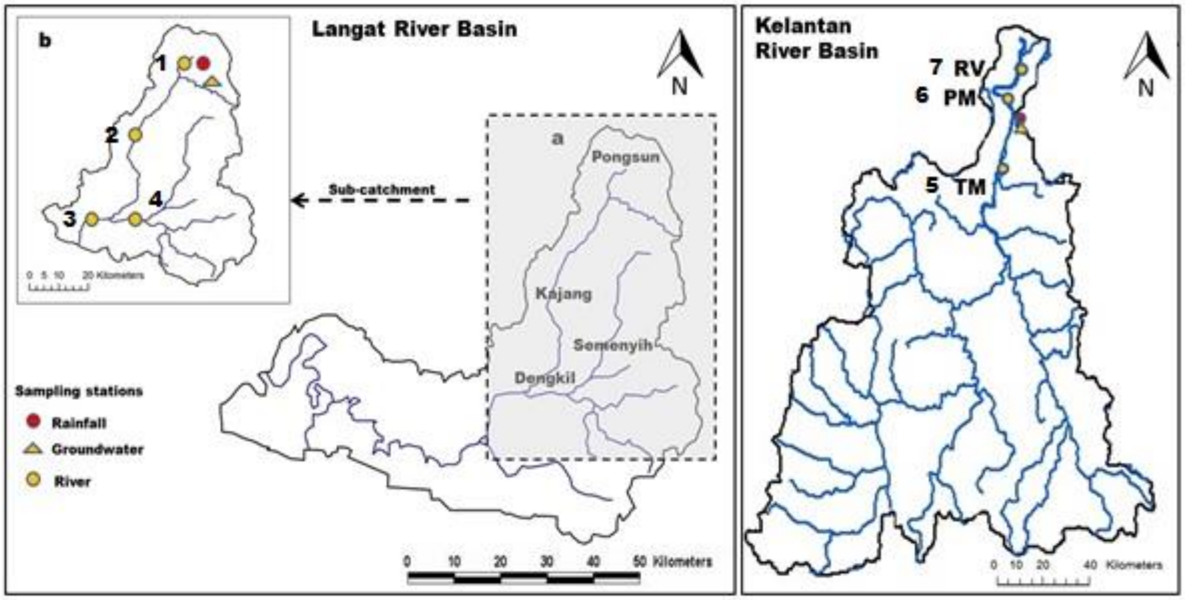

Figure 8: Sampling stations of rainfall, waters (river) and groundwater in study areas. Langat: 1) Pongsun (upstream), 2) Kajang (urban), 3) Dengkil (downstream) and 4) Semenyih (tributary). Kelantan: 5) TM (Tanah Merah- river discharge station) and downstream; 6) Pasir Mas and 7) River View.

The initial three months of sampling were performed by myself and Mr. Kern Lee. At that time we also trained local assistants who did subsequent sampling. Every four months, the samples were sent to the University of Ottawa's G.G. Hatch Isotope Laboratory for analysis. Waters were sampled in the middle of the rivers using a 250 mL Pyrex bottle. The bottle was lowered to the river from the bridge by rope to one meter depth and retrieved, while a JT-1 water sampler (code 1077) was used during the periods of higher water level and at sites with greater depth. These samples were subsequently filtered through a 25mm diameter, 0.45 µm MFS disposable membrane into 30 mL Nalgene™ bottles and kept at 4^0C before shipment to University of Ottawa.

Groundwaters were collected approximately bi-weekly from the consumption wells located at upstream Langat and downstream Kelantan. The sites were selected based on logistic availability. The water was collected directly from the pipe unfiltered, and stored in 30 mL Nalgene™ bottles at 4^{o}C prior to shipment to University of Ottawa.

3.2 Stable Isotopes of oxygen and hydrogen

The $^{18}O/^{16}O$ ratio of water samples was measured by standard CO_2-H_2O equilibration techniques [*De Groot, 2004*] at the G.G. Hatch Isotope Laboratory at the University of Ottawa. The $^{2}H/^{1}H$ ratio of water samples was determined using the zinc reduction technique [*Coleman et al., 1982*]. Oxygen-18 and deuterium content of water samples are expressed as δ values, representing deviation in parts per thousand (‰) from Vienna-Standard Mean Ocean Water (VSMOW), such that $\delta^{2}H$ or $\delta^{18}O$ = $[(R_{sample}/R_{standard})-1]*1000$ with R representing $^{18}O/^{16}O$ and $^{2}H/^{1}H$, respectively. Normalization of $\delta^{2}H$ or $\delta^{18}O$ measurements was achieved using International Atomic Energy Agency (IAEA) reference materials, and the value are reported in per mil (‰) relative to VSMOW with precision ±0.1‰ for $\delta^{18}O$ and ±2.0‰ for $\delta^{2}H$ of isotope analyses. The total number of precipitation, river and groundwater samples measured for isotopes in the Langat and Kelantan watersheds was 399 and they are listed in Appendices 9-14.

Chapter 4: Water budgets of the watersheds based on isotopic constraints

A flux of moisture from the oceans and its return via precipitation and runoff is close to a dynamic equilibrium (on an annual basis and global scale). The isotopic exchange reactions that occur between two different phases of a transition at a rate that maintains equilibrium are termed equilibrium fractionation (ie: transition of water vapor to liquid precipitation). Fractionation between water and vapor is fundamental to the hydrological cycle and plays an important role in partitioning ^{18}O and ^{2}H between the various reservoirs such as oceans, vapor, rains, runoff or groundwater [*Clark and Fritz, 1997*].

For water in a closed system, equilibrium fractionation can be expressed as:

$$H_2O_{(l)} \underset{Jc}{\overset{Je}{\longleftrightarrow}} H_2O_{(v)} \qquad \text{(a)}$$

Where *l* is the liquid phase, *v* is the water vapor phase and the rate of exchange is constant (J_e=J_c), yet it may vary for different isotopic compositions. Thus, with ^{18}O:

$$H_2{}^{18}O_{(l)} \underset{J_c^{18}}{\overset{J_e^{18}}{\longleftrightarrow}} H_2{}^{18}O_{(v)} \qquad \text{at } J_e=J_c \qquad \text{(b)}$$

Similarly, with ^{16}O:

$$H_2{}^{16}O_{(v)} \underset{J_c^{16}}{\overset{J_e^{16}}{\longleftrightarrow}} H_2{}^{16}O_{(l)} \qquad \text{at } J_e=J_c \qquad \text{(c)}$$

However, the rate of exchange for ^{18}O and ^{16}O may differ, $J_e^{18} \neq J_e^{16}$ as greater energy is needed to dissociate the stronger bonds in ^{18}O. The same is the case for H ions.

Consequently, the lighter nuclei ^{16}O and ^{1}H react more rapidly and become enriched in water vapor, leaving the heavier nuclei ^{18}O and ^{2}H enriched in the liquid.

Because the oxygen and hydrogen isotope values in precipitation fall along the Global Meteoric Water Line (GMWL), the $\delta^{18}O$ and $\delta^{2}H$ values in global precipitation are predictable, $\delta^{2}H = 8\ \delta^{18}O + 10$ ‰ [*Craig 1961*]. This relationship is primarily a reflection of differences in their equilibrium fractionation factors. The slope of the GMWL expresses this ratio, which is eight times greater for oxygen than hydrogen. The key observation is that isotopically-depleted waters associated with cold regions plot near the bottom-left and enriched waters in warm regions usually plot near the top-right of the GMWL. The above geographic dependency is due to the fact that the main global atmospheric moisture source is from the tropical ocean. Thus, precipitation at low-latitude is less depleted in ^{18}O and ^{2}H than at higher latitudes, due to proximity to its evaporative source.

Hot moist air then rises at the equator and subsequently the moisture condenses into precipitation, releasing latent heat [*Berner and Berner, 1996*]. The weak surface winds rise to equatorial doldrums, flow northward at high levels, cool and eventually sink around 30°N. The descending air is extremely dry having lost most of its moisture in the tropics, and has therefore higher capacity for uptake of moisture when warmed. Subsequently, this dry air reaches the surface, flows over the ocean, where it absorbs a substantial amount of moisture and flows southward, deflected to the right by the Coriolis force, known as Northeast trade winds. The Northeast, and Southeast, trade winds converge at the tropical convergence zone upon reaching the Equator and then rise again completing the low latitude cycle known as the Hadley Cell.

Given that ^{18}O and ^{2}H are the heavier isotopes, these continual condensation events cause the progressive depletion of the residual atmospheric moisture reservoir in ^{18}O and ^{2}H. As rain-out is related to any process that causes condensation, such as a decrease in air temperature, similar pattern of progressively lighter $\delta^{18}O$ and $\delta^{2}H$ values in precipitation are usually observed with increase distance from coastal regions (the continental effect) and in regions where a change in elevation causes orographic precipitation.

In regional conditions, the local meteoric water lines (LMWLs) differ somewhat from the GMWL and the slopes and $\delta^{2}H$-intercepts are determined by intra-annual variation in the $\delta^{18}O$ and $\delta^{2}H$ values of local precipitation. At higher latitudes, such as North America, the $\delta^{18}O$ and $\delta^{2}H$ values of precipitation vary with changes in the source of moisture, the seasonal changes in air temperature, and with the form of precipitation [*Clark and Fritz, 1997*]. Consequently, $\delta^{18}O$ and $\delta^{2}H$ values of precipitation are usually lighter during cooler months of the year, plotting near the bottom-left of a LMWL, and the isotopically heavier values, reflecting the warmer months, plot near the top-right of LMWL.

In terms of GMWL, the temperature dependent isotope separation differs with latitude [*Rozanski et al., 1993*]. In equatorial regions, where the temperature is generally consistent throughout the year and precipitation usually occurs only as rain, $\delta^{18}O$ and $\delta^{2}H$ values of precipitation depend mainly on the source of atmospheric moisture, the pathway of its transport from the source to the point of condensation, and the amount of incident rainfall (the amount-effect) [*Araguas-Araguas et al., 1998*]. In the context of Peninsular Malaysia, because of the absence of a distinct dry period, the $\delta^{18}O$ and $\delta^{2}H$ values in precipitation depend mainly on the source of atmospheric moisture, the Northeast and Southwest monsoon.

4.1 Partitioning of Evaporation and Plant Transpiration Water Fluxes

Naturally, stable isotopes of water ($^{18}O/^{16}O$ and $^{2}H/^{1}H$) in global *precipitation* exhibit systematic spatial and temporal variations and jointly define a regression line, the Global Meteoric Water Line (GMWL) [*Craig, 1961; Dansgaard, 1964; Rozanski et al., 1993*]. This relationship arises from mass-dependent isotope fractionation that accompanies the phase transitions of water (ie: evaporation and condensation).

At a regional scale, the linear trends for Local Meteoric Water Line (LMWL) and Local Evaporation Lines (LEL) can be established by a cross-plot of $\delta^{18}O$-$\delta^{2}H$ for precipitation and *river water*, respectively. In our case, LEL is defined by $\delta^{18}O$ and $\delta^{2}H$ values of *river water* collected near the river mouth, based on the assumption that this water is a product that subsumes all processes involved in the input/output balance of water cycle in the watershed [*Gibson et al., 2005*].

The slope and the $\delta^{2}H$-$\delta^{18}O$ intercept value of LMWL is governed by the main meteorological conditions of the moisture source area, rainout and the trajectory of the air mass, and by second-order kinetic effects such as those associated with snow formation and evaporation from raindrops [*Clark and Fritz, 1997; Araguas-Araguas et al., 1998*]. The isotopic composition of precipitation at a specified location is determined by an initial evaporation at the moisture source and the path of moisture transport to the location of eventual condensation of vapor mass [*Jouzel, 2006*]. The slope for LEL of surface water (river) at a given location within a watershed is primarily determined by the initial isotope composition of water input and the cumulative influence of evaporation upstream, as evaporation causes an enrichment in ^{16}O and ^{1}H in vapor mass and hence enrichment in the heavier isotopes in the residual waters [*Gibson and Edwards, 2002*].

Given the difficulties of measuring direct evaporation, the $\delta^{18}O$ and $\delta^{2}H$ values of river water collected from the point of outflow can be taken as that of the residual liquid and the LEL can be used to constrain the evaporation flux E_d. In watershed where E_d from soils and water bodies is volumetrically significant, relative to annual water input, LEL is characterized by a slope that is shallower than the $\delta^{18}O$ and $\delta^{2}H$ trend for the precipitation input.

The intersection of the LEL and LMWL provides an amount weighted estimate of the $\delta^{18}O$ and $\delta^{2}H$ values for water entering the hydrologic system that is not yet affected by evaporation within the watershed [*Gibson and Edwards, 2002*]. Fundamentally, these stable isotopes studies reflect fractionating water vapor fluxes that result from incomplete evaporation generating a residual ^{18}O-^{2}H-enriched liquid. In contrast, transpiration processes do not affect the isotope composition of soil water [*Moreira et al., 1997; Twining et al., 2006*]. Note, however, that water flux that is intercepted by the canopy results in complete evaporation, hence no isotopic fractionation. The (I_n) must therefore be estimated in other ways. The proportion of fractionating water vapor fluxes to water input can be resolved by examining the isotope separation between $\delta^{18}O$ and $\delta^{2}H$ value of water input (precipitation) and output (river outflow) from a particular geographical region [*Gonfiantini, 1986; Gibson* *et al., 1993; Lee and Veizer, 2003; Ferguson and Veizer, 2007*], such as watersheds, that can be considered as a quasi-closed hydrologic system.

The equations for isotope mass balance, were proposed for steady-state [*Gonfiantini, 1986; Gat and Bowser, 1991; Gibson et al., 1993*] as well as non-steady state hydrologic conditions [*Gibson, 2002*]. For a well-mixed hydrologic system, such as a lake or a watershed, the equation can be written as [*Gibson et al., 1993*]:

$$\frac{dV}{dt} = I - Q - E_v$$

$$\frac{d(dV\delta_L)}{dt} = I\delta_I - Q\delta_Q - E\delta_E \tag{2}$$

Where V is the volume of water in the system, dV is the change in volume over the time interval dt, I is the input of water (Appendices 1, 2), Q is the discharge (Appendices 3, 4), E_v is evaporation, and δ_L, δ_I, δ_Q, and δ_E are the isotope compositions of the respective waters in the system. In this case, precipitation is designated as the principal input of water to the system and δ_I represents the mean $\delta^{18}O$ and $\delta^{2}H$ values of precipitation. Furthermore, the isotope composition of water output $\delta_Q = (\delta_S Q_S + \delta_G Q_G)/Q$, where δ_S and δ_G are identical and considered approximately equal to δ_L (surface water), is the isotopic composition at constant volume over time for a well-mixed conditions, in order to maintain isotope mass balance. The estimate for δ_Q is possible through flow-weighted sampling of water at the river mouth. Based on a linear resistance model described by *Craig and Gordon* [*1965*] and modified by *Gibson* [*2002*], δ_E can be estimated by,

$$\delta_E = \frac{\delta_L - h\delta_A - \varepsilon}{1 - h + \varepsilon_K/1000}$$

(3)

where h is the ambient humidity normalized to saturation vapor pressure, δ_A is the isotope composition of ambient moisture, and $\varepsilon = \varepsilon^* + \varepsilon_K$ is the total isotope fractionation comprised of the equilibrium component (ε^*), considered a function of temperature, and the kinetic component (ε_K), which is controlled by the turbulent/diffusion mass transfer mechanism and humidity.

Under steady-state atmospheric and hydrologic conditions within a given watershed, $dV/dt = 0$, air-water isotope exchange will progress and surface waters will enrich (or deplete) to an isotope steady-state and this helps us to elucidate the isotope and hydrologic characteristics of the system [*Gibson, 2002*]. Assuming well-mixed conditions, substitutions in equation 4 results in:

$$V\frac{d\delta_L}{dt} + \delta_L\frac{dV}{dt} = I\delta_I - Q\delta_Q - \frac{E_v}{1 - h + \varepsilon_K/1000}(\delta_L - h\delta_A - \varepsilon)$$

(4)

Given a situation where the volumetric changes are negligible ($dV/dt=0$), that is the volume of water in a given hydrologic system is considered constant, $P-Q=ET$, and this enables characterization of isotope changes in surface water over time t. This ultimately permits quantification of evaporation (E_v) with respect to water input (I). For multi-year precipitation and river flow data, ET inter-annual changes in water volume have to be considered insignificant in order to maintain the assumption of hydrologic steady-state. In that case the steady-state isotope mass balance equation proposed by *Gonfiantini (1986)* can be used to estimate the proportion of E_v relative to the annual water input I.

$$\frac{E_v}{I} = \frac{(\delta_S - \delta_I)(1 - h + \Delta\varepsilon)}{(\delta_S + 1)\left(\Delta\varepsilon + \frac{\varepsilon}{\alpha}\right) + h(\delta_A - \delta_S)}$$

(5)

Where α is the equilibrium fractionation factor ($\ln\alpha$ = 1137 TEMP $^{-2}$ – 0.4156 TEMP $^{-1}$ - 0.00207) for oxygen and ($\ln\alpha$ = 24844 TEMP $^{-2}$ – 76.248 TEMP $^{-1}$ + 0.05261) for hydrogen isotopes during evaporation (Temperature, TEMP in Kelvin, K) [*Friedman and O'Neil, 1977*], $\Delta\varepsilon = \alpha - 1$, and δ_I, δ_A, δ_s are the mean $\delta^{18}O$ (or δ^2H) values of precipitation, ambient moisture, and outflow, respectively.

E_v/I value essentially represents the amount of evaporative water loss from a watershed required to produce the observed isotope separation between initial water input (δ_I) and output (δ_S) at the ambient climatic conditions (ie: temperature and relative humidity). In this study, the main source of the water input is rainfall, and its $\delta^{18}O$ and δ^2H values define the LMWL for the period of data collection. Note that it is also assumed that incident precipitation and throughfall are identical in terms of isotope composition.

δ_s was estimated as the flow-weighted mean $\delta^{18}O$ (or δ^2H) value of river water at the point of discharge from the watershed (ie: river mouth). A δ_s value with 95% confidence interval was used to approximate the error associated with the isotope composition of the outflow. Both δ_I and δ_s values with 95% confidence intervals were used to estimate the error associated with the *Ev/I* value from equation (5).

Mean annual value for temperature and humidity, provided by the Meteorological Department of Malaysia (Appendices 5-7), were substituted into equation (5) and used to calculate the isotope fractionation factors for this equation. The approximation of the isotope composition of atmospheric moisture and mean annual precipitation is based on equation $\delta_A=\delta_I-\varepsilon^*$ [*Gat and Matsui, 1991; Gammons et al., 2006*].

4.2 Isotopic trends in precipitation

4.2.1 Langat Basin

$\delta^{18}O$ and δ^2H values of rainfall, collected at Langat from May 2010 to December 2011, define a LMWL approximated by equation $\delta^2H= 7.7(\pm0.4).\delta^{18}O+6.3(\pm2.6)$ ‰ (Figure 9). The enriched end-member rains reflect the relative proximity of Peninsular Malaysia to moisture from the Indian Ocean and South China Sea followed by rainout effect as the moisture-laden winds encounter Main Range (Titiwangsa) in the upper reaches of the watershed. During this transit, condensation of moisture results in depletion of rainfall in ^{18}O and ^2H.

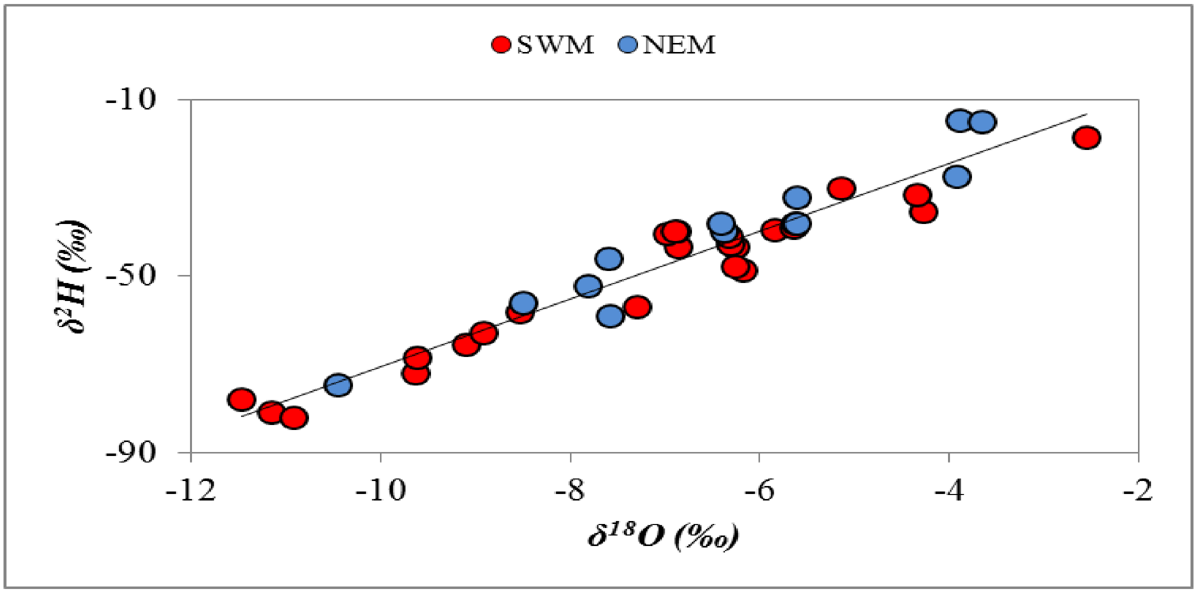

Figure 9: Monsoonal influences on the rainfall in Langat watershed (R^2=0.92, p<0.01, n=37)

Overall, the rainout effect or the degree of isotope depletion appears slightly more pronounced at the times of the SWM (Figure 9).

4.2.2 Kelantan Basin

$\delta^{18}O$ and δ^2H values of rainfall in the Kelantan watershed (Figures 10), collected between May 2010 and November 2011, plot around the LMWL of $\delta^2H = 7.8(\pm0.5).\delta^{18}O+7.1(\pm3.6)$ ‰. These samples show a somewhat more restricted isotopic range than those of the Langat rain. δ^2H and $\delta^{18}O$ for water samples collected during SWM season plot towards the top-right of Figure 10, likely reflecting a sea breeze effect. The ocean absorbs more heat and its greater heat capacity enables the ocean surface to warm up gradually, relative to the land surface. As the temperature of the land rises, the surface air is heated, becomes less dense, surges upwards and is replaced by the cooler air from the adjacent South China Sea, generating a cooler breeze in the coastal area. The strength of the sea breeze is directly proportional to the temperature gradient between sea and the land. A sea breeze front creates a boundary resulting in two masses of air of different densities. The cold air from the sea converges with the warm air from the land, creates the shallow cold front and thunderstorms result. Theoretically, the cold air is progressively moving inland replacing the warm air that is continually rising at the weather front. Note that this trend of isotopic variation in precipitation is based on the sampling station that is located in the downstream portion of the watershed. The pattern may be shifted towards greater depletion in the upper reaches of the watershed. Note nevertheless, that precipitation for both watersheds defines almost identical LMWL (Figure 11) arguing for relative isotopic homogeneity of rains across the Malaysian Peninsula.

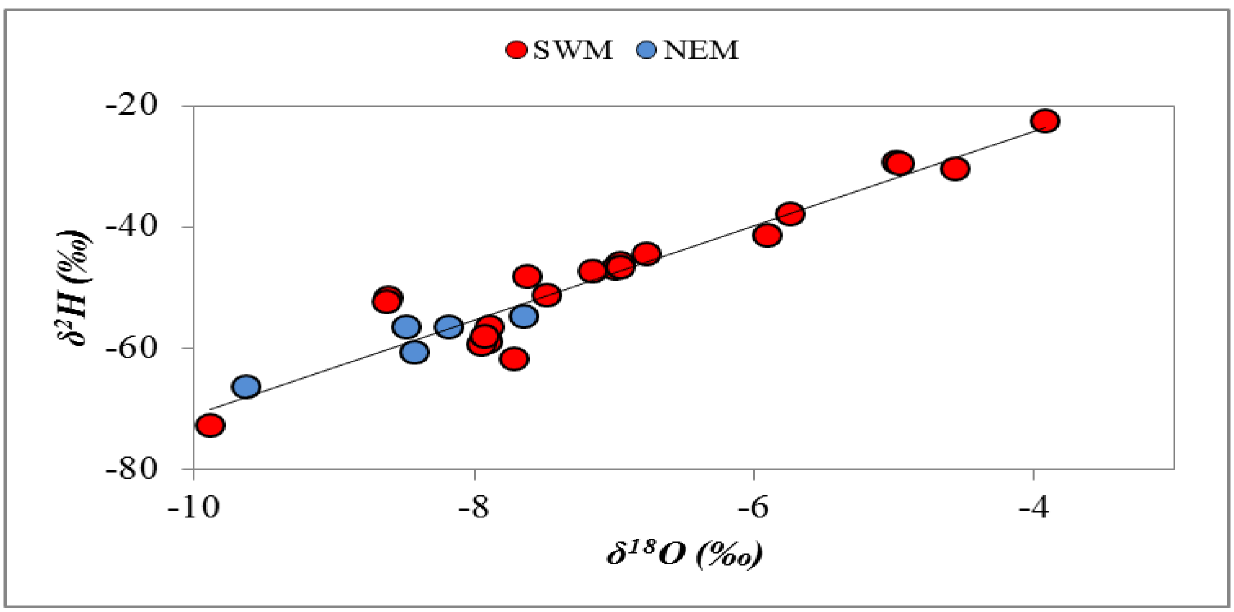

Figure 10: Monsoonal influences on rainfall in Kelantan watersheds. (R^2=0.90, p<0.01, *n*=27).

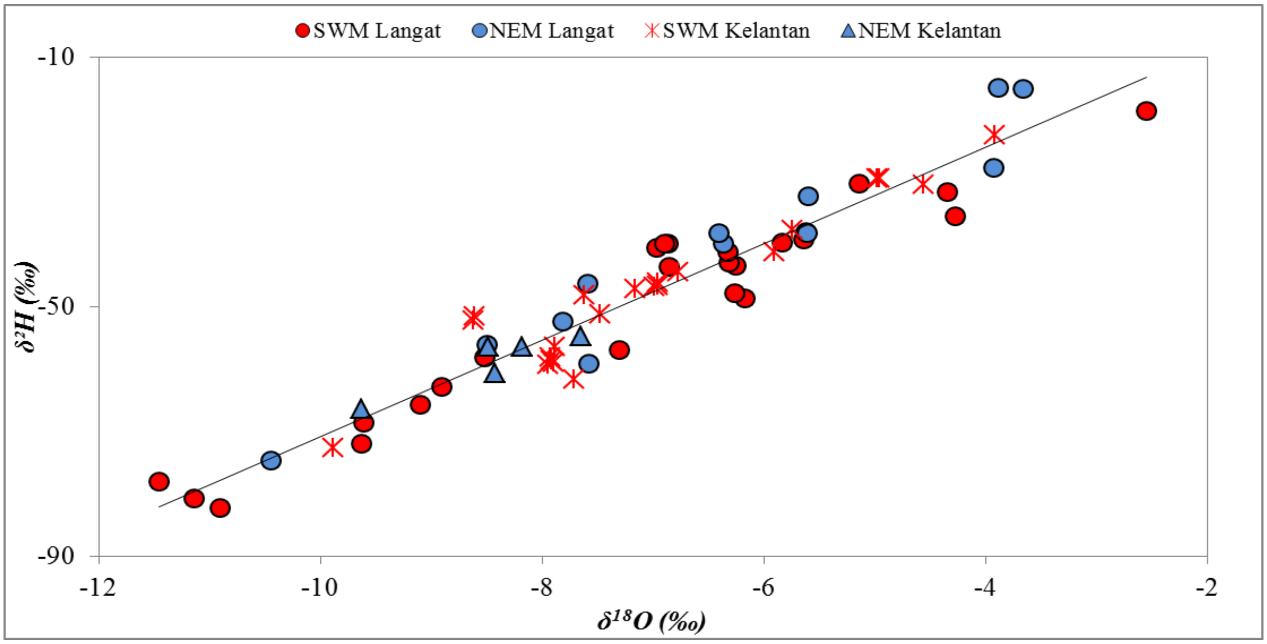

Figure 11: Composite Local Meteoric Water Line (LMWL) for the Langat and Kelantan watersheds defines $\delta^2H=7.73(\pm0.3).\delta^{18}O + 6.52(\pm2.1)$ ‰.

4.3 Isotopic trends in river water

4.3.1 Langat watershed

$\delta^{18}O$ and δ^2H values of river water collected from the upstream, tributary and downstream of Langat watershed defines a Local Evaporative Water Line (LEL) with slightly shallower slope than that of the LMWL of rainfall at Pongsun (Figure 12, Table 1). The shallower slope of 6.8 reflects evaporation at the surface of waters in the Langat watershed despite its high humidity (80%).

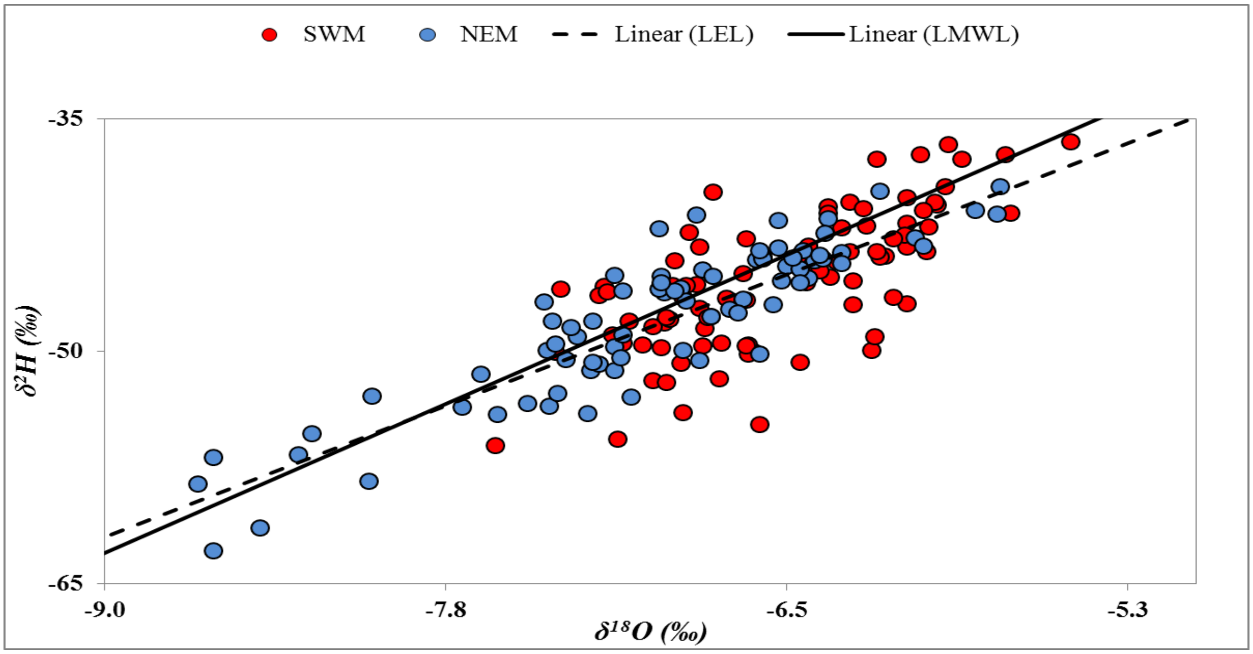

Figure 12: δ^2H and δ^{18}O values of river water collected from the upstream, tributary and downstream of Langat watershed define a LEL (dotted line).

	Langat		
LMWL	$\delta^2H = (7.7 \pm 0.4)\ .\delta^{18}O + (6.3 \pm 2.6)$	$R^2 = 0.93$	$n=37$
LEL	$\delta^2H = (6.8 \pm 0.4)\ .\delta^{18}O - (0.8 \pm 2.5)$	$R^2 = 0.68$	$n=166$
	Kelantan		
LMWL	$\delta^2H = (7.8 \pm 0.5)\ .\delta^{18}O + (7.1 \pm 3.7)$	$R^2 = 0.91$	$n=27$
LEL	$\delta^2H = (7.8 \pm 0.2)\ .\delta^{18}O + (7.5 \pm 1.1)$	$R^2 = 0.96$	$n=103$

Table 1: Local Meteoric Water Line (LMWL) and Local Evaporation Line (LEL) of the Langat and Kelantan watersheds (± are 95% confidence intervals)

Langat and Semenyih dams, located in the upstream section of the Langat sub-catchment, may contribute to this evaporation as more surface water is exposed to the atmosphere due to its increased residence time in the dams. Note also the considerably greater isotopic depletions of river waters during some intervals of the NEM, likely reflecting the greater rainout effect for moisture transported across the mountain range from the South China Sea.

4.3.2 Kelantan Watershed

$\delta^{18}O$ and $\delta^{2}H$ values of water collected from the Kelantan River defines a LEL that is similar to Kelantan LMWL (Figure 13). Note, however, that the rainfall samples for this watershed were collected from its downstream portion. Greater moisture content of air mass from South China Sea, moving inland due to earlier postulated sea breeze effect, results in higher humidity (80%) and hence less evaporation.

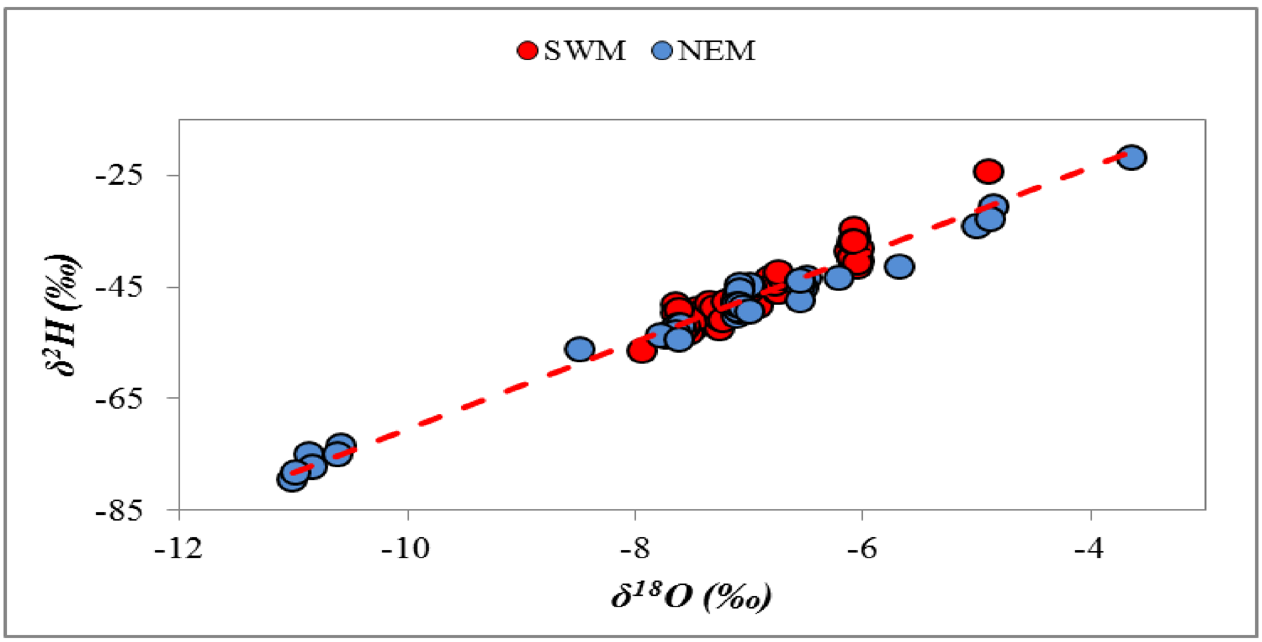

Figure 13: $\delta^{2}H$ and $\delta^{18}O$ values of river water collected from the downstream Kelantan define the LEL (red dotted line).

4.4 *Evaporation estimates*

Quantitatively, an isotope mass balance equation can now be used to estimate the amount of evaporation required to generate the observed isotope separation between initial rainfall (δ_I) and eventual outflow via river water (δ_s), provided the information on temperature, humidity and related isotope fractionation factors for oxygen and hydrogen isotopes are available. Input parameters substituted into equation (5) and the calculated *Ev/I* for Langat watershed are summarized in Table 2. Given that the LEL for the Kelantan watershed is the same as LMWL, δ_I and δ_s cannot be resolved and the *Ev/I* for Kelantan watershed becomes insignificant, reflecting its high humidity.

The δ_S values for the Langat watershed, by comparison, were approximately 1‰ heavier than the $\delta_{I,}$ implying that waters were enriched in ^{18}O and ^{2}H due to isotope fractionation during evaporation. This isotope separation between δ_I and δ_S corresponds to E_v/I value of ~11%. The present estimate includes evaporation of surface waters from the actual watercourses as well as from the dams.

Watersheds	Input parameters							Output
	T	h	δ_I	δ_A	ε	$\Delta\varepsilon$	δ_S	Ev/I
	K	%	‰	‰	‰	‰	‰	%
Langat	298.7	82	-7.8 ± 0.7	-16.9	9.3	2.5	-6.7 ± 0.1	10.6
Kelantan	298.7	82	NA	NA	NA	NA	-7.2 ± 0.2	NA

Table 2: Input parameters for steady-state isotope mass balance (equation 5) and the calculated E_v/I values from oxygen isotopes, with 95% confidence interval. E_v denotes evaporation and I is the annual water input.

4.5 *Rainfall Interception, I_n*

P and *Q* are the fundamental components of annual water balance for a watershed and the difference *ET* represents an approximation of the total flux of water vapor from a closed hydrologic system to the atmosphere. However the *ET* consists of three components, isotopically fractionating partial evaporation from water bodies E_d, non-fractionating full evaporation from canopy called interception I_n, and non-fractionating transpiration flux *T*. The variable *T* can be estimated from the balance in the *ET* component ($ET - [I_n + E_d]$), if I_n can be estimated by other means.

The proportion of gross rainfall that is captured by plant surfaces and subsequently fully evaporated is termed rainfall interception, I_n, also referred to as canopy evaporation. This component may account for a significant proportion of annual rainfall in densely-vegetated regions and varies depending on the intensity, duration and form of precipitation, the growth stage and structure of vegetation, and ambient environmental conditions, such as temperature and humidity [*Fleischbein et al., 2006; Holwerda et al., 2006*]. The studies of isotopic composition (^{18}O and ^{2}H) of throughfall waters in tropical rainforest regions, such as South America and Southeast Asia, show that the rainfall, throughfall and waters entering the soil zone have identical values [*Goller et al., 2005; Rhodes et al., 2006; Liu et al., 2007*]. Thus evaporation from canopy does not influence their isotope budget, demonstrating that this evaporation, in contrast to surface water bodies and soils, must be 100% effective. As a consequence, I_n is not reflected in the evaporation budget based on the isotope approach and must be established by additional empirical data.

In Peninsular Malaysia, the rainfall is evenly distributed throughout the year and the major vegetation type is tropical evergreen [*Stibig et al, 2007*]. The annual interception for this forest type and canopy in the Pasoh Forest Reserve (Table 3) was estimated to be ~18% (331 mm) of annual gross rainfall (1804 mm) [*Tani et al., 2003*]. In Borneo I_n was estimated to account for ~13% (352 mm) of annual gross rainfall (2740 mm) [*Kumagai et al., 2005*]. In another regional estimate, *Asdak et al.* [*1998*] reported I_n of ~11% (251 mm) of P (2199 mm) for a pristine, closed-canopy rainforest of central Borneo. In a rain-fed, inter-cropped system of cassava [*van Dijk and Bruijnzeel, 2001*] and cocoa agroforest [*Dietz et al., 2006*] in West Java and central Sulawesi (Indonesia), I_n was also estimated at 18%, (284/1577 mm and 39/214 mm), albeit based on 18 days of rainfall measurements only. In Malaysia, I_n for rubber tree and oil palm plantations [*Yusop et al., 2003*] and [*Bentley, 2007*] was estimated as 12.1% (~66/548 mm) and 40.7% (~726/1772 mm) of gross rainfall, respectively.

Langat					
Land type	Area		Interception, I_n		Rainfall, *P*
	km^2	%	%	mm	mm
Forest	635	44	18	170	944
Oil palm	491	32	41	281	686
Non-irrigated cultivation	289	20	18	77	429
Urban	43	3	NA		64
Others	14	1			21
Total	1443	100	~8%		2145
Average I_n				176	

Kelantan					
Land type	Area		Interception, I_n		Rainfall, *P*
	km^2	%	%	mm	mm
Forest	9289	68	18	292	1621
Oil palm	3850	28	41	275	672
Non-irrigated cultivation	471	3	18	NA	82
Paddy	29	0	NA		5
Urban	20	0			3
Total	13659	100	~12%		2383
Average I_n				284	

Table 3: Estimates of area-weighted I_n/P based on GLC 2000 land-cover class [*Stibig et al., 2007*] in the watersheds.

In order to estimate area-weighted I_n/P, the literature values summarized in Table 3 were assigned to each constituent GLC 2000 land-cover class in the watersheds, yielding an overall I_n approximately of 8% and 12% for the Langat and Kelantan watersheds, respectively. For Langat, which is more urbanized, and for Kelantan, the compound I_n estimates with ±95% were 176±160 and 284±102 mm, respectively.

4.6 Transpiration (T) and the water budgets of the watersheds

The river flow, Q patterns in Langat and Kelantan rivers are influenced by the intensity of the rainfall in the upstream areas, and rainfall patterns at different rainfall stations. This is particularly true for periods of consistently high daily rainfall [*Bruno et al., 2006*] due to rapid response of river flow to rainfall events. Because approximately 56% of water uptake by plants occurs at depths of 0-2 meters, the fast response argues that the proportion of P stored in the soil zone is negligible ($\Delta S = 0$). Therefore P-Q represents an approximation of ET.

Despite uncertainties related to the area of contributing drainage, rainfall clearly exceeds discharge, implying that a proportion of annual rainfall, if not stored in the watersheds, must have been transferred to the atmosphere via (E_d + I_n + T). Considering that 1 mm yr^{-1} corresponds to 10^3 g H_2O m^{-2} yr^{-1}, the magnitude of the water flux can then be calculated for a regional scale of a watershed (Table 4).

Watersheds	Values in mm or 10^3g H_2O $m^{-2}yr^{-1}$					
	P	Q	I_n	E_d	T	ET
Langat	2145 ± 237	703 ± 81	176 ± 160	236 ± 24	1030 ± 103	1442 ± 131
Kelantan	2383 ± 120	1080 ± 94	284 ± 102	0	1019 ± 102	1303 ± 71

Table 4: Components of annual water balance for the Langat and Kelantan watersheds in 2010-2011 and their 95% confidence intervals. The contributing drainage areas are 1443 km^2 for the Langat sub-catchment and 13659 km^2 for the Kelantan watershed.

The estimate for rainfall P in the Langat sub-catchment is based on a single station that exists in the basin (Appendix 1), a limitation somewhat mitigated by the small size of the sub-catchment. The Kelantan watershed rainfall is based on 13 stations. Because the location coordinates for these stations are not available, an arithmetic average (Appendix 3) is employed for the entire watersheds [*Dingman, 2008*]. With these limitations the annual estimates of water input per unit area of the studied watershed are given in Table 4. The average monthly discharge is 35.38 m^3/s for the Langat sub-catchment (Appendix 2) and 198.56 m^3/s for the Kelantan watershed (Appendix 4), normalized for the area of respective basins, define the term Q in Table 4. Based on these P and Q estimates, almost 70% of P is being transferred to the atmosphere as water vapor via ET. The water flux T, the biological transport of water to the atmosphere, is then the residual amount in rearranged equation (1); $T = P- Q- E_d- I_n$. The residual flux required for balancing the annual water input by P for the Langat and Kelantan watersheds are 1030±103 mm and 1019±102 mm, respectively. The error assigned to T is the propagated error of P at 10% for the 95% confidence intervals.

4.7 Summary

Evapotranspiration flux, ET in the water budget of the Langat and Kelantan watersheds accounts for 67% and 55% of the incoming precipitation P. ET, in turn, is partitioned into E_d, I_n and T (Figure 14). T appears to be a major component, comprising 80% of ET, whereas E_d represented only a small proportion in terms of volumetric significance, up to ~11%. The estimates for E_d and T, based on stable isotope technique, complemented by the annual water inputs (rainfall), river discharges, and spatial distribution of ecosystems within the watershed enabled a closure for the water budget for these closed, steady-state, hydrologic systems.

This approach is particularly suitable for regions where hydrologic data are sparse. I do nevertheless emphasize that spatial ambiguities encountered in this study, the impact of transition of rainfall to river via groundwater storage pathway, and the extent of a dense hydrologic network within the watersheds (especially Kelantan), necessitate further studies for tropical watersheds. Given the short-term variability of precipitation and river flow within the Langat sub-catchment and Kelantan basin, it is essential to better document the seasonal variability of E_d and T by frequent sampling over a multi-year period.

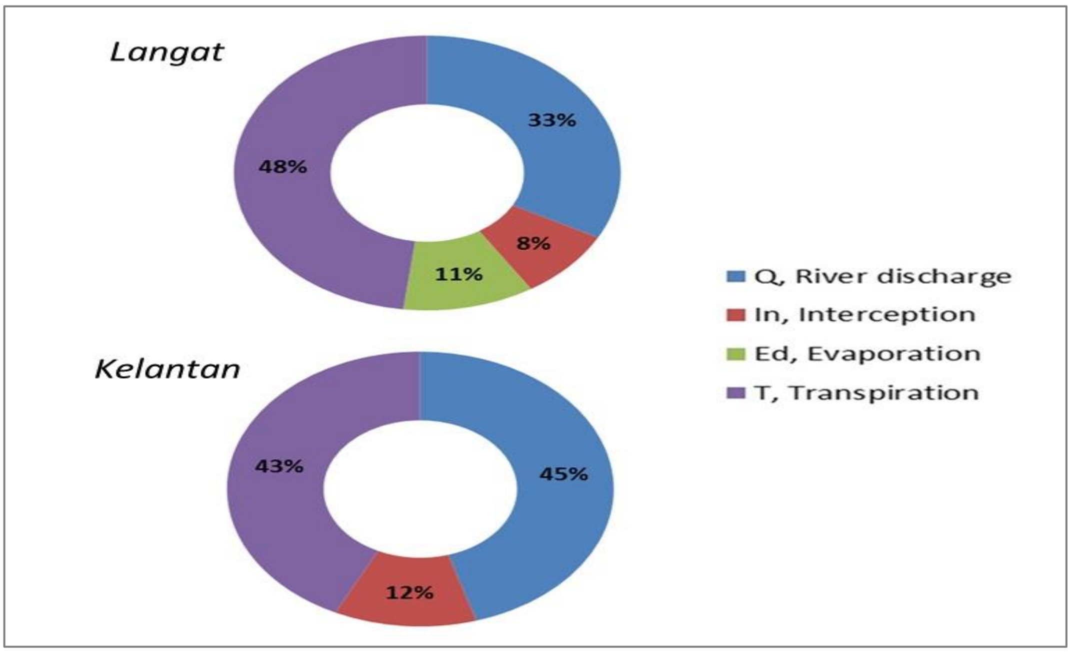

Figure 14: Apportionment of the hydrologic components in Langat and Kelantan watershed

Chapter 5: Isotopes, Climate and hydrology: Temporal variations

This chapter discusses the seasonal variations of the stable isotopes at Langat and Kelantan watersheds and their relationships with the regional climate and hydrological variables. The datasets of Precipitation (*P*) and Discharge (*Q*) (Appendices 1- 4) were obtained from the Department of Irrigation and Drainage Malaysia (DID) and those for Global Solar Radiation (*GSR*) and Temperature (*TEMP*) (Appendices 5, 6, 8), from Malaysian Meteorological Department (MMD). The stable isotope data of rainfall, waters and groundwaters in the Langat and Kelantan watersheds were collected from May 2010 to December 2011 (Appendices 9-14). Data collection of *P* and *Q* are maintained by DID whereas MMD is responsible for the *GSR* and *TEMP*.

5.1 Stable isotopes, $\delta^{18}O$ and $\delta^{2}H$

The statistical parameters for $\delta^{18}O$ and $\delta^{2}H$ in the Langat and Kelantan basin waters, (Appendices 9-14) are summarized in Table 5. Box-Whisker plot (Figure 15) demonstrates that $\delta^{18}O$ and $\delta^{2}H$ of LP, LR, LG and KR data are negatively skewed whereas KP is slightly skewed to the right. $\delta^{18}O$ of KG is positively skewed while $\delta^{2}H$ is skewed to the left. Note that, by referring to median values (Figure 15), the precipitation is isotopically enriched than river or groundwater in the Langat watershed while the relationship is the opposite for the Kelantan watershed.

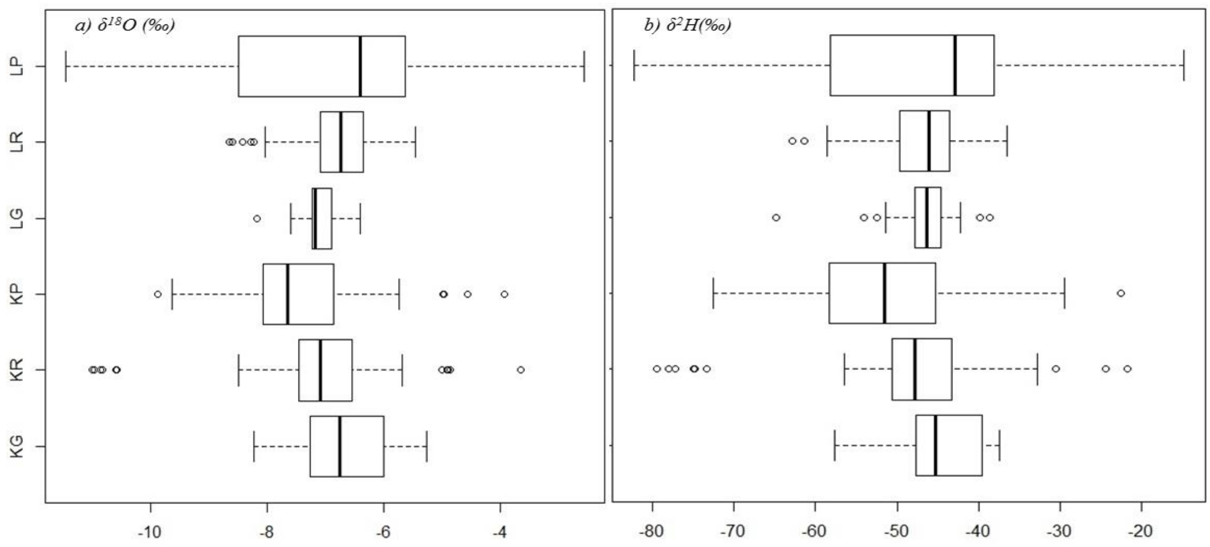

Figure 15: Box-whisker plot shows the distributions of sets of $\delta^{18}O$ and $\delta^{2}H$ for *precipitation, river waters and groundwaters*, comprising outliers (circle), lower fence (left), lower fourth, median (bold line), upper forth and upper fence (right). Dotted line indicates the range of the data distribution. LP= Langat Precipitation, LR= Langat River, LG= Langat Groundwater, KP= Kelantan Precipitation, KR= Kelantan River, KG= Kelantan Groundwater.

This is somewhat surprising considering that the precipitation station for the former is in the upstream portion and that of the latter in the downstream section of the watershed. More data are required to resolve this enigmatic observation because it is entirely possible that the overall isotopically enriched nature of Langat precipitation is due to few anomalous outliers in the summer and winter precipitation (see also Figure 9, Section 4.2.1).

	Langat					
	$\delta^{18}O$			$\delta^{2}H$		
	Rainfall	*River*	*Groundwater*	*Rainfall*	*River*	*Groundwater*
Mean	-6.93	-6.74	-7.12	-47.02	-46.61	-46.71
Standard Error	0.36	0.05	0.06	2.88	0.37	0.83
Median	-6.41	-6.72	-7.18	-42.93	-46.00	-46.32
Standard Deviation	2.19	0.59	0.34	17.49	4.81	4.68
Minimum	-11.46	-8.66	-8.18	-82.23	-62.89	-64.82
Maximum	-2.55	-5.46	-6.41	-14.80	-36.51	-38.58
Sample size (*n*)	37	166	32	37	166	32
Confidence Level (95%)	0.73	0.09	0.12	5.83	0.74	1.69

	Kelantan					
	$\delta^{18}O$			$\delta^{2}H$		
	Rainfall	*River*	*Groundwater*	*Rainfall*	*River*	*Groundwater*
Mean	-7.29	-7.09	-6.64	-49.81	-47.62	-44.66
Standard Error	0.28	0.12	0.13	2.32	0.94	0.86
Median	-7.65	-7.08	-6.77	-51.58	-47.86	-45.30
Standard Deviation	1.47	1.20	0.73	12.05	9.50	5.04
Minimum	-9.89	-11.01	-8.23	-72.62	-79.54	-57.69
Maximum	-3.92	-3.64	-5.25	-22.52	-21.73	-37.40
Sample size (*n*)	27	103	34	27	103	34
Confidence Level (95%)	0.58	0.23	0.25	4.77	1.86	1.76

Table 5: General statistics for $\delta^{18}O$ and $\delta^{2}H$ (‰) in Langat and Kelantan watersheds.

5.2 *Langat Watershed*

5.2.1 Seasonal variations in isotope signals of Langat waters

The $\delta^{18}O$ variations in the river water shows most depleted values to be associated with the winter months and the NEM (Figure 16). This is likely a reflection of the stronger rain-out effect for the moisture transported across the Titiwangsa mountain range.

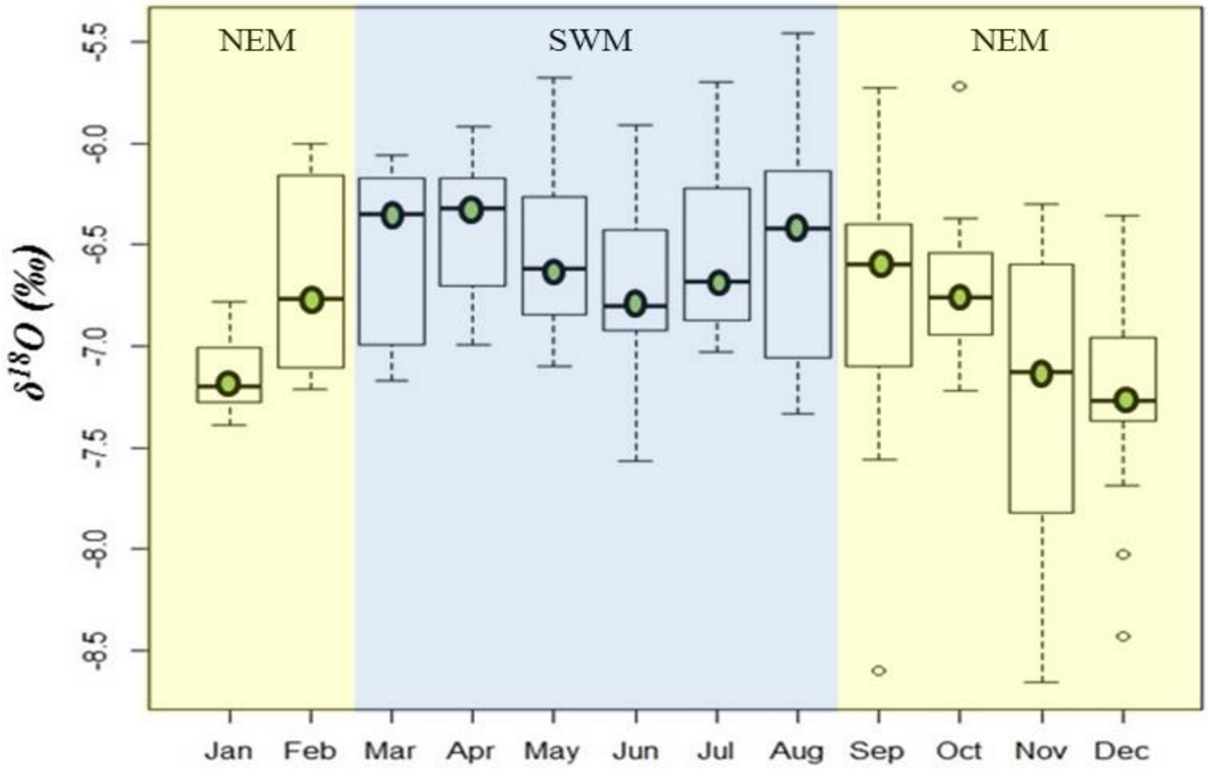

Figure 16: Seasonal variations of $\delta^{18}O$ for Langat River. Patterns as in Figure 15.

$\delta^{18}O$ and $\delta^{2}H$ values of *rainfall* collected at Langat (Appendix 8) during SWM vary from ~ -12 ‰ to ~ -2 ‰ and ~ -90 ‰ to -10 ‰, respectively. The NEM values have smaller range, with $\delta^{18}O$ and $\delta^{2}H$ from ~ -11 ‰ to ~ -4 ‰ and ~ -75 ‰ to ~ -15 ‰, respectively. No rainfall data are available for March and November. Over the sampling period, isotopically-enriched ($\delta^{18}O$ and $\delta^{2}H$) rainfalls were observed on May 29, 2010 (-4.27 ‰; -35.46 ‰), January 28, 2011 (-3.66 ‰; -15.07 ‰), August 8, 2011 (-2.55 ‰; -18.59 ‰), September 24, 2010 (-3.89 ‰; -14.8 ‰) and September 23, 2011 (5.62 ‰, -38.08 ‰). On the other hand, the isotopically-depleted rainfalls were observed in July 8, 2011 (-11.46 ‰; -78.00 ‰), September 14, 2010 (-10.45 ‰; -74.66 ‰) and May 1, 2011(-11.14 ‰; -80.77 ‰). In terms of median values, (Figure 17) the oxygen isotope data show a gradual depletion from

February (late NEM) towards the SWM (July) and then slight enrichment as the monsoon shifts to NEM.

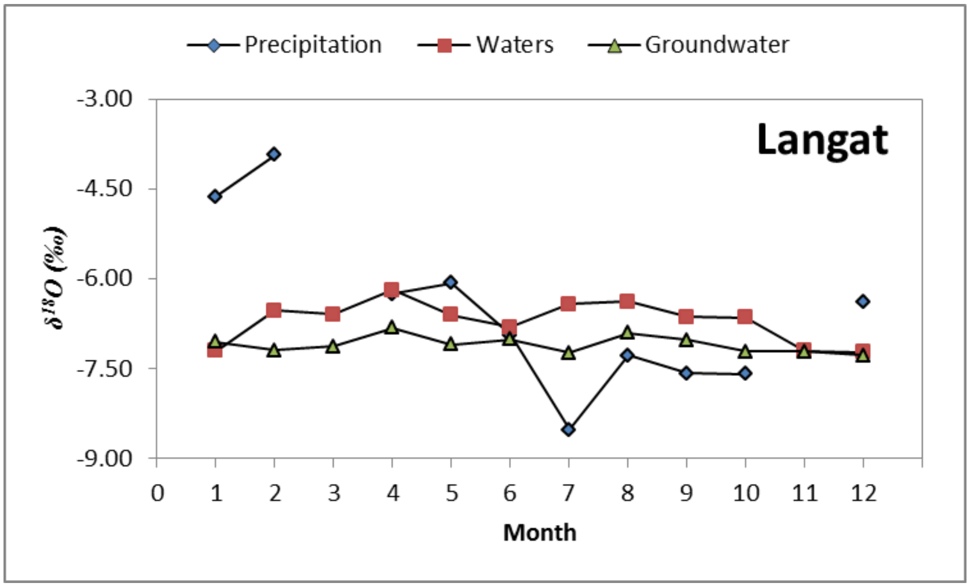

Figure 17: Monthly median δ^{18}O of precipitation, river waters and groundwater for the Langat watershed.

The bi-weekly data for δ^{18}O and δ^{2}H (Appendix 10) for *surface waters* collected at Pongsun (ILO14-upstream), Kajang (ILO5- Midstream), Dengkil (ILO3-Downstream), and Semenyih (tributary) have minimum values of δ^{18}O and δ^{2}H of -8.66 ‰ and -62.89 ‰ (September 26, 2010) The maximum values are -5.46 ‰ and -36.51 ‰ (August 26 2011), respectively. As for the composite river water set (Figure 16), the δ^{18}O and δ^{2}H in SWM appear to be more enriched in ^{18}O and ^{2}H relative to NEM at all sampling sites.

δ^{18}O and δ^{2}H values for *groundwater* (Appendix 11) have the highest values for δ^{18}O and δ^{2}H of -6.41 ‰ and -38.58 ‰. The lowest values are -8.18 ‰ and -64.82 ‰, respectively. These end-members were recorded in May 30, 2010 and May 7, 2011. Overall the isotopic variations with time appear relatively minor (Figure 17), resembling the trend, albeit slightly depleted, for surface river waters.

Taking the river water seasonal isotopic trends (Figure 16) as the most representative dataset, it appears that the isotopic pattern appears to be related to the two monsoonal systems that control the local climate. Is this pattern a reflection of variations in precipitation and river flow amounts? Is there a relationship to seasonal temperatures or solar flux?

5.2.2 Seasonal variations in environmental variables for the Langat watershed.

The environmental variables potentially influencing the hydrology and the isotope signature of the Langat watershed are precipitation (Appendix 1), river flow/discharge (Appendix 3), temperature (Appendix 5) and global solar radiation, *GSR* (Appendix 13). Their temporal trends are summarized in Figure 18. The first order optical evaluation clearly shows that precipitation and discharge co-vary, both being larger during the NEM. Similarly, solar flux (*GSR*) and temperature co-vary, both declining in winter during the NEM.

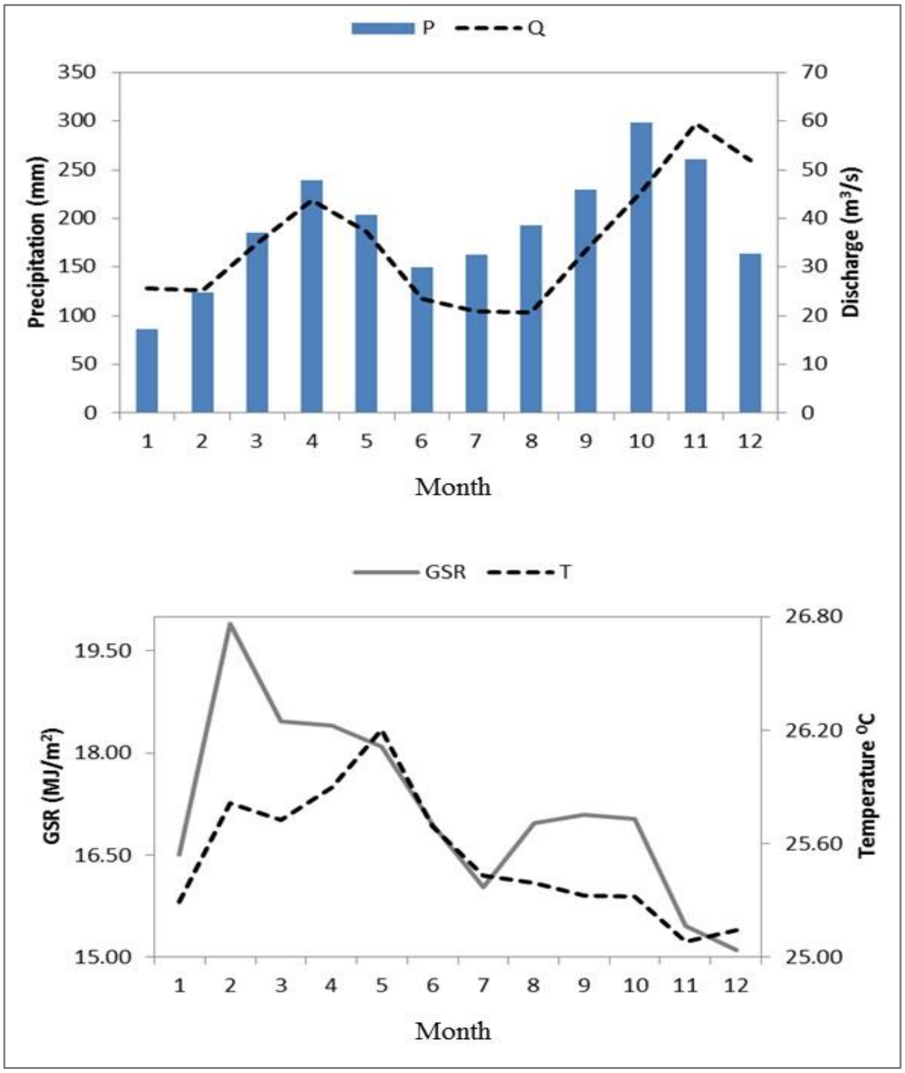

Figure 18: Seasonal trends of precipitation, discharge, Global Solar Radiation (*GSR*) and temperature for the Langat watershed.

5.3 Kelantan Watershed

5.3.1 Seasonal variation in isotope signals of the Kelantan waters

Similar to Langat watershed, the $\delta^{18}O$ variations for river water based on their median values (Figure 19) shows depleted signals during the NEM. *Rainfall* (Appendix 12) has the highest $\delta^{18}O$ and $\delta^{2}H$ values at -3.92 ‰ and -22.52 ‰, observed in June 24, 2011. The lowest values, -9.89 ‰ and -72.62 ‰, respectively, were observed on May 21, 2010. Similar to river waters, the $\delta^{18}O$ and $\delta^{2}H$ during the SWM are somewhat higher than during NEM (Figure 20).

The minimum *river water* values of $\delta^{18}O$ and $\delta^{2}H$, -11.01 ‰ and -79.84 ‰ and the maximum, -3.64 ‰ and -21.73 ‰ (Appendix 13), were observed on November 13, 2010 and November 12, 2011, respectively. The spread of $\delta^{18}O$ and $\delta^{2}H$ values during NEM was larger (~ -11 to ~ -3 ‰) than during SWM (~ -8 to ~ -5 ‰).

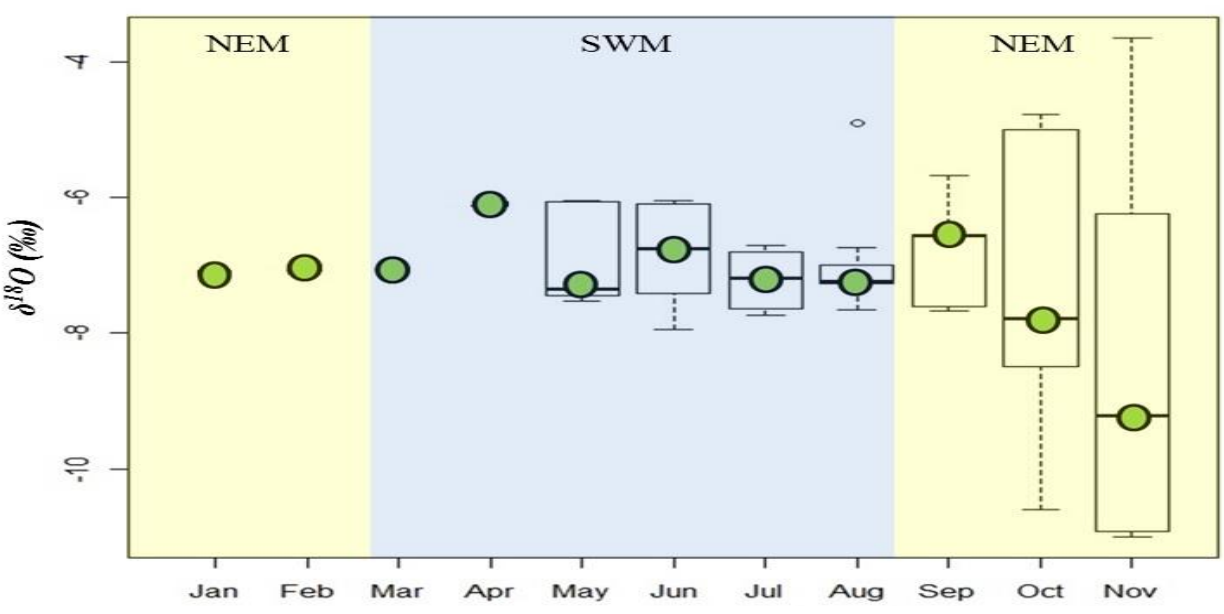

Figure 19: Seasonal variations of $\delta^{18}O$ for Kelantan River. Patterns as in Figure 15.

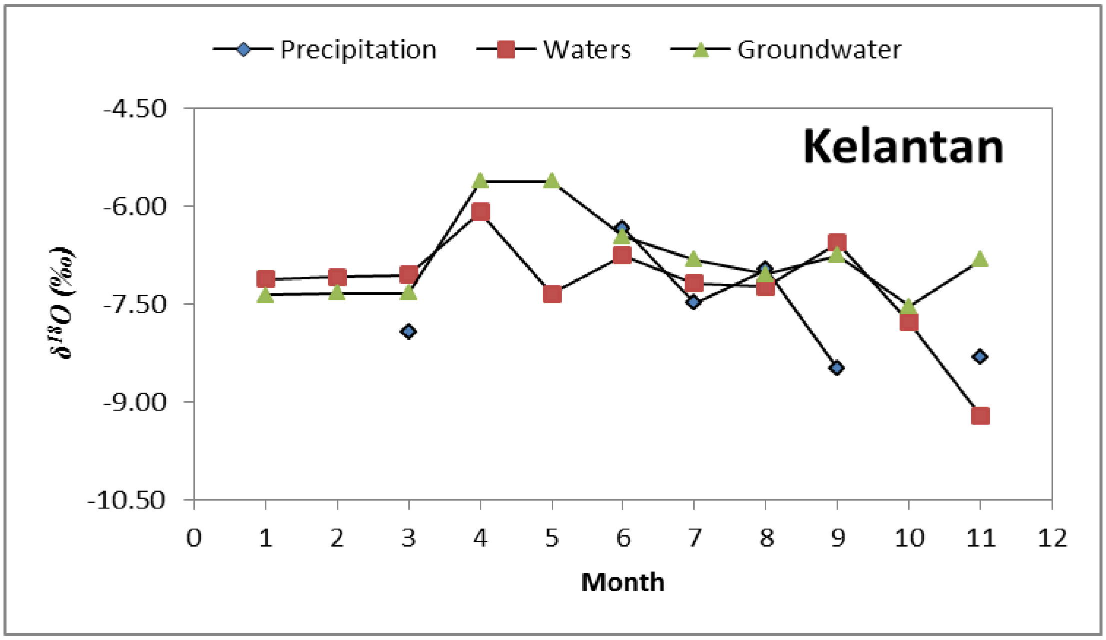

Figure 20: Monthly median δ^{18}O of precipitation, river waters and groundwater for the Kelantan watershed.

Maximum δ^{18}O and δ^{2}H values for the *groundwater* (Appendix 14) were -5.52 ‰ and -37.40 ‰ and the minimum -8.23 ‰ and -57.69 ‰, respectively. Overall, the isotopes of oxygen and deuterium in precipitation, groundwater and river water (Figure 20) yield a consistent temporal pattern with respect to monsoons, SWM and NEM.

5.3.2 Seasonal variations in environmental variables for the Kelantan watershed

Seasonal variations in precipitation (Appendix 3), discharge (Appendix 4), *GSR* (Appendix 6), temperature (Appendix 7) are summarized in Figure 21.

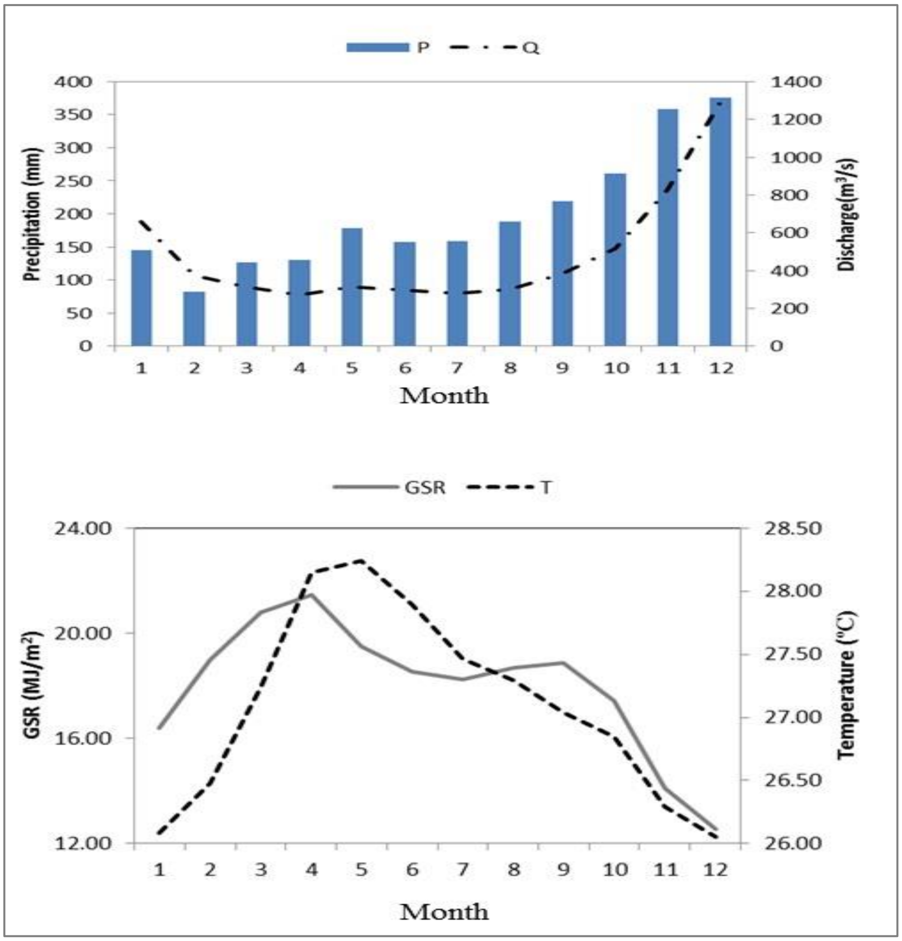

Figure 21: Seasonal trends of Precipitation, Discharge, Global Solar Radiation (*GSR*) and Temperature for Kelantan watershed.

5.4 Non-parametric Kendall's Tau statistical test

The Kendall's Tau statistics are employed for testing of potential *seasonal* inter-relationships among environmental variables and isotopic signal of river water. The Tau-b statistic [*Gibbons and Chakraborti, 2011*] determines a correlation of two non-parametric data samples with ties. The values of tau-b range from −1 to +1 for perfect inversion or agreement while zero indicates an absence of association.

The Kendall tau-B coefficient is defined as:

$$\tau_B = \frac{n_c - n_d}{(n_0 - n_1)(n_0 - n_2)}$$

(6)

where;

$n_0 = n(n-1)/2$
$n_1 = \sum_i t_i\ (t_i - 1)/2$
$n_2 = \sum_j u_j (u_j - 1)/2$
n_c = *Number of concordant pairs*
n_d = *Number of discordant pairs*
t_i = *Number of tied values in the* i^{th} *group of ties for the first quantity*
u_j = *Number of tied values in the* j^{th} *group of ties for the second quantity*

As expected (Table 6), global solar flux and temperature correlate at 95% confidence level in both watersheds (Figure 18, 21). For the Langat watershed, the $\delta^{18}O$ of river water is isotopically enriched during the summer SWM, coincident with the enhanced solar radiation. The evaporative effect of ~11% (Section 4.4) is likely the reason for this observed isotopic enrichment. The same covariance of *GSR* and temperature is evidence also in the Kelantan watershed (Table 6), but in this case inversely related with discharge, clearly a reflection of the winter NE monsoon as the source of moisture. This role of NEM and the negative correlation between *GSR* and *P* was a dominant feature controlling the hydrology in the watershed as far back as the available record (Figure 22), some three decades. As already used, the NEM is isotopically-depleted relative to SWM, a feature reflected in the inverse correlation with discharge for both precipitation and river water.

The overall seasonal variability, of hydrology and its isotopic characteristics are clearly controlled by solar flux (*GSR*) as the principal driver. This opens the following question: Is the stronger solar flux during SWM solely an outcome of higher incoming solar radiation or is it a measure of lesser cloud cover (and rain)? Considering that the *GSR* was measured at the surface below cloud cover, the latter alternative is the more likely explanation. Nevertheless, the possibility of temporal variations in intensity of incoming solar flux cannot be entirely discounted, since it was demonstrated in decadal and centennial archives for the Asian monsoonal system. While the records for environmental variables in the studied areas are available for only few decades, this perhaps may prove sufficient to answer the above/below clouds quandary.

Langat					
	δ^{18}O-P	*δ^{18}O-Q*	*P*	*Q*	*GSR*
δ^{18}O-Q	-0.2				
P	-0.3	0.3			
Q	0.1	-0.2	0.4		
GSR	0.1	**0.6**	0.1	-0.1	
Temperature	0.1	0.4	-0.1	-0.1	**0.5**

Kelantan					
	δ^{18}O-P	*δ^{18}O-Q*	*P*	*Q*	*GSR*
δ^{18}O-Q	-0.1				
P	-0.3	**-0.5**			
Q	**-0.6**	-0.4	**0.5**		
GSR	-0.1	**0.5**	**-0.5**	**-0.5**	
Temperature	**0.7**	0.2	-0.3	**-0.7**	**0.5**

Kendall's Tau test is significant at $p<0.05$ (bold)

Table 6: Summary of the Kendall`s Tau statistical test for stable isotopes, climate and hydrology for the Langat and Kelantan watersheds. δ^{18}O =Waters (‰), P=Rainfall (mm), Q=River discharge (m^3/s), GSR=Global Solar Radiation (MJ/m^2) and Temperature (ºC).

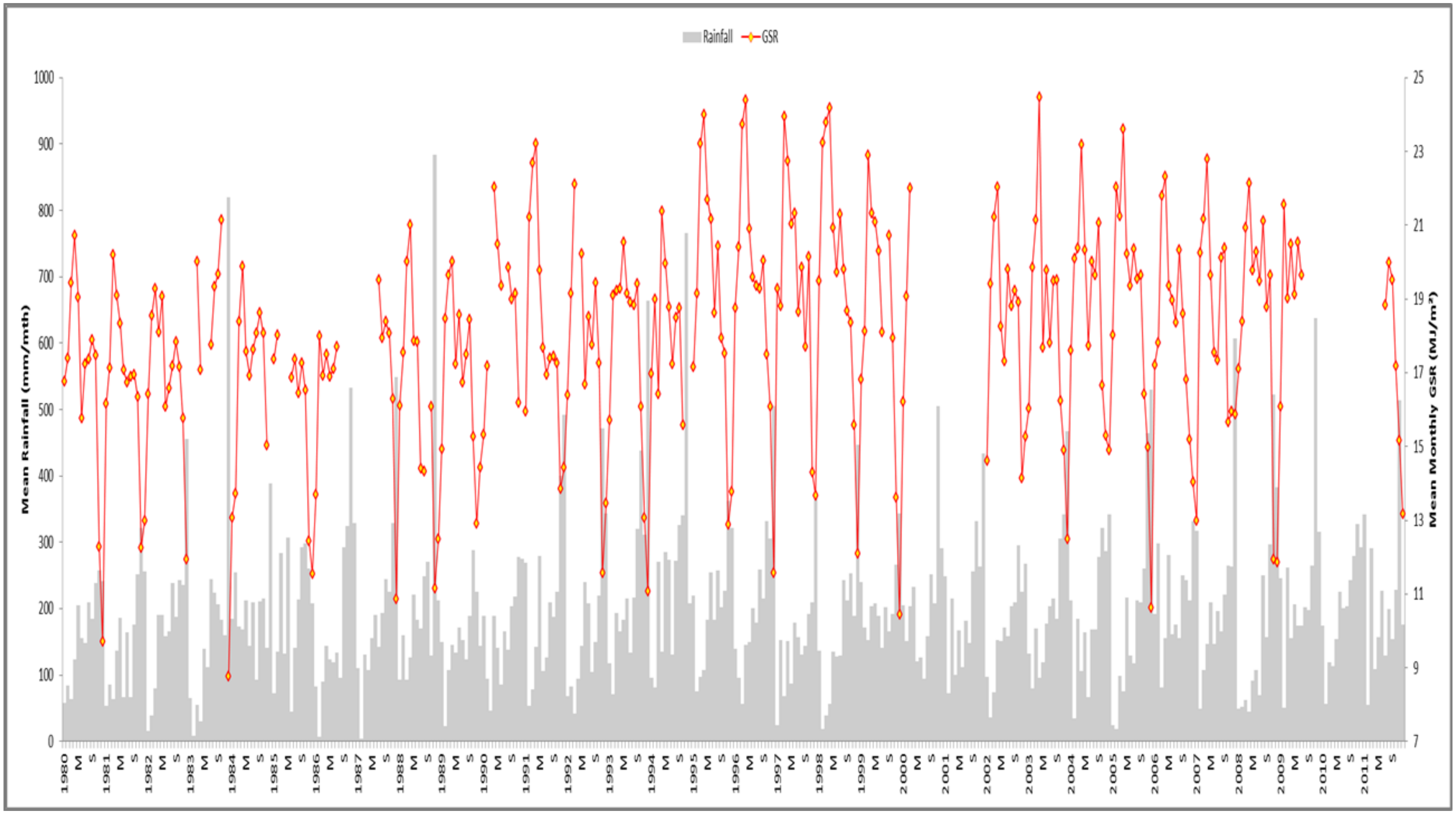

Figure 22: In Kelantan watershed GSR shows inverse seasonal (monthly) correlations of GSR and *P* (n=312, $p<0.05$). Data are listed in Appendices 2a and 8. As Peninsular Malaysia is a tropical maritime region, cloudiness may be considered as an important factor in discussing variations in incoming solar radiation. During the monsoon period, more precipitation, discharge, and more clouds result in less incoming solar radiation to the Earth's surface and thus colder temperatures.

5.5 Decadal environmental trends

High solar activity was correlated with higher precipitation over Arabia and India, resulting from the upwelling in the equatorial troposphere that produces a north-south seesaw of convective activity [*Kodera, 2004*]. As well, it is known that the 11 year (Schwabe) solar cycle may act to balance moisture across the world [*Wasko and Sharma, 2009*]. In China, solar variability was known to dominate variations in summer precipitation [*Zhao et al., 2012*]. These studies demonstrate the importance of solar forcing for the earth's climate [*Sud et al.,2002; Lambert et al., 2004; Meehl et al., 2009; Liu et al., 2009; Wasko and Sharma, 2009*], especially on regional precipitation trends on decadal time scales [*Zhao et al., 2012*]

Increase in solar flux, apart from enhancement of thermal energy input, may also results in more intense solar wind, which attenuates the incoming Cosmic Rays Flux (CRF) to the earth, diminishing the atmospheric ionization rate [*Ney, 1959; Svensmark, 1998*; *Dickenson, 1975; Harrison and Aplin, 2001; Eichkorn et al., 2002; Yu, 2002; Tinsley and Yu, 2003*], potentially resulting in less clouds, thus enhancing the planetary energy balance. The observed coincidence of hydrologic regimes across the world (ie: South Africa, Southeast Asian Monsoon and China) with records of past solar variability indicate a possible solar-climate connection [*Alexander, 2005; Bhattacharyya and Narasimha, 2005; Zhao et al., 2012*], with ENSO acting as a mediator between Sun and the Earth's climate on centennial to millennial timescales [*Emilea-Geay et al., 2007*].

In addition, during the El Nino period in the western part of the Pacific, including the Malaysian region, the atmospheric pressure increases and results in a relatively drier climate, especially during the SWM. Nevertheless, the variability of rainfall in Peninsular Malaysia (1976-2006) is not significantly affected [*Wong et al., 2009; MMD, 2009*]. For the period of NEM, dry north easterly wind becomes moist during the passage over the South China Sea and subsequently interacts with the land along the coastal area, developing deep convection clouds and resulting in rainfall [*Chang et al., 2005*]. Despite the overall high amount of rainfall across Peninsular Malaysia [*Wong et al., 2009*], it is the NEM that brings the highest mean rainfall to the east coast, more so than to the inland and west coast regions.

Evidence for such dynamic response to sun in the troposphere over longer, centennial and millennial, timescales is found in the sediment of Lake Naivasha, East Africa, with dry conditions pronounced during periods of high solar activity [*Verschuren et al.*, 2000], suggesting significant role of the ITCZ within variety of timescales [*Kodera*, 2004]. Displacement of the Hadley cell [*Haigh et al., 2005*] depends on the magnitude of solar radiation, which modulates rainfall across affected regions.

Given that Peninsular Malaysia is located near the equator and receives high solar radiation and rainfall intensity all year round, the specific mechanism that governs the Malaysian climate on decadal time scales can perhaps be elucidated. Should solar variability be the cause of cloudiness, by a scenario similar to the one described above, the measured *GSR* and the hydrological parameters would have to correlate with a measure of solar variability, such as the Solar Sunspot Number (*SSN*).

5.5.1 Solar Sunspots Number (SSN) and related statistics

Solar Sunspot Number (SSN) is the measure of solar intensity and the relevant dataset was obtained from the Solar Influence Data Analysis Centre (SIDC), Belgium (http://sidc.oma.be/aboutSIDC/). The sunspot index is based on visual observations of sunspots (Appendix 15). It consists of counting sunspots and groups of sunspots. The sunspot index determination is now based on statistical processing of observations from a worldwide network of about 80 stations, but the method used and numbers of available observations have varied over time [*Clette et al., 2007*].

The statistical evaluation of interrelationships among environmental trends and *SSN* on decadal time scales will be restricted to the Kelantan watershed because not all time series for the Langat basin cover the entire 30 years interval. The *SSN-GSR* for Kelantan is also limited to only 17 years of *GSR* data in the 1980-2011 time span. The statistical evaluation is based on the Tau statistical test described in section 5.4.

Kelantan	*SSN*	*GSR*	*T*	*P*
GSR	**-0.50**			
T	-0.11	**0.41**		
P	**-0.26**	0.13	-0.11	
Q	-0.19	0.12	**-0.28**	**0.44**

Kendall's Tau test is significant at p<0.05(bold)

Table 7: Decadal environmental trends for the Kelantan watershed.

The statistical evaluation (Table 7) shows that the Kelantan watershed *SSN* correlates negatively with *GSR* and *P* (Figure 23). Considering that the fragmentary *GSR* records spans only three eleven year (Schwabe) *SSN* cycles, the above τ statistics is not informative. For the continuous GSR stretches, such as the post 2000 cycle, there seems to be no clear variability with the declining *SSN*. If so, the observed *GSR* values are clearly a reflection of cloudiness and not of variability in incoming solar flux. In contrast to incomplete *GSR* series the precipitation data cover the entire 30 year interval suggest a weak tendency towards more precipitation during solar minima (Figure 23). In that case dynamical processes (ITCZ) must be the factor influencing the regional climate. Hence the seasonal monsoonal variations appear to be of regional nature, dominated by the ITCZ oscillation, with clouds muting the *GSR* and enhancing precipitation. On decadal time scales, there may exist a tentative relationship between hydrology and the 11 year solar cycle (Figure 23b).

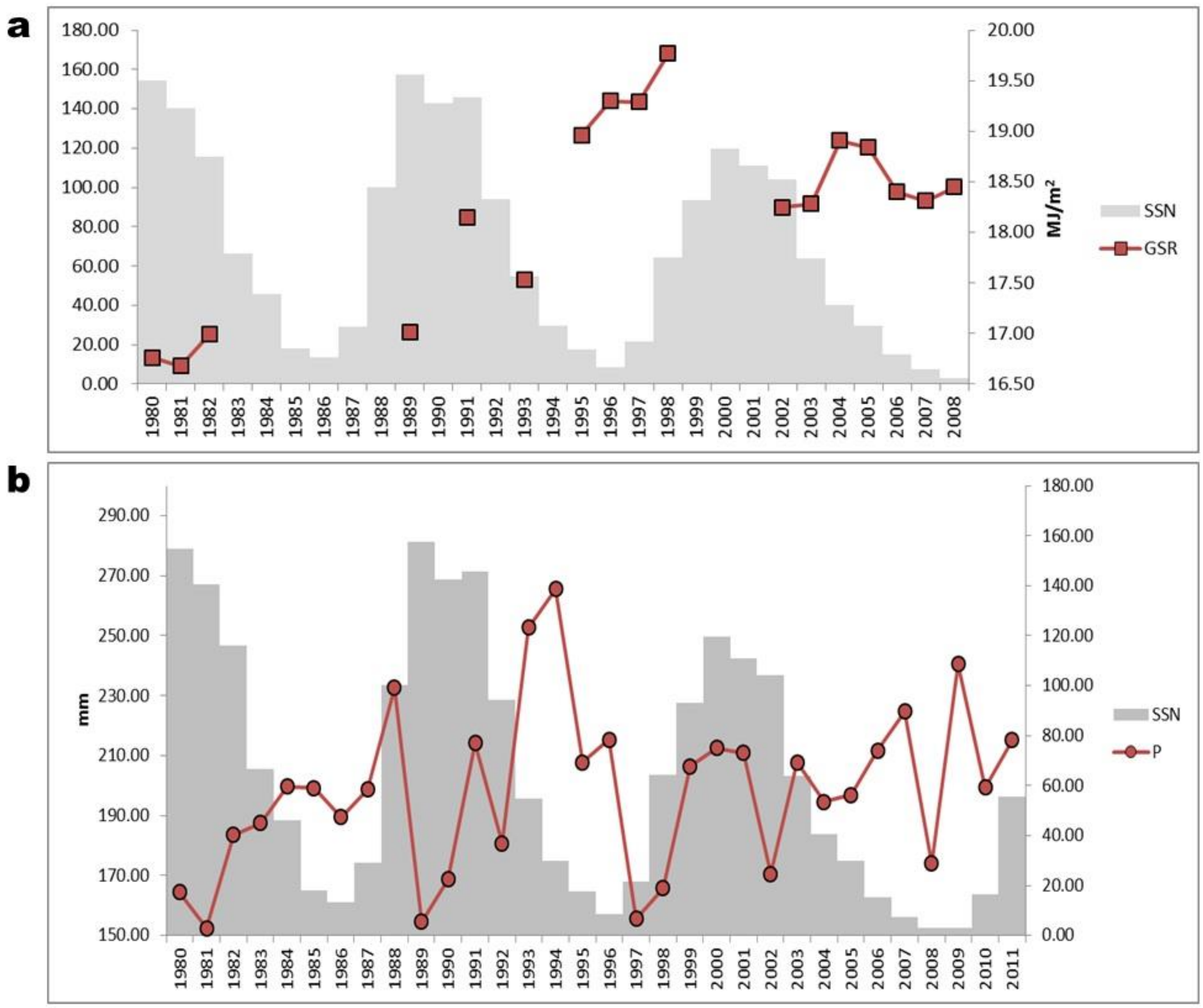

Figure 23: a) Inverse correlations of SSN-GSR (*n*= 17, p<0.05). b) Inverse trend of annual SSN (*n*=32) and annual amount of *P* (*n*=32), with lesser, but still statistically significant (τ= -0.26, *p*<0.05) relationship.

5.6 Summary

In both watersheds situated on the opposite sides of the Malaysian Peninsula, the hydrologic system and the hydrologic properties appear to be responding to seasonal monsoonal variations. The causative factor is apparently the seasonally differing solar energy flux over the broader region of south-eastern Asia. Given that the Malaysian peninsula is located at the near equatorial position, the local variability in the seasonal energy flux results mostly from an indirect impact, the variability in cloud coverage. Clouds, because of their strong albedo can reflect the solar energy back into space resulting in diminished *GSRs* at the surface, below cloud cover. This seasonal scenario affects also the local hydrologic cycle and its isotopic composition, with moisture associated with the summer SWM, being slightly isotopically heavier, likely due to an isotopically documented evaporation effect.

Chapter 6: Implications for Carbon Cycle

6.1 The energy, water and carbon cycles

The difference between annual water input by precipitation (*P*) and river discharge (*Q*) is a measure of total evapotranspiration (*ET*), the collective fluxes of water vapour from plants, soils, and water bodies. The *ET* for both Langat and Kelantan, watersheds appears to be the greatest component of terrestrial water cycle, and thus is a nexus for interplay of planetary energy and carbon cycles.

Long term observations show that *ET* was relatively stable with respect to variations in the long term annual rainfall in the Southeast Asian rainforests [*Kumagai et al., 2009; Kume et al., 2011*]. Since an increase in solar radiation enhances *ET* and photosynthetic capacity [*Tani et al., 2003; Goulden et al., 2004; Saleska et al., 2007*], the ability of tropical forests to maintain stable *ET* during dry seasons is attributed to deep root systems [*Oliveira et al., 2005; Bruno et al., 2006*]. If this is so, what would be the mechanism that maintains *ET*?

The isotope-based technique employed here can be used to constraint not only water budget but also carbon fluxes, an approach applied previously to large watersheds (Table 8) in North America, South America, Africa, Australia and New Guinea [*Telmer and Veizer, 2000; Lee and Veizer, 2003; Ferguson et al. 2007; Freitag et al., 2008 ; Karim et al., 2008 and Brunet et al., 2009*] (see also *Schulte et al., 2011* and *Jasechko et al., 2013*).

Watersheds	Water input by precipitation LMWL	Discharge at downstream river LEL	Location	
Southeast Asia				
Langat	$\delta^2H = 7.7 \pm 0.4\ \delta^{18}O + 6.3$	$\delta^2H = 6.6 \pm 0.3\ \delta^{18}O - 1.5$	West coast, Peninsular Malaysia	
Kelantan	$\delta^2H = 7.8 \pm 0.5\ \delta^{18}O + 7.1$	$\delta^2H = 7.8 \pm 0.2\ \delta^{18}O + 7.5$	East coast, Peninsular Malaysia	
Ok Tedi	$\delta^2H = 8.2 \pm 0.1\ \delta^{18}O + 11.8$	$\delta^2H = 6.7 \pm 0.8\ \delta^{18}O - 1.1$	Konkoda, Papua New Guinea	[*Ferguson and Veizer, 2007*]
Upper Fly	$\delta^2H = 8.2 \pm 0.1\ \delta^{18}O + 11.8$	$\delta^2H = 7.3 \pm 0.8\ \delta^{18}O + 3.3$	Kiunga, Papua New Guinea	[*Ferguson and Veizer, 2007*]
Africa				
Bani	$\delta^2H = 6.2 \pm 0.6\ \delta^{18}O - 0.4$	$\delta^2H = 4.3 \pm 0.3\ \delta^{18}O - 6.2$	Douna, Burkina Faso	[*after Feguson and Veizer, 2007]*
Upper Niger	$\delta^2H = 6.2 \pm 0.6\ \delta^{18}O - 0.4$	$\delta^2H = 4.8 \pm 0.2\ \delta^{18}O - 4.1$	Banankoro,Guinea	[*after Feguson and Veizer, 2007]*
Black Volta	$\delta^2H = 6.1 \pm 0.8\ \delta^{18}O - 0.6$	$\delta^2H = 4.7 \pm 0.7\ \delta^{18}O - 7.1$	Bondouku, Ivory Coast	[*Freitag et.al., 2007*]
White Volta	$\delta^2H = 6.1 \pm 0.8\ \delta^{18}O - 0.6$	$\delta^2H = 4.8 \pm 0.9\ \delta^{18}O - 6.0$	Tamale, Ghana	[*Freitag et.al., 2007*]
Oti	$\delta^2H = 6.1 \pm 0.8\ \delta^{18}O - 0.6$	$\delta^2H = 4.9 \pm 0.7\ \delta^{18}O + 6.3$	Sokode, Togo	[*Freitag et.al., 2007*]
Nyong	$\delta^2H = 8.1 \pm 0.2\ \delta^{18}O + 10.9$	$\delta^2H = 7.7 \pm 1.1\ \delta^{18}O + 7.7$	Dehane, Cameroon	[*after Feguson and Veizer, 2007*]
South America				
Piracicaba	$\delta^2H = 9.1 \pm 1.3\ \delta^{18}O + 16.7$	$\delta^2H = 6.3 \pm 0.6\ \delta^{18}O - 0.9$	Artemis, Brazil	[*Martinelli et.al., 2004*]

Table 8: Local Meteoric Water Line (LMWL) and Local Evaporation Line (LEL) in tropical and sub-tropical watersheds. Modified from *Ferguson and Veizer* [*2007*].

In Peninsular Malaysia, the *ET* flux accounts for around ~50-70% of the incoming precipitation *P*. In section 4.4 we used stable isotopes of oxygen and hydrogen to partitioning the flux of water due to plant transpiration from the direct evaporative flux from soils, water bodies and plant. Our results showed that *T* comprises 80% of *ET*, while E_d represented only a small portion in terms of volumetric significance, up to ~11%.

The causative factor is apparently the seasonally differing solar energy flux over the broader region of south-eastern Asia. Given that the Malaysian peninsula is located at near equatorial position, the local variability in the seasonal energy flux results mostly from an indirect impact, the variability in cloud coverage.

The high values of *T* in the Langat (1030±103 mm yr^{-1}) and Kelantan (1019±102 mm yr^{-1}) water budgets reflect that water is an essential component of the biological web. Solar radiation, temperature and water availability are essential for the Net Primary Productivity

(*NPP*) and hence the plant growth [*Nemani et al., 2002*]. In the extratropics [*Ferguson and Veizer, 2007*], the *NPP* clearly declines with lower rainfall whereas the correlations with air temperature are marginal at best [*Lee and Veizer, 2003*]. In the tropics, by comparison, the intensity of solar radiation appear to be the limiting factor of photosynthesis, regionally such as in Peninsular Malaysia [*Tani et al., 2003; Kumagai et al., 2004*] and globally [*Myneni et al., 2007*].

On a global scale, the annual photosynthesis/respiration flux of C is about 120 Pg [*Denman et al., 2007*], most of it in the tropics where it is driven by the photosynthetically active solar radiation (PAR) [*Myneni et al., 2007*]. Note, that the carbon intake during the photosynthesis is regulated by stomata in order to maximize the carbon gain per unit of water loss [*Frank and Beerling, 2009*; *Katul et al., 2010*; *de Boer et al., 2011*]. Thus transpiration (*T*) reflects the *NPP* [*Lee and Veizer, 2003*]. The theoretical upper limit for biological transformation of solar light energy (photons) to chemical energy is 11%, but natural ecosystems operate mostly with 3-6% efficiency [*Miyamoto, 1997*].

Our estimates show that about 40-50% of *P* in Peninsular Malaysia was transferred to the atmosphere as water vapour via *T*. Estimated *T(s)* in the Langat and Kelantan watersheds are consistent with *T(s)* in other tropical regions (Table 9). Such large *T* reflects the efficiency of nutrients recycling through plant biomass, resulting in high primary productivity of tropical rainforests. Considering that the tropics have abundant water [*Tani et al., 2003*], its availability does not represent a rate-limiting factor for plant growth.

In our study, the amount of *P* in Langat and Kelantan watersheds is considerably smaller than at Ok Tedi and Upper Fly in New Guinea (Table 9), yet their *T* still reaches the tropical plateau (Figure 34), suggesting that the system is solar radiation limited [*Tani et al., 2003; Kumagai et al., 2004; Huete et al., 2006; Mynenei et al., 2007*].

	Annual Values (mm or 10^3 g H_2O m^{-2} yr^{-1})				
Watersheds	*P*	*Q*	I_n	E_d	*T*
Southeast Asia					
Langat	2145	703	176	236	1030
Kelantan	2383	1080	284	0	1019
Ok Tedi	7056	4583	1129	344	1000
Upper Fly	6540	4032	961	324	1223
Africa					
Bani	1068	100	192	82	694
Upper Niger	1545	488	268	60	729
Black Volta	955	60	166	111	618
White Volta	969	85	107	140	641
Oti	970	189	110	131	540
Nyong	1835	527	178	0	1130
South America					
Piracicaba	1468	355	202	27	979

P,*precipitation; Q, river runoff;*
I_n,*Interception;* E_d, *Evaporation; T, transpiration*

Table 9: Components of annual water balances for the watersheds in tropical region; Southeast Asia, Africa and South America. Modified from *Ferguson and Veizer* [*2007*]

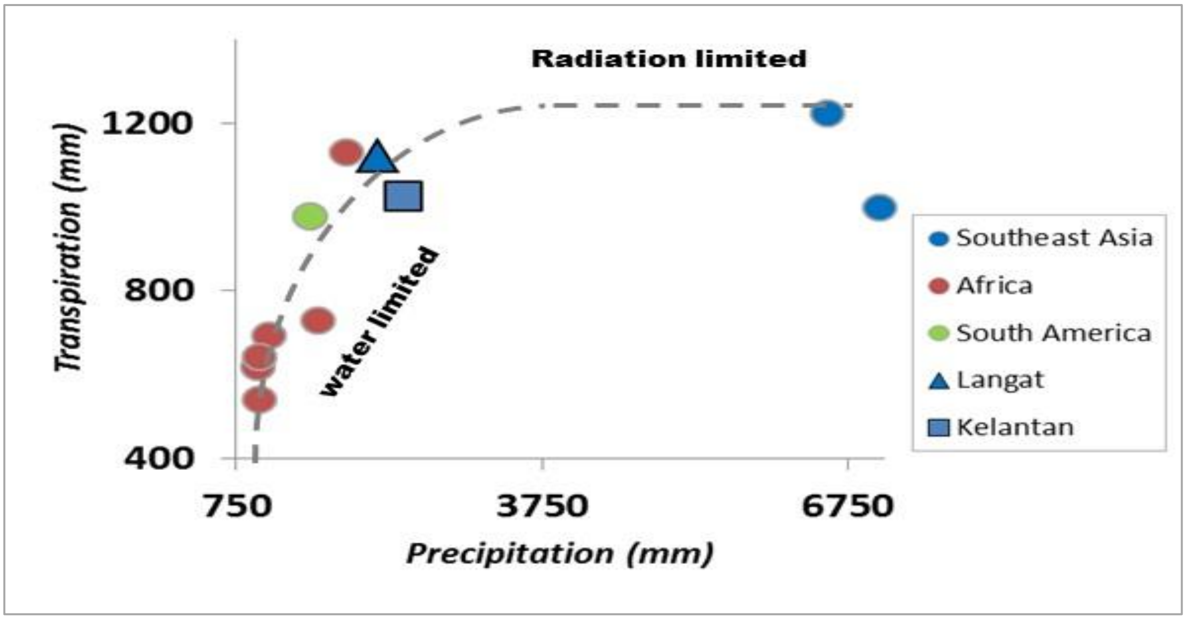

Figure 24: Cross-plot of transpiration (*T*) versus precipitation (*P*) in tropical and sub-tropical regions. Modified after *Ferguson and Veizer* [*2007*] and see also Figure 2.

In this understanding, enhanced solar activity will result in elevation of the *T* plateau and invigoration of the water cycle and the entire pattern in Figure 24 will shift up and to the right. A decline in PAR results in an opposite shift. The coupled water - carbon system thus oscillates in phase with solar activity. The Net Primary Productivity (*NPP*) is expressed in units of g C m^{-2} yr^{-1} where 1 mm of *T* represents 10^3 g H_2O m^{-2} yr^{-1}. The fixation of atmospheric CO_2 as organic C is proportional to the *T* flux by the Water Use Efficiency (WUE) factor, with an average value of 1 molecule of C per 500 or 250 molecules of H_2O for C3 and C4 plants, respectively [*Taiz and Zeiger*, *2006*]. Given that the estimated *T* for the Langat watershed relates to steady state condition on annual basis, and the plants are almost exclusively of C3 type, the long term WUE of 500 has been utilized for calculation of the *NPP*, giving the carbon fixation amount for Langat and Kelantan are 1373±137 g C m^{-2} yr^{-1} and 1359±136 g C m^{-2} yr^{-1}, respectively.

Interpolating for the entire watersheds, the transpiration fluxes of water for Langat (~5.7 x 10^4 mol H_2O m^{-2} yr^{-1}) and Kelantan (~5.66 x 10^4 mol H_2O m^{-2} yr^{-1}) are far larger than the respective carbon intakes; ~1.14 x 10^2 mol CO_2 m^{-2}yr-^{1} and ~1.13 x 10^2 mol CO_2 $m^{-2}yr^{-1}$. Considering that only about 2% of this carbon is exported to the ocean by the rivers [*Lee et al., 2013*; *Lee, 2013*], the remaining 98% must be re-exported to the atmosphere by respiration, demonstrating the importance of interplay of water and biology for the global carbon cycle.

As pointed out by [*Jasechko et al., 2013*], the flux *T* appropriates about half of all solar energy absorbed by the continents. Yet, the efficiency of photosynthesis is only some 3-6% [*Miyamoto, 1997*]. The bulk of this energy is therefore required not for the photosynthesis itself, but for the continuous pumping of water that delivers food (nutrients) to the plant, thus emphasizing the role of water cycle as a "conveyor belt" essential for nutrient transport in terrestrial ecosystems [*Syakir et al., 2014*]

Chapter 7: Hydrology and river chemistry

Peninsular Malaysia is a tropical region with high annual rainfall (> 2000 mm), dense vegetation and rich soils with potentially strong influence on the chemistry of water. Most natural water constituents are derived from weathering, atmospheric input, and anthropogenic sources. Historically, rivers play a critical role in urbanization as they provide an easy access to water resources and serve as the main course for transportation. Population growth, economic progress and technological advancement are the main factors that drive the urban dynamics [*Lyon and Harmon, 2012*]. Cities demand an immense amount of energy for their growth and expansion, impeding the environmental quality of air, soil and water, and affecting fate and transport of elements in the system.

Urban atmospheres contain gases and particles from vehicle exhaust, industrial emissions and dust that enter the urban hydrologic cycle by wet (dissolved in precipitation) and dry (particle and vapor) deposition [*Albanese and Cicchella, 2012*]. Atmospheric deposits include HNO_3, H_2SO_4, metals (e.g. Cd, Hg, Ni, Pb) and industrial organic compounds (polycyclic aromatic hydrocarbons (PAHs)).

Stormwater runoff contains a variety of constituents leached from the urban environment (e.g. atmosphere, roads, parking lots, buildings). Moreover, urban runoff can have elevated turbidity and high concentration of suspended sediments, nutrients, bacteria, metals (commonly Cu, Fe, Pb, Zn), pesticides and herbicides that all can degrade the quality of surface water and groundwater [*Wong et al., 2012*]. Furthermore, fertilizers, pesticides and herbicides are not only applied in agriculture but also to green areas such as gardens and golf courses, resulting in substantial loading of nutrients and organic pollutants to surface water. The leakage, direct discharge, or land application (i.e. irrigation) of treated wastewater all can degrade water quality. Waters receiving treated wastewater [*Wong et al., 2012*] can have also increased concentrations of constituents that are used in water treatment process, such as Cl (product of chlorination), Na and K (exchange ions in water softeners), or those that are in detergents (Ca, SO_4).

Given that water cycle permeates the entire biosphere, any pollutants in the system are inevitably introduced into the water cycle, ultimately resulting in water quality deterioration. In order to understand how seasonal hydrological parameters are reflecting the interplay of geogenic factors and anthropogenic pollution on water quality and transport of constituent from land to sea, the same samples that were measured for isotopes have been tested for their dissolved load, that is major ions contents. The data are evaluated by statistical techniques, the Correlation and the Principal Component Analysis (PCA).

7.1 Analytical procedures and results

The concentration of cations in water samples were analyzed by Inductively Coupled Plasma Atomic Emission Spectroscopy (ICP-AES) with precision of ±5% and accuracies of ±15%. The concentrations of anions were analyzed by Ion Chromatography (Dionex DX-100) with precisions better than 17% at the 0.1 ppm level. Samples were measured in 5 ml volumes following acidification to 1% with HNO_3 for cation analyses. Overall, up to 196 and 106 samples were analyzed for the Langat and Kelantan watersheds, respectively. The results are listed in Appendices 16-19.

7.2 Major ion chemistry of Langat watershed

The concentrations of major cations (Ca^{2+}, K^{+}, Mg^{2+}, Na^{+}) and anions (Cl^{-}, SO_4^{-}, NO_3^{-}) in Langat River and groundwater, together with measurement (in-situ) of *pH* are listed in Appendix 16 and 17 respectively. Concentrations of HCO_3^{-} were provided by *Lee* [*2013*] based on indirect measurement of dissolve inorganic carbon (DIC) in laboratory. The charge balance for the Langat River (Table 10) shows that 50% of the data falls within 5% charge-balance neutrality (Figure 24). For the groundwater, the missing values for anions result in a significant deviation from equality, with only 30% of major ions satisfying the electroneutrality condition. The mean concentrations of dissolved ions and the average pH values of Langat waters are summarized in Table 11.

For *river water*, Na^{+} was the dominant cation comprising approximately 40% of all cations on a molar basis (Table 11). The concentrations of K^{+}, Ca^{2+} and Mg^{2+} decreased in the order 31%, 25% and 4%, respectively. HCO_3^{-}, the dominant anion, representing approximately 48% of total, is followed by Cl^{-} (36%), SO_4^{2-} (10%) and NO_3^{-} (6%). In *groundwater*, the dominant cation, at 52%, is Na^{+}, followed by K^{+} (27%), Ca^{2+} (17%) and Mg (5%), while dominant anion is Cl^{-} at 46%, followed by HCO_3^{-} (37%), SO_4^{2-} (10%) and NO_3^{-} (7%).

	Ca^{2+}	K^{+}	Mg^{2+}	Na^{+}	Cl-	$SO4^{2-}$	NO^{3-}	HCO^{3-}	ΣCation	ΣAnion
				µeq/L					µeq/L	
Langat	43701	23030	7715	29325	33507	15798	5001	41627	103771	95934
Langat Groundwater	3107	7862	879	10837	6647	2979	1055	4900	22684	15580

HCO_3 for Langat waters was obtained from [Kern Lee, 2013]

Table 10: Summary of the electroneutrality condition for major ions of samples collected monthly, from May 2010 to December 2011 in the Langat watershed.

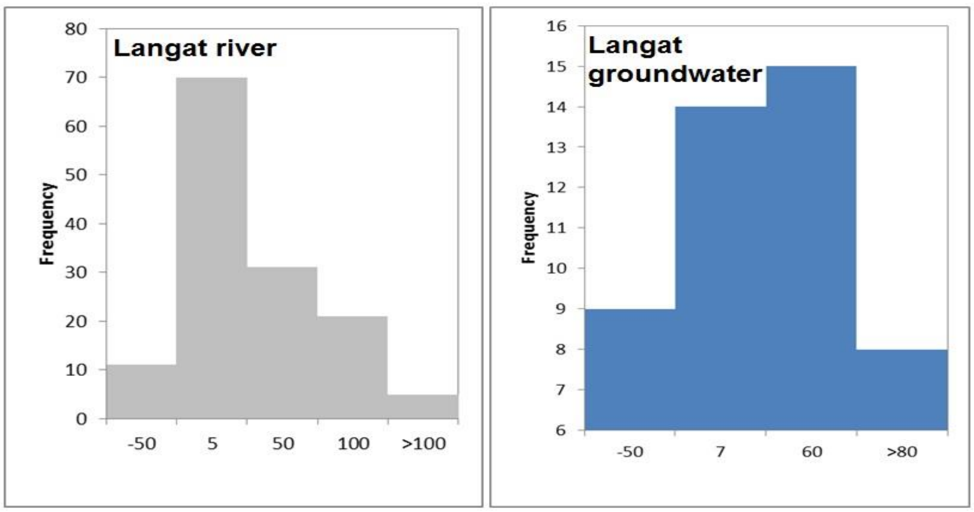

$$\frac{\Sigma cation - \Sigma anion}{\Sigma cation + \Sigma anion}(\%)$$

Figure 25: Error distributions for major ions in the Langat watershed

Rivers (all stations)	Ca^{2+}	K^{+}	Mg^{2+}	Na^{+}	$Cl-$	SO_4^{2-}	NO_3^-	HCO_3^-	pH
	μM								
Mean	164.56	202.21	28.50	260.91	302.89	84.86	68.61	340.26	6.82
Standard Error	9.11	39.26	0.91	38.36	28.53	8.13	6.35	22.13	0.03
Standard Deviation	111.62	480.82	11.14	469.77	312.50	89.08	57.83	261.90	0.38
Sample Size (n)	150	150	150	150	120	119	83	140	140
Confidence Level (95%)	18.01	77.58	1.80	75.79	56.49	16.10	12.63	43.76	0.06
Groundwater	Ca^{2+}	K^{+}	Mg^{2+}	Na^{+}	$Cl-$	SO_4^{2-}	NO_3^-	HCO_3^-	pH
	μM								
Mean	33.93	55.70	9.62	106.30	221.55	49.65	95.92	154.48	6.25
Standard Error	5.47	8.65	0.53	13.06	51.51	11.10	25.84	19.55	0.07
Standard Deviation	37.07	58.70	3.62	88.55	282.12	60.81	85.71	115.68	0.41
Sample Size (n)	46	46	46	46	30	30	11	35	35
Confidence Level (95%)	11.01	17.43	1.08	26.30	105.35	22.71	57.58	39.74	0.14
Pongsun	Ca^{2+}	K^{+}	Mg^{2+}	Na^{+}	$Cl-$	SO_4^{2-}	NO_3^-	HCO_3^-	pH
	μM								
Mean	58.06	79.21	28.46	90.22	238.77	73.13	87.01	173.50	6.80
Standard Error	5.26	16.97	1.53	5.94	52.26	10.92	16.63	12.36	0.07
Standard Deviation	31.97	103.25	9.33	36.15	286.23	59.82	70.56	73.10	0.43
Sample Size (n)	37	37	37	37	30	30	18	35	35
Confidence Level (95%)	10.66	34.43	3.11	12.05	106.88	22.34	35.09	25.11	0.15
Kajang	Ca^{2+}	K^{+}	Mg^{2+}	Na^{+}	$Cl-$	SO_4^{2-}	NO_3^-	HCO_3^-	pH
	μM								
Mean	264.60	226.32	29.98	298.24	418.47	138.00	81.64	536.62	6.87
Standard Error	18.78	30.45	2.04	24.66	58.78	29.99	13.95	55.36	0.04
Standard Deviation	111.82	183.94	12.08	153.93	311.03	34.42	64.76	332.14	0.25
Sample Size (n)	37	37	37	37	28	25	22	36	36
Confidence Level (95%)	37.28	61.33	4.03	51.32	120.60	14.21	28.71	112.38	0.09
Dengkil	Ca^{2+}	K^{+}	Mg^{2+}	Na^{+}	$Cl-$	SO_4^{2-}	NO_3^-	HCO_3^-	pH
	μM								
Mean	214.81	174.55	31.96	273.33	303.65	70.92	66.90	406.72	6.82
Standard Error	14.38	34.94	1.94	21.57	60.02	8.23	12.23	43.40	0.07
Standard Deviation	112.68	182.69	12.24	147.98	311.03	155.85	63.92	256.74	0.39
Sample Size (n)	36	36	36	36	28	27	21	35	35
Confidence Level (95%)	38.13	61.81	4.14	50.07	120.60	61.65	29.09	88.19	0.13
Semenyih	Ca^{2+}	K^{+}	Mg^{2+}	Na^{+}	$Cl-$	SO_4^{2-}	NO_3^-	HCO_3^-	pH
	μM								
Mean	115.03	181.64	23.09	224.90	258.32	66.47	47.13	235.59	6.80
Standard Error	18.78	30.45	2.04	24.66	58.78	29.99	13.95	17.95	0.07
Standard Deviation	112.68	182.69	12.24	147.98	311.03	155.85	63.92	104.67	0.43
Sample Size (n)	36	36	36	36	28	27	21	34	34
Confidence Level (95%)	38.13	61.81	4.14	50.07	120.60	61.65	29.09	36.52	0.15

Table 11: Summary of statistical parameters for concentrations of major ions and pH collected at monthly sampling sites from May 2010 to December 2011.

7.3 Major ions chemistry of Kelantan watershed

The concentrations of major cations (Ca^{2+}, K^{+}, Mg^{2+}, Na^{+}) and anions (Cl^{-}, SO_4^{-}, NO_3^{-}) in Kelantan River and groundwater are listed in Appendix 18. The charge balances for the *river waters* and *groundwater* (Table 12) are incomplete and only 33% and 20% of samples fall within the 0-5% error, respectively (Figure 26). The negative imbalances in electroneutrality are due to missing values in the datasets, mostly because the estimated HCO_3^- values were based on bulk annual pH (2005-2011) that were provided by the Department of Environment Malaysia (Appendix 19). The mean concentrations of dissolved ions and average pH values of the Kelantan waters are summarized in Table 13.

	Ca^{2+}	K^{+}	Mg^{2+}	Na^{+}	Cl-	$SO4^{2-}$	NO^{3-}	HCO^{3-}	ΣCation	ΣAnion
				μeq/L					μeq/L	
Kelantan	9361	8225	3415	13818	7298	517	3555	28440	34819	39810
Kelantan Groundwater	3294	1713	1471	8036	3457	1314	1655	17385	14514	23812

HCO_3 in Kelantan was obtained from [Kern Lee, 2013]and is based on bulk pH values of all seasons

Table 12: Summary of the electroneutrality condition of major ions for samples collected monthly, from May 2010 to October 2011 in the Kelantan watershed.

Rivers (all stations)	Ca^{2+}	K^{+}	Mg^{2+}	Na^{+}	Cl-	SO_4^{2-}	NO_3^-	HCO_3^-	pH
	µM								
Mean	115.98	99.38	41.53	164.82	115.71	7.30	56.87	363.82	6.87
Standard Error	5.12	30.25	1.67	13.58	35.44	0.63	7.34	32.91	0.01
Standard Deviation	45.82	272.27	15.04	122.21	302.78	5.07	56.35	303.45	0.14
Sample Size (*n*)	80	81	81	81	73	64	59	85	85
Confidence Level (95%)	10.20	60.20	3.33	27.02	70.64	1.27	14.69	65.45	0.03
Groundwater	Ca^{2+}	K^{+}	Mg^{2+}	Na^{+}	Cl-	SO_4^{2-}	NO_3^-	HCO_3^-	pH
	µM								
Mean	63.35	213.29	28.28	309.08	304.92	25.27	91.97	861.31	6.88
Standard Error	7.75	104.91	3.05	26.00	118.53	5.53	16.22	81.00	0.03
Standard Deviation	39.49	534.92	15.53	132.56	604.40	28.21	68.81	436.22	0.14
Sample Size (*n*)	26	26	26	26	26	26	18	29	29
Confidence Level (95%)	15.95	216.06	6.27	53.54	244.12	11.40	34.22	165.93	0.05
Tanah Merah	Ca^{2+}	K^{+}	Mg^{2+}	Na^{+}	Cl-	SO_4^{2-}	NO_3^-	HCO_3^-	pH
	µM								
Mean	121.31	100.70	44.86	192.72	126.22	6.38	71.98	342.79	6.87
Standard Error	8.52	39.53	2.65	26.22	49.06	1.16	14.66	47.76	0.03
Standard Deviation	46.69	216.52	14.49	143.62	245.31	5.54	65.55	278.46	0.14
Sample Size (*n*)	30	30	30	30	25	23	20	34	31
Confidence Level (95%)	17.44	80.85	5.41	53.63	101.26	2.40	30.68	97.16	0.05
Pasir Mas	Ca^{2+}	K^{+}	Mg^{2+}	Na^{+}	Cl-	SO_4^{2-}	NO_3^-	HCO_3^-	pH
	µM								
Mean	115.75	131.21	40.51	130.85	145.98	8.67	44.14	467.05	6.90
Standard Error	6.71	71.74	2.43	11.86	84.53	1.02	9.96	99.81	0.02
Standard Deviation	36.12	392.95	13.34	64.96	439.25	5.19	43.42	446.34	0.14
Sample Size (*n*)	29	30	30	30	27	26	19	20	34
Confidence Level (95%)	13.74	146.73	4.98	24.26	173.76	2.10	20.93	208.89	0.05
River View	Ca^{2+}	K^{+}	Mg^{2+}	Na^{+}	Cl-	SO_4^{2-}	NO_3^-	HCO_3^-	pH
	µM								
Mean	108.10	48.25	37.88	175.54	61.00	5.93	53.86	320.27	6.80
Standard Error	12.98	5.07	4.04	32.96	11.72	0.91	12.65	34.45	0.02
Standard Deviation	58.03	22.69	18.08	147.41	52.42	3.40	56.57	191.83	0.09
Sample Size (*n*)	20	20	20	20	20	14	20	31	20
Confidence Level (95%)	27.16	10.62	8.46	68.99	24.53	1.96	26.47	70.36	0.04

Table 13: Summary of statistical parameters of concentrations of major ions in waters of the Kelantan watershed collected monthly, from May 2010 to October 2011.

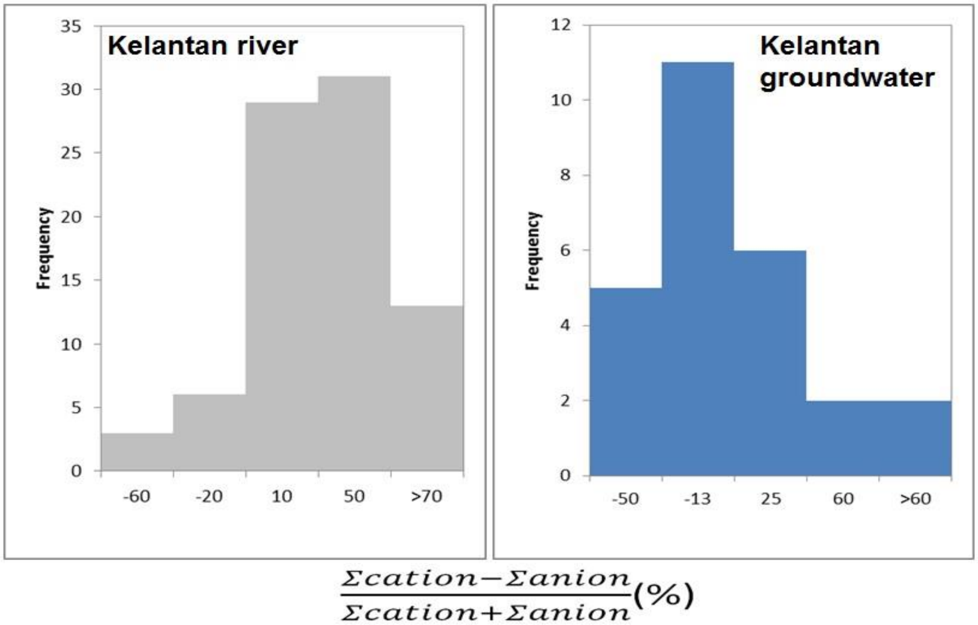

Figure 26: Error distributions for major ions in the Kelantan watershed.

For *river water*, Na^{+} was the dominant cation, accounting for ~40% of all cations on molar basis. The concentrations of Ca^{2+}, K^{+} and Mg^{2+} accounted for 27%, 24% and 10%, respectively. HCO_3^{-} was again the dominant anion in river water [*Lee, 2013*], accounting for 71% of total anions, followed by Cl^{-} (20%), NO_3^{-} (8%) and SO_4^{2-} (1%). In *groundwater*, Na^{+} is the dominant cation (50%) followed by K^{+} (35%), Ca^{2+} (10%) and Mg^{2+} (5%). HCO_3^{-} was the dominant anion, at 71%, followed by Cl^{-} (23%), NO_3^{-} (5%) and SO_4^{2-} (2%).

7.4 *Regional Variations*

7.4.1 Langat watershed

Kajang, the urban location, has the highest average concentrations of Ca^{2+}, K^{+}, Na^{+}, *Cl-*, and SO^{2-}. The downstream Dengkil is marked by the highest value of Mg^{2+}, while the groundwater (GW) contains the highest NO_3^-. *pH* values for river water and groundwater samples during this period were slightly acidic, at 6.82 to 6.25.

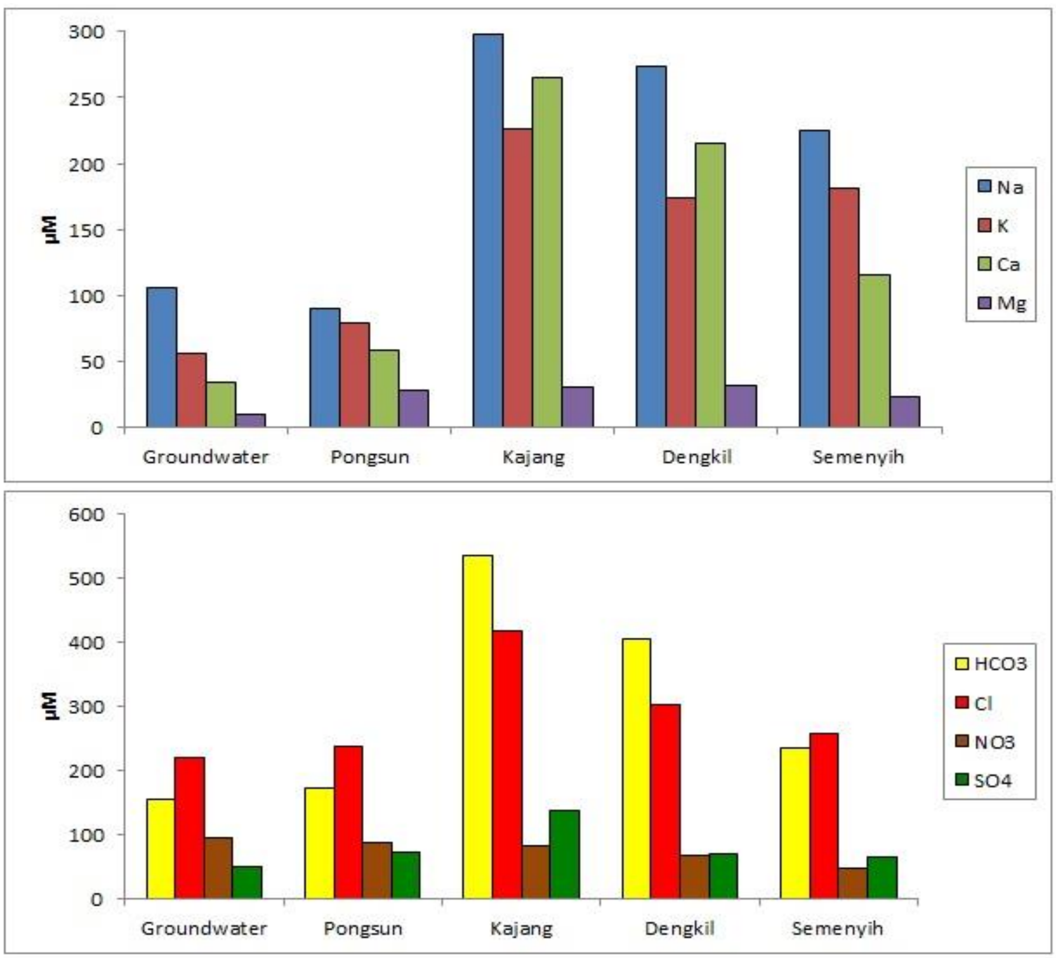

Figure 27: Spatial variations (average values) of major ions in the Langat watershed.

7.4.2 Kelantan watershed

Considering that all sampling stations are from the downriver section, the *regional variability* in major ion chemistry is to be expected minimal, albeit more dilute than in local groundwaters (Figure 28). The highest average concentrations for Ca^{2+}, Mg^{2+}, Na^{+} and NO_3^{-} were observed at Tanah Merah and for K^{+}, Cl^{-} and SO_4^{2-} at Pasir Mas.

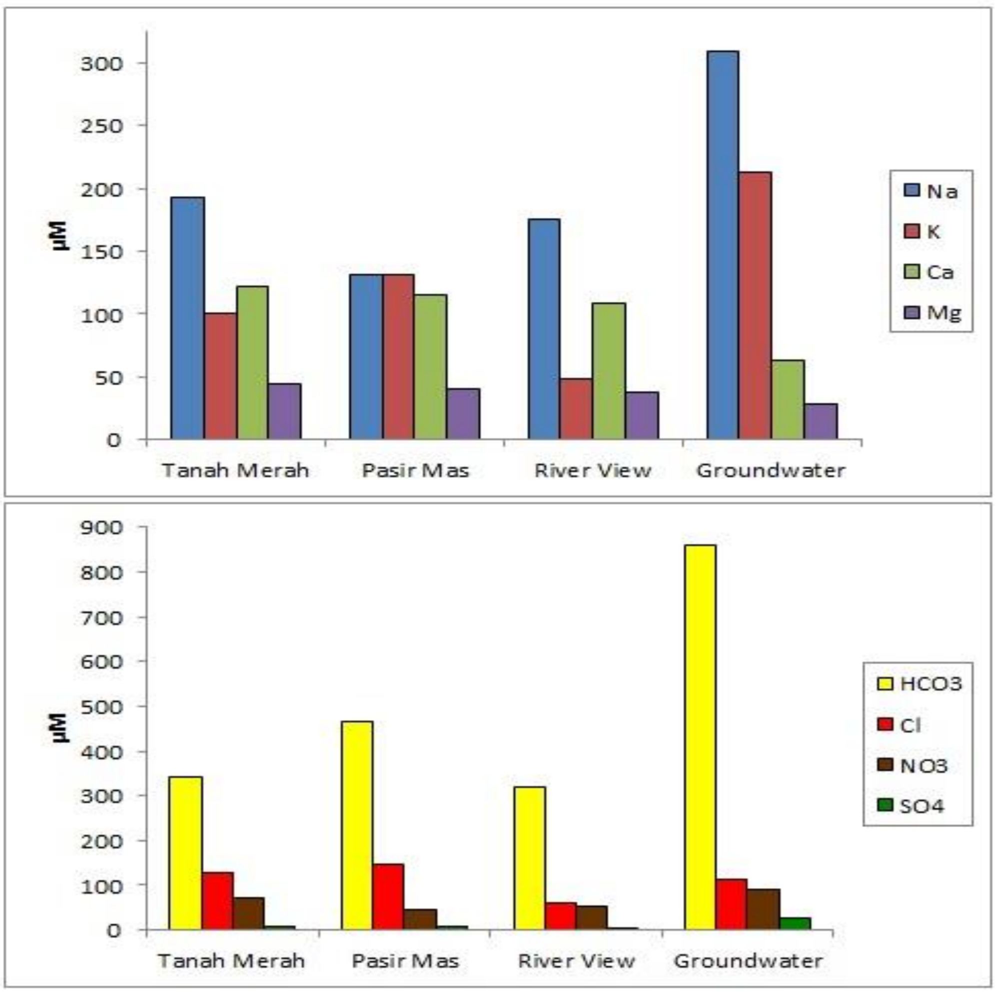

Figure 28: Spatial variations (average values) of major ions in Kelantan watershed.

7.5 Statistical evaluation of major ions in Langat and Kelantan watersheds.

The interrelationships among the major ions and their relationship to hydrology are evaluated via correlation and Principal Component Analysis (PCA). *Correlation coefficient* is an index of the degree of linear association between two random variables [*Ayyub and McCuen, 2011*]. In this study, the *Pearson product moment correlation coefficient* (*r*) is employed to measure the strength and the direction of a linear relationship between two variables, *x* and *y*. *n* is the number of pairs in the data.

$$r = \frac{n\sum xy - \left(\sum x\right)\left(\sum y\right)}{\sqrt{n\left(\sum x^2\right) - \left(\sum x\right)^2}\sqrt{n\left(\sum y^2\right) - \left(\sum y\right)^2}} \tag{7}$$

Principal Component Analysis (PCA) is a tool for evaluation of the datasets for the Langat and Kelantan rivers. The aim is to identify variables that are responsible for spatial variations of geochemistry, to ascertain key factors which describe the structure of datasets, and to quantify the influence of possible natural and anthropogenic sources on these two rivers.

PCA analyzes a dataset (matrix/table of data) comprising number of samples (rows) and variables (columns), which are, in general, inter-correlated [*Jackson, 2003*]. It can be simply explained by the equation; *X= SL'*. *X* is modelled as a product of Scores (*S*) and Loadings (*L'*). The Scores and Loadings have *f* columns which represent the number of components, selected at Eigen-value >1. The scores and loadings matrix are determined by the least squares method. Each principal component consists of score and loading vector, where Component 1 represents the leading variable, followed by Component 2 which is orthogonal to Component 1 (in scores and loadings), followed by Component 3, etc.

The components of PCA can plot as a score plot, which illustrates the vectors (length & direction) and angle that characterizes the variability and correlation between two variables, respectively. The score values explain the degree of loading on a given vector for different variables. In addition, PCA model is based on the centered data, a pre-processing operation of orthogonal linear transformation where the dataset is transformed into a new coordinate system centered in a data cloud. PCA aims to extract the important information from the data matrix, compress the size of the dataset by holding only main information, simplify the description of dataset and analyze the structure of the observations (samples) and the variables.

7.5.1 The Langat watershed

The correlation matrix of major ions in Langat *river water* (Table 14) shows strong-positive correlations for [Ca^{2+}, Mg^{2+}, Na^{+} and HCO_3^{-}]; [K^{+} and Cl^{-}]; [SO_4^{2-} and NO_3^{-}] and these will be discussed further during evaluation by PCA.

Langat River	*Ca*	*K*	*Mg*	*Na*	*Cl*	SO_4	NO_3
K	0.2						
Mg	**0.8**	0.1					
Na	**0.9**	**0.2**	**0.8**				
Cl	0.1	**0.7**	0.0	0.1			
SO4	0.1	0.0	0.1	0.2	0.3		
NO3	0.2	-0.1	**0.4**	0.2	0.1	**0.6**	
HCO3	**0.6**	0.2	**0.3**	**0.5**	0.2	0.2	0.0

Langat groundwater	*Ca*	*K*	*Mg*	*Na*	*Cl*	SO_4	NO_3
K	-0.1						
Mg	**0.4**	0.0					
Na	0.0	**1.0**	0.1				
Cl	**0.4**	-0.1	0.3	-0.1			
SO4	**0.4**	0.2	0.1	-0.4	**0.4**		
NO3	**0.3**	-0.1	0.2	-0.2	**0.3**	**0.7**	
HCO3	0.2	**0.3**	0.1	**0.3**	0.2	-0.2	-0.2

Coorelation coefficient is significant at p<0.05 (bold)

Table 14: Correlation-coefficient analysis of river and groundwater for Langat watershed.

For Langat *groundwater* (Table 14) significant positive correlations are shown for [Ca^{2+}, Mg^{2+}, Cl^-, SO_4^{2-} and NO_3^-] and [K^+, Na^+ and HCO_3^-]. The groundwater datasets for the Langat watershed is small and has many missing values. Only 30% satisfy the electroneutrality condition. For this reason, no additional statistical treatment beyond simple correlation analysis is employed. The strong relationship of K^+ and Na^+ and the significant correlation coefficient with HCO_3^- potentially may reflect weathering of the granitoid country rocks [*Hamdan and Burnham, 1996*] by soil derived acids. The covariance of [Ca^{2+}, Cl^-, SO_4^{2-}, NO_3^-] may result from anthropogenic influences via atmospheric and agricultural inputs into soils.

Similar to correlation matrix, the *PCA analysis* of Langat *river water* (Table 15) shows that the first component (CI-Langat), which accounts for 42% of the total variance, groups together Na^{+}, Ca^{2+}, Mg^{2+} and HCO_3^{-}. In order to understand its meaning, the scores derived from PCA analysis were considered separately for each sampling stations, that is Pongsun (upstream), Kajang (urban), Dengkil (downstream) and Semenyih (tributary). Positive values were set into percentages based on total number of scores (positive and negative values), termed score impact (Figure 29, Appendix 20). For Semenyih, 79% score impact is attributed to CI-Langat followed by Pongsun with 73%, Dengkil 50% and Kajang 44%. Given that the loadings for CI-Langat are negative (Table 15), the urban Kajang with the lowest score is presumably the most polluted locality [*Juahir et al., 2010*], suggesting that the CI-Langat is a geogenic factor reflecting the weathering of the country rocks.

The second component (CII-Langat) that represents 20% of the total variance correlates positively K^{+} and Cl^{-}. Kajang contributes 50% to the score impact followed by Semenyih 42%, Pongsun 33% and Dengkil 25%. The same argument as above would point out to anthropogenic pollution as the major source of these constituents.

The third component (CIII-Langat) represents 18% of the total variance, with loading by SO_4 and NO_3. Kajang contributes 75% to the score impact followed by Pongsun 47%, Dengkil 45% and Semenyih 37%. Again, only more so, anthropogenic pollution is likely the major source of these anions. Fallout from the atmosphere, either as wet deposition (rain) containing dilute sulfuric (H_2SO_4) and nitric (HNO_3) acid, or as dry deposition of SO_x and NO_x [*Albanese and Cicchella, 2012*] may be implicated. Rainwater dissolves and incorporates sea salt aerosol, sulphate, ammonium and nitrate from natural and anthropogenic sources, such as power plants, automobile exhaust, smelters and agriculture. This water can also be chemically altered as it reacts with dry particulate aerosols on the ground accumulated between precipitation events [*Zhu and Schwartz, 2011*]. Nitrate in soils originates from various sources, such as mineralization of soil organic nitrogen, application of organic and inorganic N fertilizers, and atmospheric deposition. Moreover, nitrate fertilizers are highly mobile in soils [*Mengis et al., 2001*] and readily leached to the groundwater.

	Langat		
	Component		
	I	II	III
Proportion of variance (%)	42	20	18
Ca	**-0.5**	0.0	-0.2
K	-0.2	**0.7**	0.2
Mg	**-0.5**	-0.2	-0.1
Na	**-0.5**	0.0	-0.2
Cl	-0.2	**0.5**	0.4
SO_4	-0.2	-0.3	**0.5**
NO_3	-0.2	-0.4	**0.5**
HCO_3	**-0.3**	0.1	-0.3

Table 15: Loadings for PCA components for Langat river waters

In summary, the Langat River chemical make-up is the reflection of the dominant geogenic (CI-Langat) and superimposed anthropogenic (CII-Langat, CIII-Langat) inputs, with latter two becoming more visible in the urbanized reaches of the river. Note, nevertheless that the river waters have a chemistry that is a mixture of these three principal components (Figure 29), superimposed at differing proportions in space and time.

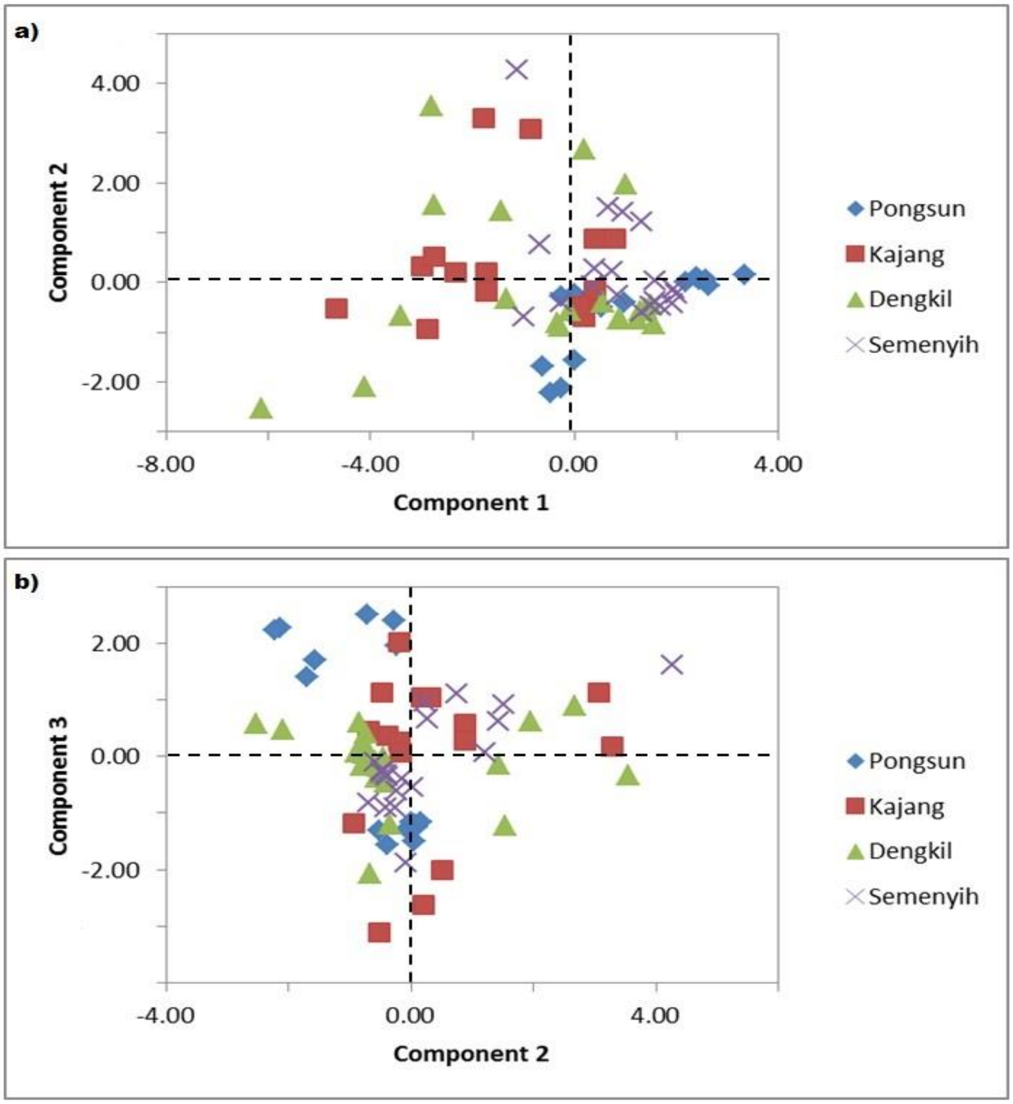

Figure 29: Bi-plot for the Langat river water: a) Component 1 vs Component 2; b) Component 2 vs Component 3. Only scores with positive values are utilized for standardization of analysis and interpretation (see Appendix 20).

7.5.2 The Kelantan watershed

In the Kelantan *river*, strong *correlations* (Table 16) exist for almost all major ions with the exception of HCO_3^- which was not measured in the field, but was calculated from data provided by *Lee* [*2013*]. The attribution, as for the Langat watershed, has to rely on PCA, as discussed below. The correlation matrix of major ions for *groundwater* dataset for the Kelantan watersheds is small and has many missing values. Only 20% satisfy the electroneutrality condition. For this reason, and similar to Langat no additional statistical treatment beyond simple correlation analysis is employed for the geochemistry of groundwaters (Table 16).

Kelantan river	*Ca*	*K*	*Mg*	*Na*	*Cl*	*SO_4*	*NO_3*
K	**0.4**						
Mg	**0.9**	**0.4**					
Na	0.1	**0.7**	0.1				
Cl	**0.5**	**0.6**	**0.4**	**0.5**			
SO4	**-0.3**	**0.4**	-0.2	-0.1	0.1		
NO3	**0.4**	**0.8**	**0.4**	**0.9**	**0.8**	0.1	
HCO3	0.2	0.1	0.1	-0.1	0.2	0.0	0.0

Kelantan groundwater	*Ca*	*K*	*Mg*	*Na*	*Cl*	*SO_4*	*NO_3*
K	0.0						
Mg	**0.7**	**0.7**					
Na	**-0.6**	**0.6**	-0.1				
Cl	**-0.7**	0.0	**-0.6**	**0.6**			
SO4	**-0.4**	0.2	-0.3	**0.6**	**0.7**		
NO3	**-0.4**	**0.9**	0.4	**0.9**	0.2	0.2	
HCO3	0.3	0.3	0.3	-0.1	**-0.5**	-0.2	0.3

Coorelation coefficient is significant at $p<0.05$ (bold)

Table 16: Correlation-coefficient analyses of river and groundwater for Kelantan watershed.

The *PCA analysis* (Table 17) for Kelantan *river* shows that the first component (CI-Kelantan) accounts for 46% of the total variance, and groups K^+, Na^+, NO_3^- and Cl^-. The score impacts (Figure 30, Appendix 21) attributed to this component increase downriver, from Tanah Merah (TM) 65% to Pasir Mas (PM) 78% and River View (RV) 86%, and is likely a reflection of anthropogenic pollution and/or spray deposition. Yet, considering these negative loadings, dilution downriver may be an alternative, or more likely a complementary phenomenon contributing to this component. Note, nevertheless, that the scores for all localities are not that different due to their relative proximity in the downriver section of the watershed.

	Kelantan		
	Component		
	I	II	III
Proportion of variance (%)	46	22	14
Ca	-0.3	**-0.5**	0.1
K	**-0.5**	0.2	0.3
Mg	-0.3	**-0.5**	0.1
Na	**-0.4**	0.3	-0.4
Cl	**-0.4**	0.0	0.0
SO_4	0.0	**0.5**	**0.6**
NO_3	**-0.5**	0.2	-0.1
HCO_3	0.0	-0.2	**0.6**

Table 17: Loading for PCA component for Kelantan waters.

The second component (CII-Kelantan) represents 22% of the total variance with inverse loadings of Ca^{2+} and Mg^{2+} vs SO_4^{2-}. In this case the highest impact also increases from TM (30%), to PM (39%) and RV (43%), that is down river (Figure 30). The proposed interpretation is that the component represents principally a geogenic factor for Ca^{2+} and Mg^{2+} that is being overprinted downriver by the third component (CIII-Kelantan), the latter (SO_4^{2-}) accounting for 14% of total variance.

The loads of the third component in the downriver stations (50 and 36%) are almost double of the upriver TM, at 20%. This third factor is again likely a pollution and/or marine derived constituent. Note that the HCO_3^- values for the Kelantan *river* were estimated from the bulk annual pH values provided by the Department of Environment Malaysia [*Lee, 2013*] and thus may not be strictly relevant to this issue.

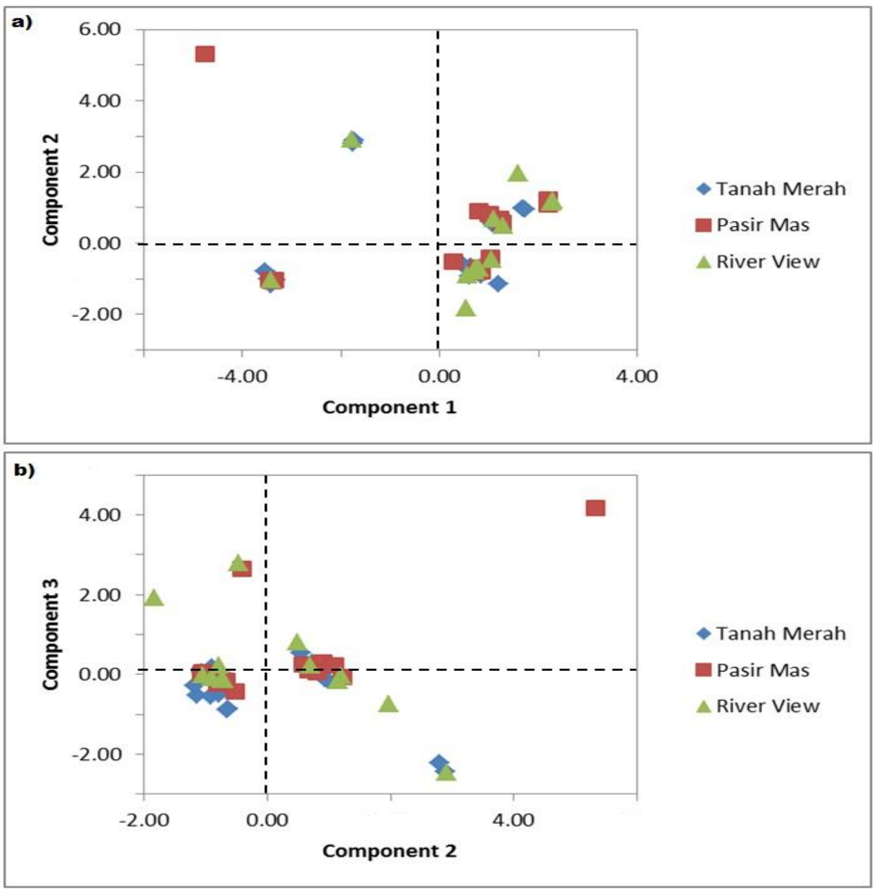

Figure 30: Bi-plot for the Kelantan waters: a) Component 1 vs Component 2; b) Component 2 vs Component 3. Only scores with positive values are utilized for standardization of analysis and interpretation (see Appendix 21).

7.6 Seasonal variations

7.6.1 Langat watershed

In terms of *seasonal variations* for *river water*, higher concentrations for major ions at all sampling stations were observed from April to October (Figure 31a, 32a), associated mostly with the SWM regime. The relative uniform SO_4^{2-} concentrations were an exception from this pattern. The Cl^- concentrations at Kajang, Dengkil and Semenyih were high particularly from July to December. NO_3^- increased steadily throughout the year, with higher concentrations observed from July to December.

In *groundwaters* (Figure 31b, 32b), Ca^{2+} and K^+ increase steadily from January to December. Na^+ is higher in the first three month of the year followed by a sharp decline in April and gradual increases throughout the year. Mg^{2+} is relatively consistent throughout the year. Concentrations of Cl^-, SO_4^{2-} and NO_3^- in groundwater show large seasonal variation with sharp increases during the NEM.

7.6.2 Kelantan watershed

Seasonally (Figure 33a, 34a), the concentrations of major ions at all riverine sampling stations are variable, but peak values for most are, as in the Langat watershed, associated with the SWM regime.

In *groundwater* (Figure 33b, 34b), Cl^- and SO_4^{2} concentrations appear to increase throughout the year. NO_3^-, Ca^{2+}, Mg^{2+}, K^+ are variable, but higher concentrations are associated mostly with the summer months (SWM). This seems to be the case also for Na^+, albeit with lesser seasonal variability.

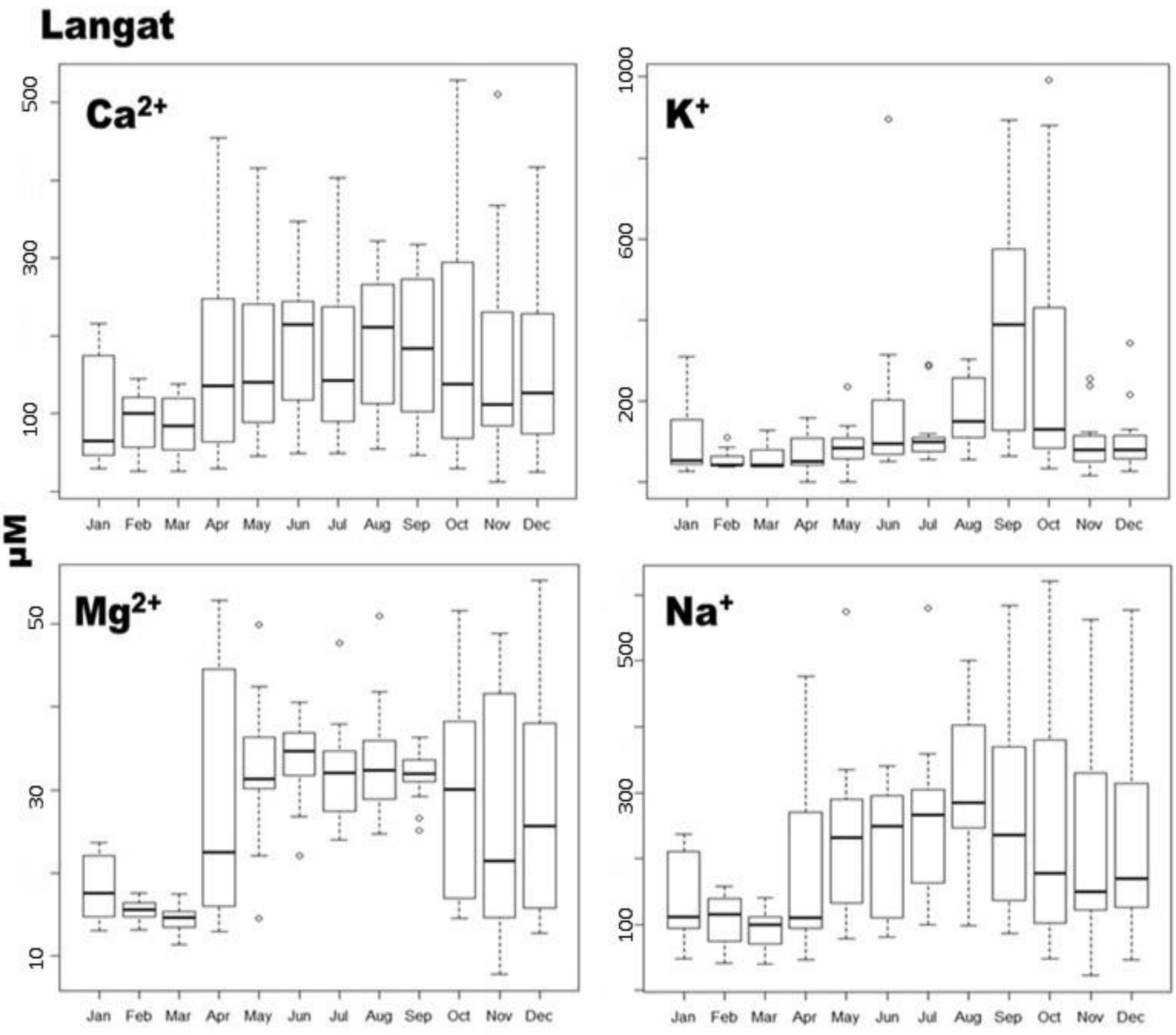

Figure 31a: Seasonal variations of Ca^{2+}, K^+, Mg^{2+} and Na^+ in river water of the Langat watershed.

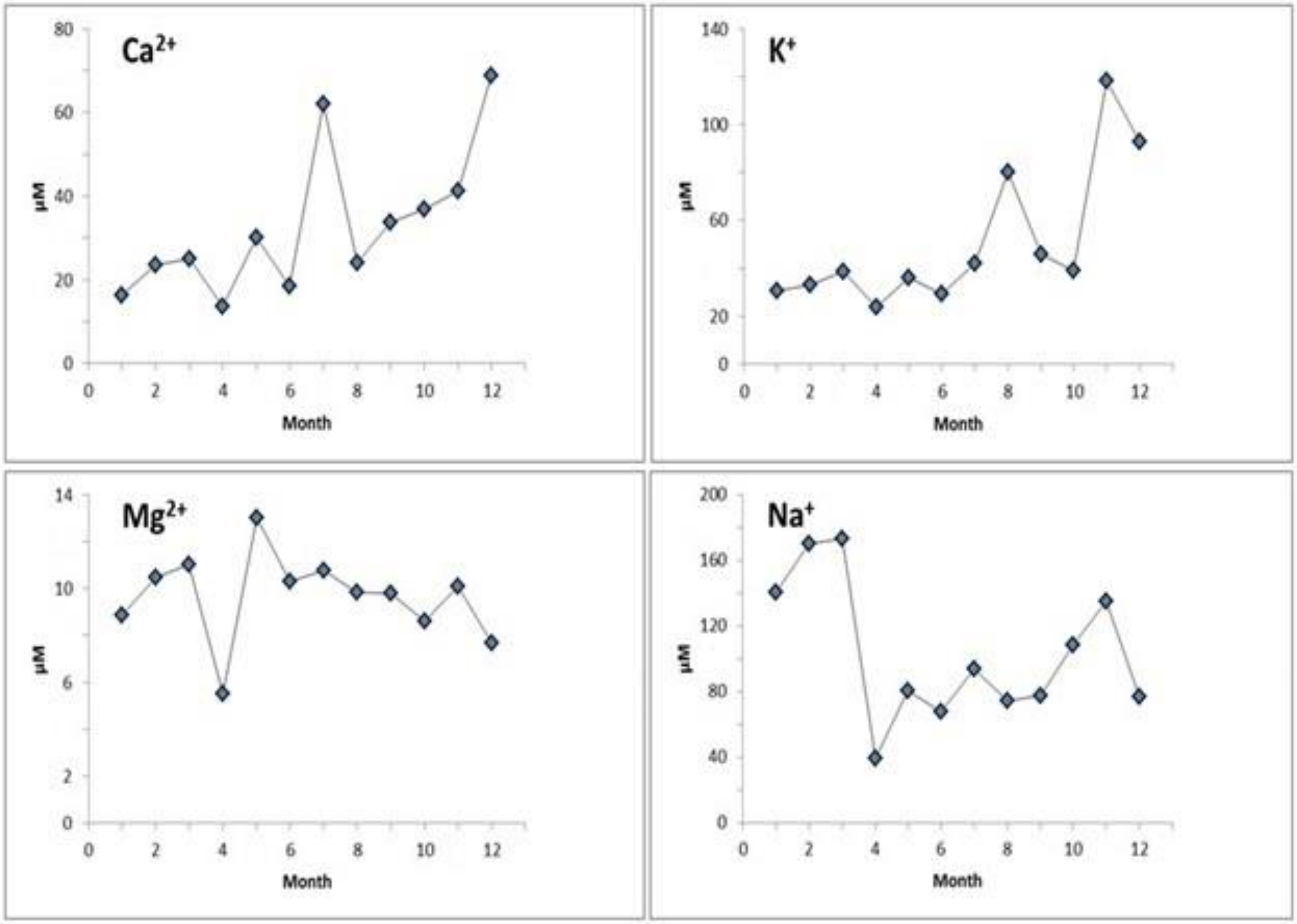

Figure 31b: Seasonal variations of Ca^{2+}, K^{+}, Mg^{2+} and Na^{+} in *groundwater* of the Langat watershed.

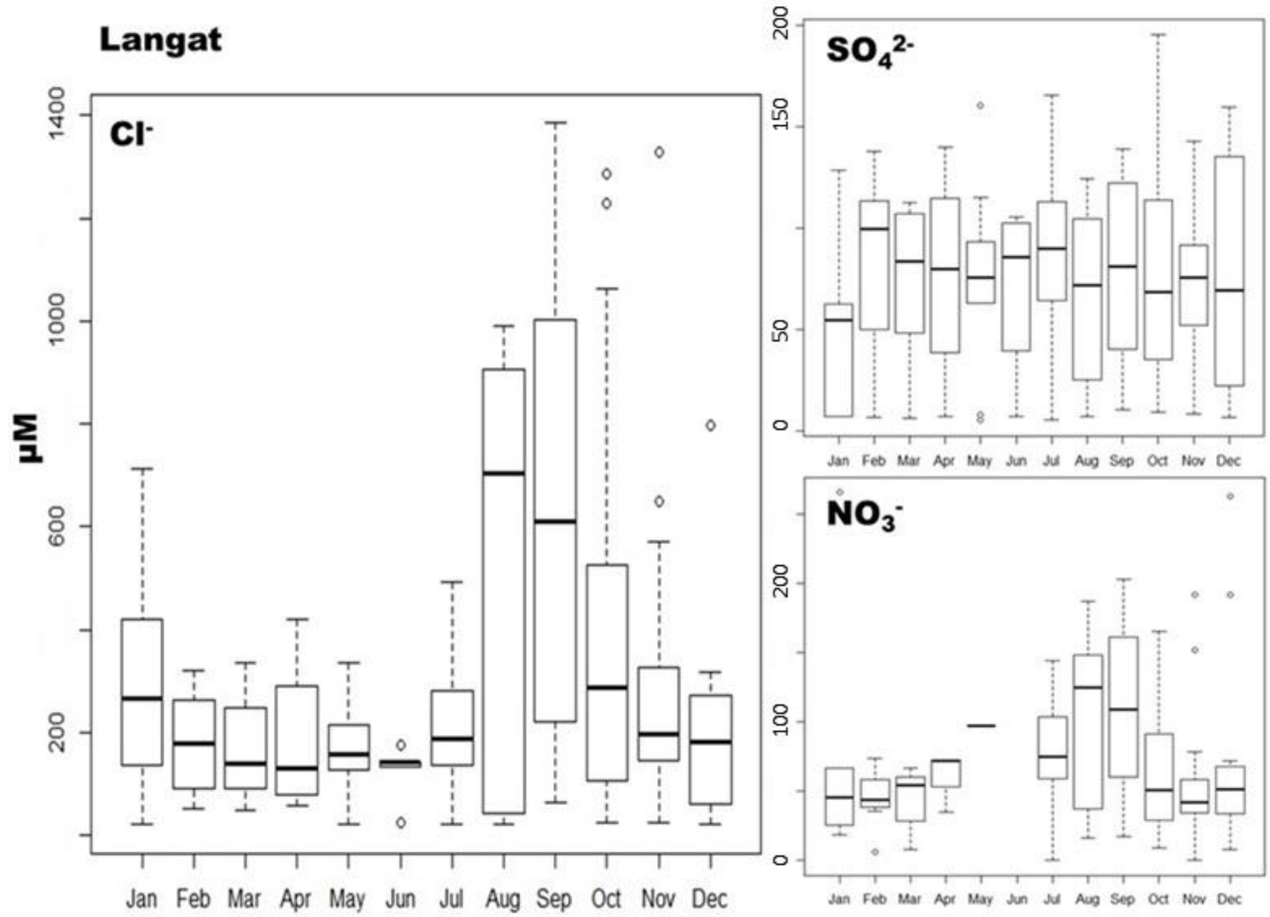

Figure 32a: Seasonal variations of Cl^{-}, NO_3^{-}, and SO_4^{2-} in river water of the Langat watershed.

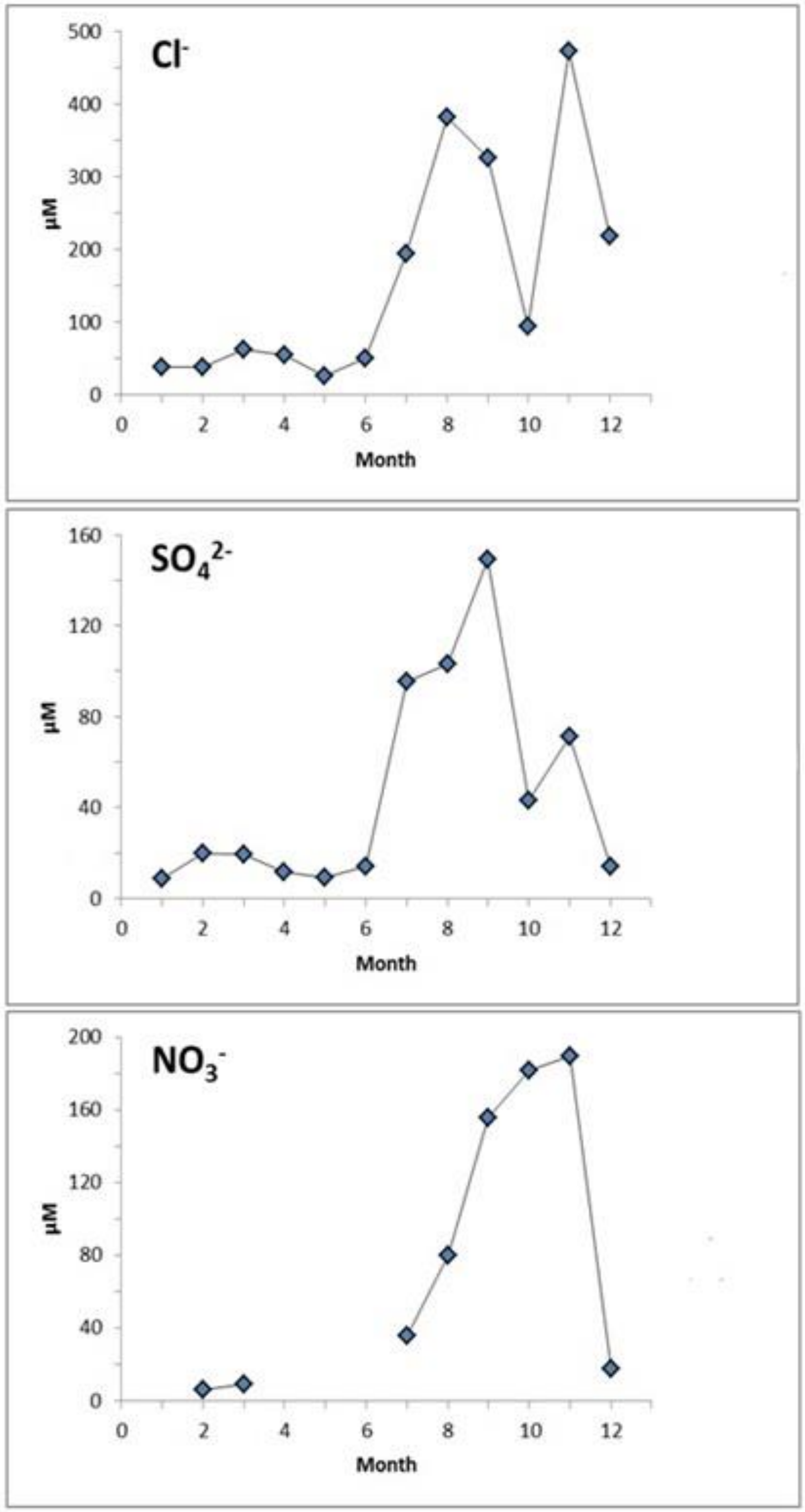

Figure 32b: Seasonal variations of Cl^-, NO_3^-, and SO_4^{2-} in *groundwater* of Langat watershed.

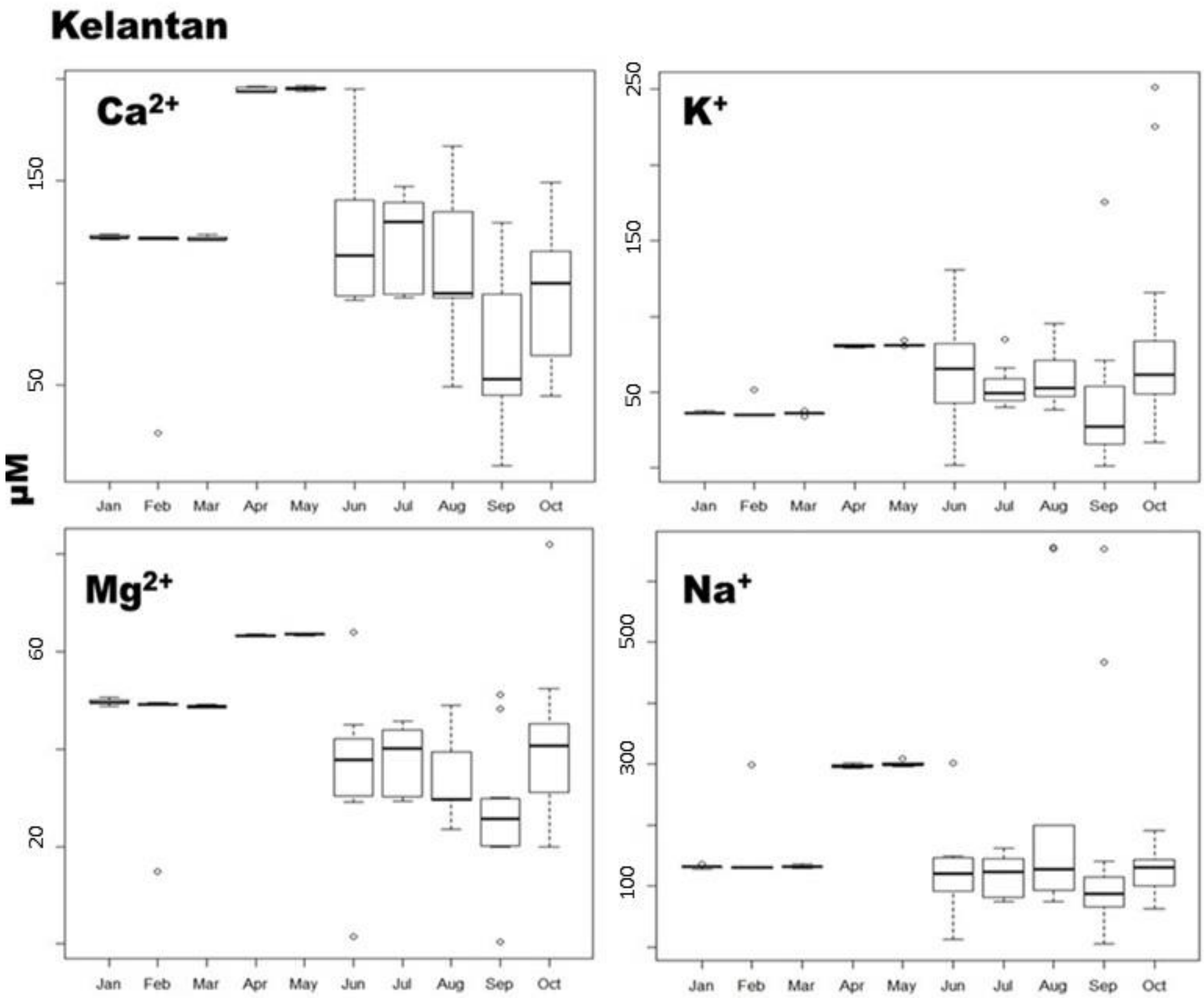

Figure 33a: Seasonal variations of Na^{+}, Ca^{2+}, K^{+}, Mg^{2+} in river water of the Kelantan watershed.

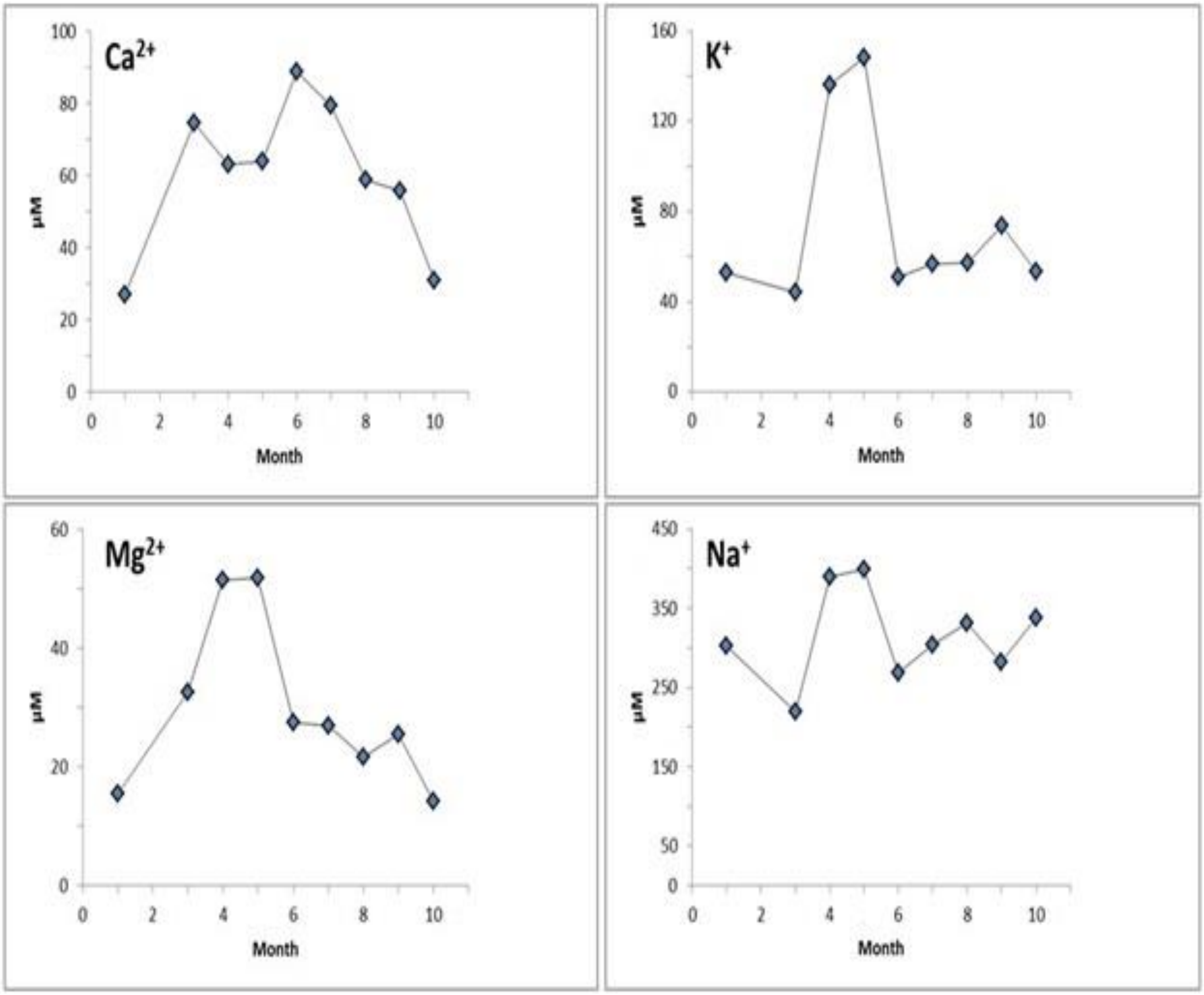

Figure 33b: Seasonal variations of Na^{+}, Ca^{2+}, K^{+}, Mg^{2+} in *groundwater* of the Kelantan watershed.

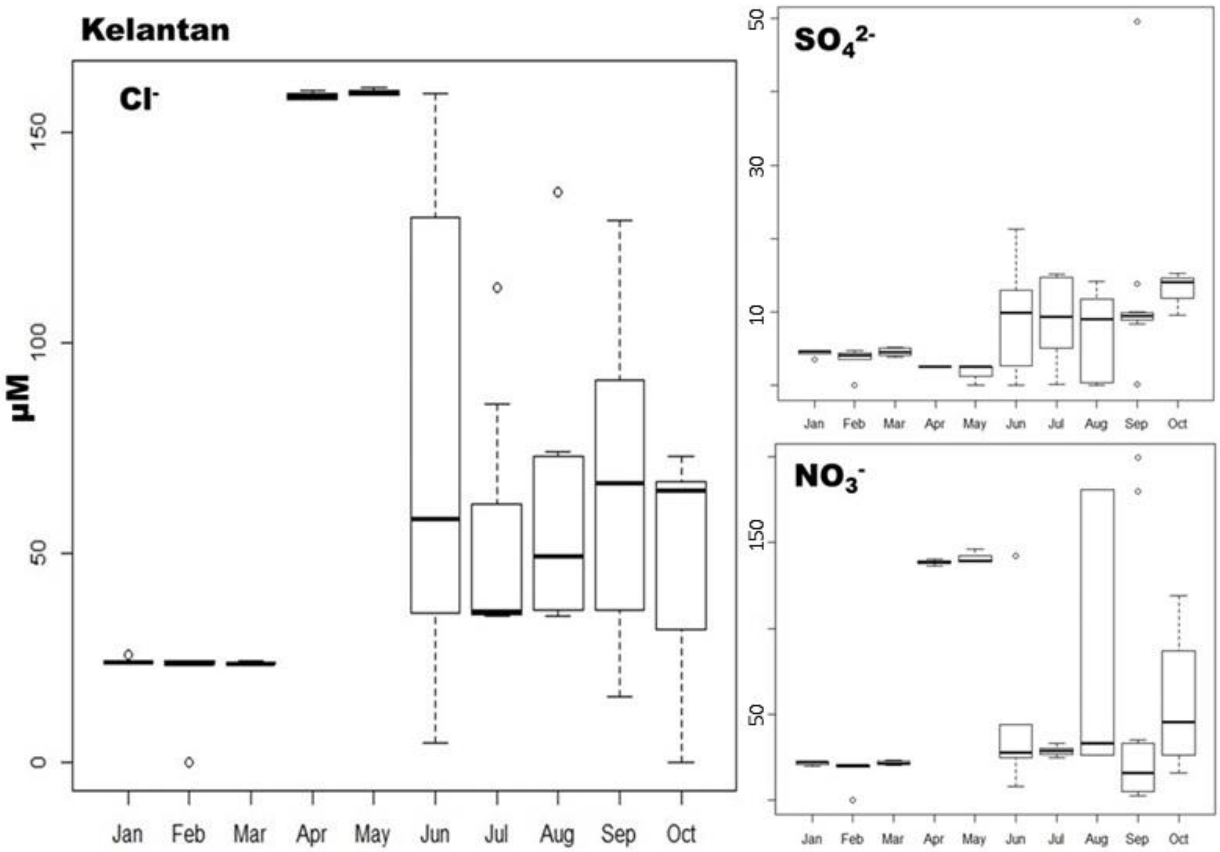

Figure 34a: Seasonal variations of Cl^-, NO_3^- and $^-$ SO_4^{2-} in river water of the Kelantan watershed.

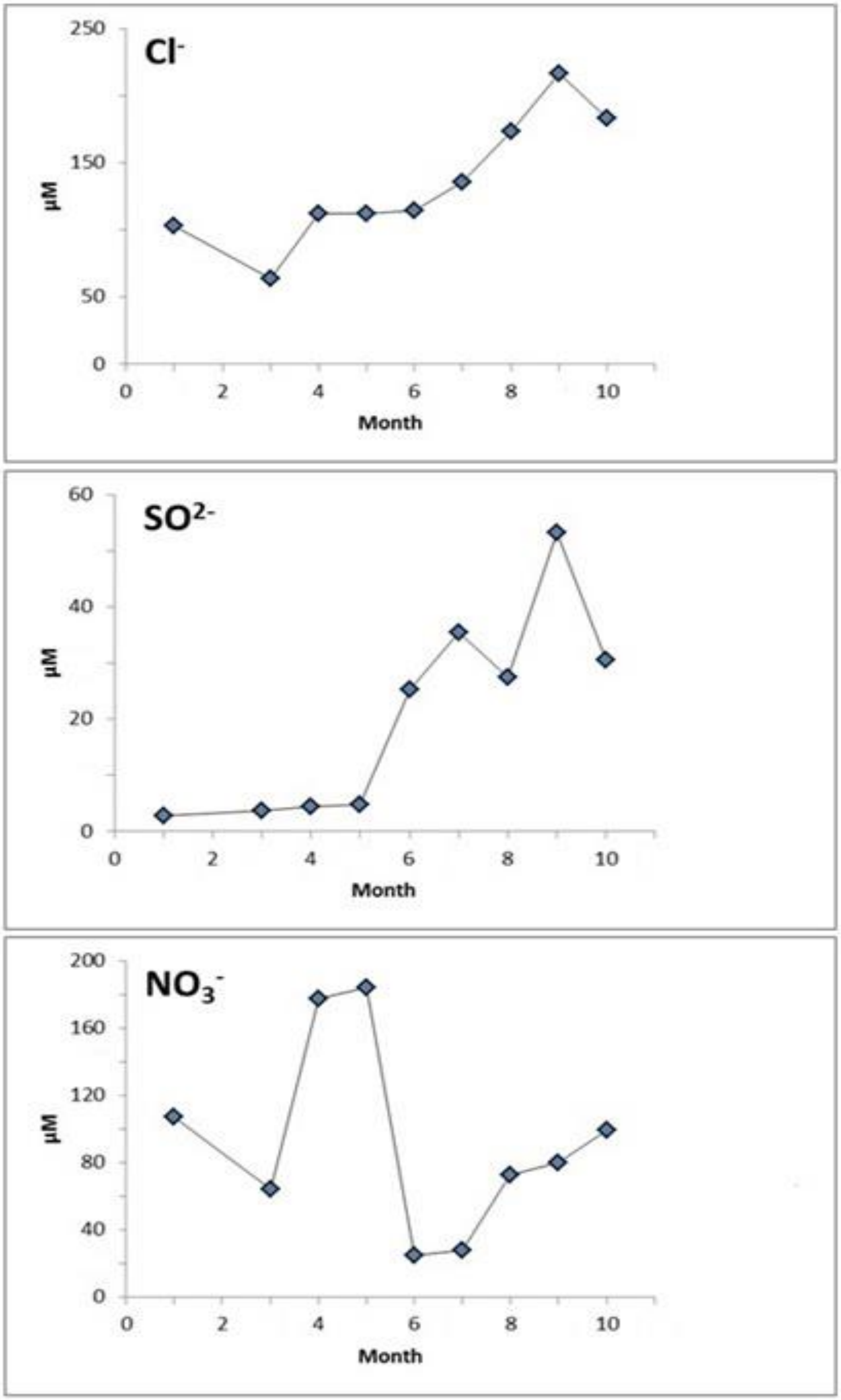

Figure 34b: Seasonal variations of Cl^-, NO_3^- and SO_4^{2-} in *groundwater* of the Kelantan watershed.

7.6.3 Seasonal variations of major ions and environmental factors

Comparison with the environmental factors, such as the earlier discussed (Chapter 5) seasonal rainfall (*P*), discharges (*Q*), Global Solar Radiation (*GSR*) and temperature (*TEMP*), does not show any clear correlations for major ions.

7.7 Summary

PCA analysis for major ions datasets (Table 18) shows that the main characteristics of geochemistry of the Langat and Kelantan rivers are characterized by three components with Eigen-value >1. These explain 80% and 82% of total variances, respectively, reflecting principally the geogenic factor with superimposed pollution, the latter particularly pronounced in the urbanized sections of the rivers.

Major Ion	Langat	CI	CII	CIII
	Component	Na, Ca, Mg, HCO_3	K, Cl	SO_4 ,NO_3
	Proportion of variance (%)	42	20	18
	Cumulative proportion (%)	42	62	80
	Factor	Weathering/Anthropogenic	Anthropogenic	Anthropogenic
	Possible pollutant	Weathering overprinted down river by pollution	Fertilizer	Atmospheric/Fertilizer
Major Ion	Kelantan	CI	CII	CIII
	Component	K, Na, NO_3,Cl	Ca, Mg	HCO_3,SO_4
	Proportion of variance (%)	46	22	14
	Cumulative proportion (%)	46	68	82
	Factor	Anthropogenic	Weathering	Anthropogenic/ Marine
	Possible pollutant	Fertilizer		

Table 18: Proposed factors, possible pollutants and sources of pollution in the Langat and Kelantan watersheds.

For the Kelantan river, in contrast to the Langat river, the anthropogenic impact appears to be the dominant influence, likely because all sampling stations are within the down-river portion of the watershed. Atmospheric inputs, biological and physical components are all closely coupled to the geogenic factor, and play a key role in the geochemistry and water quality of the rivers. There appears to be no significant correlation between seasonal variations in major ion chemistry and environmental variables such as precipitation, discharge, temperature or solar activity.

Chapter 8: Summary and Conclusion

8.1 Isotope constraints on water and carbon fluxes

Evapotranspiration, a nexus for planetary energy and carbon cycles, is as yet poorly constrained for tropical watersheds. Here I use stable isotopes of oxygen and hydrogen to partition flux of water due to plant transpiration from the direct evaporative flux from soils, water bodies and plants. The study areas, Langat and Kelantan watersheds, represent examples of domains dominated by the respective Southwest and Northeast monsoons on two sides of the main orographic barrier (Titiwangsa mountain range).

Mean annual rainfall (P) for the Langat watershed, obtained from 30 years of hydrological data, is 2145 ± 237 mm. Tentatively, 48% of this precipitation returns to the atmosphere via transpiration (T), 33% is partitioned into discharge (Q), 8% into interception (I_n), and 11% into evaporation (E_d). In Kelantan watershed, the mean annual rainfall, also based on the 30 year hydrological data, is 2383 ± 120 mm. Similar to Langat, the T accounts for 43% of precipitation, 45% is discharged into South China Sea (Q), 12% is interception (I_n) and tentatively evaporation (E_d) is negligible.

E_d for the Langat represented only a small proportion in terms of volumetric significance, up to ~11%, but this is sufficient to the isotopic fingerprint of waters associated with the summer Southwest Monsoon (SWM). In contrast, the E_d for the Kelantan watershed is negligible, perhaps a reflection of the fact that the precipitation as well as river sampling stations are all in down-river coastal portions of the watershed. The coastal storm front may thus dominate both the precipitation and the riverine regime. Furthermore, humidity is high (80%) for both watersheds.

Overall, T is a major component comprising 80% of ET, accounting for 1030±103 mm yr^{-1} in Langat and 1019±102 mm yr^{-1} in the Kelantan water budgets. This biological flux of water driven by solar radiation controls the Net Primary Productivity (NPP) of the Malaysian ecosystems. The associated carbon sequestration fluxes for the Langat and Kelantan watersheds are 1373±137 g C $m^{-2}yr^{-1}$ and 1359±136 g C $m^{-2}yr^{-1}$, respectively. These fluxes are independent of P. Considering that only about 2% of this carbon is exported to the ocean by the rivers, the remaining 98% must be re-exported to the atmosphere by respiration, demonstrating the importance of interplay of water and biology for the global carbon cycle.

8.2 Hydrochemistry

Geochemistries of the Langat and Kelantan rivers are characterized by three principal components that explains 80% and 82% of total the variances, respectively. For the Langat river, the dominant factor is geogenic with superimposed pollution, particularly pronounced in urbanized sections of the river. The concentrations of major ions appear to be somewhat higher during the Southwest monsoon season, albeit not related to environmental variables, such as precipitation, discharge, temperature or solar activity. The geochemistry of the Kelantan river, the other hand, appears to dominated by anthropogenic pollution factors, possibly a reflection of the fact that present study was limited to the costal downstream section of the watershed.

8.3 Conclusion

Transpiration, *T* appropriates about half of all solar energy absorbed by the continents. This flux in Malaysia, ~$1000*10^3$ g H_2O m^{-2} yr^{-1} is comparable to other tropical regions with a 900-$1200*10^3$ g H_2O m^{-2} yr^{-1}. Vegetation response to solar incidence via *T* and photosynthesis reflects the importance of stomatal regulation of the water and carbon fluxes. In order to maintain high transpiration in the tropical region, "constant" water supply is required for continuous pumping of water that delivers nutrients to the plant, suggesting that water and carbon cycles are co-driven by the energy of the sun and the existence of the water conveyor belt is a precondition for nutrient delivery, hence for operation of the carbon cycle. Potentially, this may change our perspective on the role that biology plays in the water cycle. In such perspective, the global water cycle is the medium that redistributes the incoming solar energy across the planet and the anatomical structures of plants then help to optimize the loop of energy transfer in the hydrologic cycle via evaporation and precipitation.

References

Albanese, S. and D. Cicchella. "Legacy Problems in Urban Geochemistry." *Elements* 8, no. 6 (2012): 423-428.

Alexander, W.J.R. "Linkages between Solar Activity and Climatic Responses." *Energy & Environment* 16, no. 2 (2005): 239-254.

Araguas-Araguas, L. K. Froehlich, and K. Rozanski. "Stable Isotope Composition of Precipitation Over Southeast Asia." *Journal of Geophysical Research-Atmospheres* 103, no. D22 (1998): 28721-28742.

Asdak, C., P.G. Jarvis, P. Van Gardingen, and A. Fraser. "Rainfall Interception Loss in Unlogged and Logged Forest Areas of Central Kalimantan, Indonesia." *Journal of Hydrology* 206, no. 3 (1998): 237-244.

Ayyub, B. and McCuen. R. *Probability, Statistics, and Realibility for Engineers and Scientists.* CRC Press (2011): 440

Baede, A.P.M, E. Ahlonsou, Y. Ding, D. Schimel, B. Bolin, and S. Pollonais. "The Climate System: An Overview." *Climate Change* (2001): 85-98.

Bentley, A. "Interception loss in Sedenak Oil Palm Plantation" *Undegraduate Thesis*. Universiti Teknologi Malaysia. (2007)

Berner, E. K. and R. A. Berner. *Global Environment: Water, Air, and Geochemical Cycles* Prentice Hall (1996): 9-17

Berry, S. L. and M. L. Roderick. "Gross Primary Productivity and Transpiration Flux of the Australian Vegetation from 1788 to 1988 AD: Effects of CO2 and Land use Change." *Global Change Biology* 10, no. 11 (2004): 1884-1898.

Betts, R. "Implications of Land Ecosystem-Atmosphere Interactions for Strategies for Climate Change Adaptation and Mitigation." *Tellus Series B-Chemical and Physical Meteorology* 59, no. 3 (2007): 602-615.

Bhattacharyya, S. and R. Narasimha. "Possible Association between Indian Monsoon Rainfall and Solar Activity." *Geophysical Research Letters* 32, no. 5 (2005): L05813.

Bowen, G. J. "A Faster Water Cycle." *Science* 332, no. 6028 (2011): 430-431.

Brunet, F., K. Dubois, J. Veizer, G. R. N. Ndondo, J. N. Ngoupayou, J. Boeglin, and J. Probst. "Terrestrial and fluvial carbon fluxes in a tropical watershed: Nyong basin, Cameroon." *Chemical Geology* 265, no. 3 (2009): 563-572.

Bruno, R. D., H. R. da Rocha, H. C. de Freitas, M. L. Goulden, and S. D. Miller. "Soil Moisture Dynamics in an Eastern Amazonian Tropical Forest." *Hydrological Processes* 20, no. 12 (2006): 2477-2489.

Burns, S. J, D. Fleitmann, M. Mudelsee, U. Neff, A. Matter, and A. Mangini. "A 780-Year Annually Resolved Record of Indian Ocean Monsoon Precipitation from a Speleothem from South Oman." *Journal of Geophysical Research-Atmospheres* 107, no. D20 (2002): 4434.

Camerlengo, A. and M. I. Demmler. (1997) “Wind-driven circulation of Peninsular Malaysia’s eastern continental shelf.” *Scientia Marina*, 61 (1997) 203–211

Calder, I. R., I. R. Wright, and D. Murdiyarso. "A Study of Evaporation from Tropical Rain-Forest - West Java." *Journal of Hydrology* 89, no. 1-2 (1986): 13-31.

Chahine, M.T. "The Hydrological Cycle and its Influence on Climate." *Nature* 359, no. 6394 (1992): 373-380.

Chang, C. P., P. A. Harr, and H. Chen. "Synoptic Disturbances Over the Equatorial South China Sea and Western Maritime Continent during Boreal Winter." *Monthly Weather Review* 133, no. 3 (2005): 489-503.

Chen, D-X. and M. B. Coughenour. "Photosynthesis, Transpiration, and Primary Productivity: Scaling Up from Leaves to Canopies and Regions using Process Models and Remotely Sensed Data." *Global Biogeochemical Cycles* 18, no. 4 (2004).

Choudhury, B. J. "Seasonal and Interannual Variations of Total Evaporation and their Relations with Precipitation, Net Radiation, and Net Carbon Accumulation for the Gediz Basin Area." *Journal of Hydrology* 229, no. 1 (2000): 77-86.

Choudhury, B. J. and N. E. DiGirolamo. "A Biophysical Process-Based Estimate of Global Land Surface Evaporation using Satellite and Ancillary Data - I. Model Description and Comparison with Observations." *Journal of Hydrology* 205, no. 3-4 (1998): 164-185.

Choudhury, B. J., N.E. DiGirolamo, J. Susskind, W. L. Darnell, S. K. Gupta, and G. Asrar. "A Biophysical Process-Based Estimate of Global Land Surface Evaporation using Satellite and Ancillary Data - II. Regional and Global Patterns of Seasonal and Annual Variations." *Journal of Hydrology* 205, no. 3-4 (1998): 186-204.

Clark, I. D. and P. Fritz. *Environmental Isotopes in Hydrogeology* CRC press (1997): 26, 37

Clette, F., D. Berghmans, P. Vanlommel, R. A. M. Van der Linden, A. Koeckelenbergh, and Laurence Wauters. "From the Wolf Number to the International Sunspot Index: 25 Years of SIDC." *Advances in Space Research* 40, no. 7 (2007): 919-928.

Coleman, M.L., T.J. Shepherd, J.J. Durham, J.E. Rouse, and G.R. Moore. “Reduction of water with zinc for hydrogen isotope analysis.” *Analytical Chemistry.* 54 (1982):995

Cox, P. M., R. A. Betts, C. D. Jones, S. A. Spall, and I. J. Totterdell. "Acceleration of Global Warming due to Carbon-Cycle Feedbacks in a Coupled Climate Model." *Nature* 408, no. 6809 (2000): 184-187.

Craig, Harmon. "Isotopic Variations in Meteoric Waters." *Science* 133, no. 3465 (1961): 1702-1703.

Craig, H. and L. Gordon. “Deuterium and oxygen-18 variation in the ocean and marine atmosphere” *Stable Isotopes in Oceanographic Studies and Paleotemperatures*, edited by E. Tongiorgi, Lab. di Geol. Nucl, Cons. Naz. delle Rich, Pisa, Italy (1965): 9-130

da Rocha, H. R., M. L. Goulden, S. D. Miller, M. C. Menton, L. D. V. O. Pinto, H. C. de Freitas, and A. M. E. S. Figueira. "Seasonality of Water and Heat Fluxes over a Tropical Forest in Eastern Amazonia." *Ecological Applications* 14, no. 4 (2004): S22-S32.

Dansgaard, W. "Stable Isotopes in Precipitation." *Tellus* 16, no. 4 (1964): 436-468.

de Boer, H. J., E. I. Lammertsma, F. Wagner-Cremer, D.L. Dilcher, M. J. Wassen, and S. C. Dekker. "Climate Forcing due to Optimization of Maximal Leaf Conductance in Subtropical Vegetation Under Rising CO2." *Proceedings of the National Academy of Sciences* 108, no. 10 (2011): 4041-4046.

de Groot P.A. editor, Handbook of Stable isotope Analytical Techniques, Vol 1, *Elsevier*, (2004): Chapter 1, 1-37.

de Smet, M.E.M. and A. J. Barber. “Tertiary Stratigraphy”. In: Barber, A.J., Crow, M.J. and Milsom, J.S. (eds). *Sumatra: Geology, resources and tectonic evolution*. Geological Society of London Memoir 31, (2005): 86-97

Delire, C., N. de Noblet-Ducoudre, A. Sima, and I. Gouirand. "Vegetation Dynamics Enhancing Long-Term Climate Variability Confirmed by Two Models." *Journal of Climate* 24, no. 9 (2011): 2238-2257.

Denman, K. L., G. Brasseur, A. Chidthaisong, P. Ciais, P. M. Cox, R. E. Dickinson, D. Hauglustaine, C. Heinze, E. Holand, D. Jacob, U. Lohmann, S. Ramachandran, P. L. da Silva Dias, S. C. Wofsy, and X. Zhang . Couplings between changes in climate system and biogeochemistry, in Climate Change 2007: *The Physical Scientific Basis: Contribution of Working I to the Fourth Assessment Report of the Intergovernmental Panel on Climate Change* (eds Solomon, S.D., Q.M. Manning, Z. Chen, M. Marquis, K. B. Averyt, M. Tignor, and H. L. Miller) Cambridge University Press (2007): 501-587

Dickenson, R. E. "Solar variability and the lower atmosphere" *Bulletin of the American Meteorological Society*, v. 56, (1975): 1240–1248.

Dingman, S. Lawrence. *Physical hydrology*. 2nd edition. Waveland Press, Inc. (2008): 119, 220, 294

"DID Manual 2009" *Government of Malaysia Department of Irrigation and Drainage*, Vol 4. retrieved September 5, (2012): 4-1 http://forum.mygeoportal.gov.my/smanre/aduan/Volume%204_Hydrology%20and%20Water%20Resources.pdf

Dietz, J., D. Hölscher, and C. Leuschner. "Rainfall Partitioning in Relation to Forest Structure in Differently Managed Montane Forest Stands in Central Sulawesi, Indonesia." *Forest Ecology and Management* 237, no. 1 (2006): 170-178.

Eichkorn, S., S. Wilhelm, H. Aufmhoff, K. H. Wohlfrom, and F. Arnold. "Cosmic Ray-Induced Aerosol-Formation: First Observational Evidence from Aircraft-Based Ion Mass Spectrometer Measurements in the Upper Troposphere." *Geophysical Research Letters* 29, no. 14 (2002): 1698.

Emile-Geay, J., Mark C., R. Seager, A. Kaplan, and P. Almasi. "El Nino as a Mediator of the Solar Influence on Climate." *Paleoceanography* 22, no. 3 (2007): PA3210.

Farquhar, G. D., K. T. Hubick, A. G. Condon, and R. A. Richards. "Carbon isotope fractionation and plant water-use efficiency." in *Stable Isotopes in Ecological Research*, edited by P. W. Rundel, J. R. Ehleringer, and K. A. Nagy, Springer, New York, (1989): 21-37

Fekete, B.M., J. J. Gibson, P. Aggarwal, and C. J. Vörösmarty. "Application of Isotope Tracers in Continental Scale Hydrological Modeling." *Journal of Hydrology* 330, no. 3 (2006): 444-456.

Fereres, E., F. Orgaz., and V. Gonzalez-Dugo. "Reflections on Food Security under Water Scarcity." *Journal of Experimental Botany* 62, no. 12 (2011): 4079-4086.

Ferguson, P. R. and J. Veizer. "Coupling of Water and Carbon Fluxes Via the Terrestrial Biosphere and its Significance to the Earth's Climate System." *Journal of Geophysical Research-Atmospheres* 112, no. D24 (2007): D24S06.

Ferguson, P. R., N. Weinrauch, L. I. Wassenaar, B. Mayer, and J. Veizer. "Isotope constraints on water, carbon, and heat fluxes from the northern Great Plains region of North America." Global biogeochemical cycles 21, no. 2 (2007): GB2023.

Ferretti, D. F., E. Pendall, J. A. Morgan, J. A. Nelson, Daniel Lecain, and A. R. Mosier. "Partitioning Evapotranspiration Fluxes from a Colorado Grassland using Stable Isotopes: Seasonal Variations and Ecosystem Implications of Elevated Atmospheric CO2." *Plant and Soil* 254, no. 2 (2003): 291-303.

Fleischbein, K., W. Wilcke, C. Valarezo, W. Zech, and K. Knoblich. "Water Budgets of Three Small Catchments Under Montane Forest in Ecuador: Experimental and Modelling Approach." *Hydrological Processes* 20, no. 12 (2006): 2491-2507.

Franks, P. J. and D. J. Beerling. "Maximum Leaf Conductance Driven by CO(2) Effects on Stomatal Size and Density Over Geologic Time." *Proceedings of the National Academy of Sciences of the United States of America* 106, no. 25 (2009): 10343-10347.

Freitag, H., P. R. Ferguson, K. Dubois, E. K. Hayford, V. von Vordzogbe, and J. Veizer. "Water and Carbon Fluxes from Savanna Ecosystems of the Volta River Watershed, West Africa." *Global and Planetary Change* 61, no. 1 (2008): 3-14.

Friedman, I., and J. R. O'Neil. “Compilation of stable isotope fractionation factors of geochemical interest”. Vol. 440. USGPO, (1977).

Foo, K.Y. “The Palaezoic sedimentary rocks of Peninsular Malaysia- stratigraphy and correlation.” *Proceedings of workshop on stratigraphic correlation of Thailand and Malaysia*, 1: Technical paper, Geological Society of Thailand & Geological Society of Malaysia, (1983): 1-19.

Gammons, C. H., S. R. Poulson, D. A. Pellicori, P. J. Reed, A. J. Roesler, and E. M. Petrescu. "The Hydrogen and Oxygen Isotopic Composition of Precipitation, Evaporated Mine Water, and River Water in Montana, USA." *Journal of Hydrology* 328, no. 1-2 (2006): 319-330

Gat, J. R., and C. Bowser. “The heavy isotope enrichment of water in coupled evaporative systems, in Stable Isotope Geochemistry.” edited by H. P. Taylor, J. R. O'Neil, and I. R. Kaplan, Special Publication *Geochemical Society*. 3, (1991): 159-168.

Gat, J. R. and E. Matsui. "Atmospheric Water-Balance in the Amazon Basin - an Isotopic Evapotranspiration Model." *Journal of Geophysical Research-Atmospheres* 96, no. D7 (1991): 13179-13188.

Gibbons, J. D., and S. Chakraborti. *“Nonparametric statistical inference”.* 5th edition. CRC press (2011): 389

Gedney, N., P. M. Cox, R. A. Betts, O. Boucher, C. Huntingford, and P. A. Stott. "Detection of a Direct Carbon Dioxide Effect in Continental River Runoff Records." *Nature* 439, no. 7078 (2006): 835-838.

Gibson, J. J, T.W. D Edwards, S. J Birks, N. A St Amour, W. M Buhay, P. McEachern, B. B Wolfe, and D. L Peters. "Progress in Isotope Tracer Hydrology in Canada." *Hydrological Processes* 19, no. 1 (2005): 303-327.

Gibson, J. J., T.W.D. Edwards, G. G. Bursey, and T. D. Prowse. "Estimating Evaporation using Stable Isotopes: Quantitative Results and Sensitivity Analysis for Two Catchments in Northern Canada." *Nordic Hydrology* 24, (1993): 79-94.

Gibson, J. J. and T. W. D. Edwards. "Regional Water Balance Trends and Evaporation-Transpiration Partitioning from a Stable Isotope Survey of Lakes in Northern Canada." *Global Biogeochemical Cycles* 16, no. 2 (2002): 1026.

Goller, R., W. Wilcke, M. J. Leng, H. J. Tobschall, K. Wagner, C. Valarezo, and W. Zech. "Tracing Water Paths through Small Catchments under a Tropical Montane Rain Forest in South Ecuador by an Oxygen Isotope Approach." *Journal of Hydrology* 308, no. 1-4 (2005): 67-80.

Gonfiantini, R. “Environmental isotopes in lake studies.” *Handbook of Environmental Isotope Geochemistry,* edited by P. Fritz and J. C. Fontes, pp, Elsevier Sci, Amsterdam. (1986): 113-168.

Goulden, M. L., S. D. Miller, H. R. da Rocha, M. C. Menton, H. C. de Freitas, A. M. E. S. Figueira, and C. A. D. de Sousa. "Diel and Seasonal Patterns of Tropical Forest CO2 Exchange." *Ecological Applications* 14, no. 4 (2004): S42-S54.

Hamdan, J. and C. P. Bumham. "The Contribution of Nutrients from Parent Material in Three Deeply Weathered Soils of Peninsular Malaysia." *Geoderma* 74, no. 3 (1996): 219-233.

Harding, R. J., C. Huntingford, and P. M. Cox. "Modelling Long-Term Transpiration Measurments from Grassland in Southern England." *Agricultural and Forest Meteorology* 100, no. 4 (2000): 309-322.

Harrison, R. G and K. L. Aplin. "Atmospheric Condensation Nuclei Formation and High-Energy Radiation." *Journal of Atmospheric and Solar-Terrestrial Physics* 63, no. 17 (2001): 1811-1819.

Heldt, H. and B. Piechulla. *Plant Biochemistry* Academic Press, (2010): 221

Henderson-Sellers, A., K. McGuffie, D. Noone, and P. Irannejad. "Using Stable Water Isotopes to Evaluate Basin-Scale Simulations of Surface Water Budgets." *Journal of Hydrometeorology* 5, no. 5 (2004): 805-822.

Hodnett, M. G, L. P. da Silva, H. R. Da Rocha, and R. C. Senna. "Seasonal Soil Water Storage Changes Beneath Central Amazonian Rainforest and Pasture." *Journal of Hydrology* 170, no. 1 (1995): 233-254.

Holwerda, F., F. N. Scatena, and L. A. Bruijnzeel. "Throughfall in a Puerto Rican Lower Montane Rain Forest: A Comparison of Sampling Strategies." *Journal of Hydrology* 327, no. 3 (2006): 592-602.

Huete, A. R., K. Didan, Y. E. Shimabukuro, P. Ratana, S. R. Saleska, L. R. Hutyra, W. Yang, R. R. Nemani, and R. Myneni. "Amazon Rainforests green-up with Sunlight in Dry Season." *Geophysical Research Letters* 33, no. 6 (2006).

Hutchison, C.S., D. N. K. Tan. *"Geology of Peninsular Malaysia".* University of Malaya (2009).

Huxman, T. E., M. D. Smith, P. A. Fay, A. K. Knapp, M. R. Shaw, M. E. Loik, S. D. Smith, et al. "Convergence Across Biomes to a Common Rain-use Efficiency." *Nature* 429, no. 6992 (2004): 651-654.

Immerzeel, W. W. and M. F. P. Bierkens. "Asia's Water Balance." *Nature Geoscience* 5, no. 12 (2012): 841-842.

Jackson, J. E. *"A user's guide to principal components."* Wiley.com, (2003): 10.

Jasechko, S., Z. D. Sharp, J. J. Gibson, S. J. Birks, Y. Yi, and P. J. Fawcett. "Terrestrial Water Fluxes Dominated by Transpiration." *Nature* (2013).

Jouzel, Jean. "Water stable isotopes: Atmospheric composition and applications in polar ice core studies", in *Treatise on Geochemistry*, 4, The Atmosphere, edited by R. F. Keeling, Elsevier-Pergamon, Oxford, U. K. (2006).

Juahir, H., S. M. Zain, A. Z. Aris, M. K. Yusoff, and M. Mokhtar. "Spatial Assessment of Langat River Water Quality using Chemometrics." *Journal of Environmental Monitoring* 12, no. 1 (2010): 287-295.

Kabat, P."Water at a crossroads". *Nature Climate Change*. doi:10.1038/nclimate1780. Published online 25 November 2012

Karim, A., J. Veizer, and J. Barth. "Net Ecosystem Production in the Great Lakes Basin and its Implications for the North American Missing Carbon Sink: A Hydrologic and Stable Isotope Approach." *Global and Planetary Change* 61, no. 1 (2008): 15-27.

Katul, G., S. Manzoni, S. Palmroth, and R. Oren. "A Stomatal Optimization Theory to Describe the Effects of Atmospheric CO_2 on Leaf Photosynthesis and Transpiration." *Annals of Botany* 105, no. 3 (2010): 431-442.

Khoo, H. P. “Mesozoic Stratigraphy in Peninsula Malaysia”. In: *Proceedings of the workshop on Stratigraphic correlation of Thailand and Malaysia*, 1: Technical paper, Geological Society of Thailand & Geological Society of Malaysia (1983): 370-383.

Khoo, K. K. Geology and Moneral Resources of Kuala Pilah Area, Negeri Sembilan. *Geological Survey of Malaysia Map Report*, 11, (1998): 93

Ki-Moon, B. *The Global Water Crisis* (2012) http://www.un.org/works/sub3.asp?lang=en&id=124

Knapp, A. K. and M. D. Smith. "Variation among Biomes in Temporal Dynamics of above ground Primary Production." *Science* 291, no. 5503 (2001): 481-484.

Kodera, K. "Solar Influence on the Indian Ocean Monsoon through Dynamical Processes." *Geophysical Research Letters* 31, no. 24 (2004): L24209.

Kuchment, L. S, V. N Demidov, and Z. P Startseva. "Coupled Modeling of the Hydrological and Carbon Cycles in the soil–vegetation–atmosphere System." *Journal of Hydrology* 323, no. 1 (2006): 4-21.

Kumagai, T., T. M. Saitoh, Y. Sato, T. Morooka, O. J. Manfroi, K. Kuraji, and M. Suzuki. "Transpiration, Canopy Conductance and the Decoupling Coefficient of a Lowland Mixed Dipterocarp Forest in Sarawak, Borneo: Dry Spell Effects." *Journal of Hydrology* 287, no. 1-4 (2004): 237-251.

Kumagai, T., T. M. Saitoh, Y. Sato, H. Takahashi, O. J. Manfroi, T. Morooka, K. Kuraji, M. Suzuki, T. Yasunari, and H. Komatsu. "Annual Water Balance and Seasonality of Evapotranspiration in a Bornean Tropical Rainforest." *Agricultural and Forest Meteorology* 128, no. 1-2 (2005): 81-92.

Kumagai, T., N. Yoshifuji, N. Tanaka, M. Suzuki, and T. Kume. "Comparison of Soil Moisture Dynamics between a Tropical Rain Forest and a Tropical Seasonal Forest in Southeast Asia: Impact of Seasonal and Year-to-Year Variations in Rainfall." *Water Resources Research* 45, (2009): W04413.

Kume, T., N. Tanaka, K. Kuraji, H. Komatsu, N. Yoshifuji, T. M. Saitoh, M. Suzuki, and T. Kumagai. "Ten-Year Evapotranspiration Estimates in a Bornean Tropical Rainforest." *Agricultural and Forest Meteorology* 151, no. 9 (2011): 1183-1192.

Lambert, F. H, P. A Stott, M. R. Allen, and M. A Palmer. "Detection and Attribution of Changes in 20th Century Land Precipitation." *Geophysical Research Letters* 31, no. 10 (2004): L10203.

Lee, K. "Carbon Cycling in Tropical Rivers: A Carbon Isotope Reconnaissance Study of the Langat and Kelantan Basins" *PhD Thesis*. University of Ottawa (2013), submitted.

Lee, K. Y., M. I. Syakir, I. D. Clark, and J. Veizer. "Isotope Constraints on the Aquatic Carbon Budget: Langat Watershed, Malaysia." Aquatic Geochemistry: (2013): 1-33.

Lee, D. H. and J. Veizer. "Water and Carbon Cycles in the Mississippi River Basin: Potential Implications for the Northern Hemisphere Residual Terrestrial Sink." *Global Biogeochemical Cycles* 17, no. 2 (2003): 1037.

Liu, W. J., W. Y. Liu, P. J. Li, L. Gao, Y. X. Shen, P. Y. Wang, Y. P. Zhang, and H. M. Li. "Using Stable Isotopes to Determine Sources of Fog Drip in a Tropical Seasonal Rain Forest of Xishuangbanna, SW China." *Agricultural and Forest Meteorology* 143, no. 1 (2007): 80-91.

Liu, J., B. Wang, Q. Ding, X. Kuang, W. Soon, and E. Zorita. "Centennial Variations of the Global Monsoon Precipitation in the Last Millennium: Results from ECHO-G Model." *Journal of Climate* 22, no. 9 (2009): 2356-2371.

Loescher, H. W., H. L. Gholz, J. M. Jacobs, and S. F. Oberbauer. "Energy Dynamics and Modeled Evapotranspiration from a Wet Tropical Forest in Costa Rica." *Journal of Hydrology* 315, no. 1-4 (2005): 274-294.

Lyons, W. B. and R. S. Harmon. "Why Urban Geochemistry?" *Elements* 8, no. 6 (2012): 417-422.

Martinelli, L. A., J. R. Gat, P. B. De Camargo, L. L. Lara, and J. P. H. B. Ometto. "The Piracicaba River basin: Isotope hydrology of a tropical river basin under anthropogenic stress." Isotopes in Environmental and Health Studies 40, no. 1 (2004): 45-56.

MMD: Climate change scenarios for Malaysia 2001–2099, Malaysian Meteorological Department, (2009).

Meehl, G. A., J. M. Arblaster, K. Matthes, F. Sassi, and H. van Loon. "Amplifying the Pacific Climate System Response to a Small 11-Year Solar Cycle Forcing." *Science* 325, no. 5944 (2009): 1114-1118.

Mengis, M., U. Walther, S. M. Bernasconi, and B. Wehrli. "Limitations of using $\delta^{18}O$ for the Source Identification of Nitrate in Agricultural Soils." *Environmental Science & Technology* 35, no. 9 (2001): 1840-1844.

Metcalfe, I. "Tectonic Evolution of the Malay Peninsula." *Journal of Asian Earth Sciences* (2013).

Miyamoto, K. "Renewable biological systems for alternative sustainable energy production". Vol. 128. *FAO Agricultural Service Bulletin*, 1997.

Moreira, M. Z., L. D. S. L. Sternberg, L. A. Martinelli, R. L. Victoria, E. M. Barbosa, L. C. M. Bonates, and D. C. Nepstad. "Contribution of Transpiration to Forest Ambient Vapour Based on Isotopic Measurements." *Global Change Biology* 3, no. 5 (1997): 439-450.

Mu, Qiaozhen, M. Zhao, and S. W. Running. "Evolution of Hydrological and Carbon Cycles Under a Changing Climate." *Hydrological Processes* 25, no. 26 (2011): 4093-4102.

Myneni, R. B., W. Yang, R. R. Nemani, A. R. Huete, R. E. Dickinson, Y. Knyazikhin, K Didan, et al. "Large Seasonal Swings in Leaf Area of Amazon Rainforests." *Proceedings of the National Academy of Sciences of the United States of America* 104, no. 12 (2007): 4820-4823.

Nemani, R., M. White, P. Thornton, K. Nishida, S. Reddy, J. Jenkins, and S. Running. "Recent Trends in Hydrologic Balance have enhanced the Terrestrial Carbon Sink in the United States." *Geophysical Research Letters* 29, no. 10 (2002): 1468.

Ney, E.P. "Cosmic Radiation and the Weather." *Nature* 183, no. 4659 (1959): 451-452.

Nobel, P. S. “Physicochemical and Environmental Plant Physiology” 3rd ed., *Elsevier Acad*., Burlington, Mass(2005): 540

Oki, T. and S. Kanae. "Global Hydrological Cycles and World Water Resources." *Science* 313, no. 5790 (2006): 1068-1072.

Oliveira, R. S., T. E. Dawson, S. S. O. Burgess, and D. C. Nepstad. "Hydraulic Redistribution in Three Amazonian Trees." *Oecologia* 145, no. 3 (2005): 354-363.

Palle, E., P. Montanes-Rodriguez, P. R. Goode, S. E. Koonin, M. Wild, and S. Casadio. "A Multi-Data Comparison of Shortwave Climate Forcing Changes." *Geophysical Research Letters* 32, no. 21 (2005): L21702.

Raj, J.K. “Clay mineral in the weathering profile of graphite-quartz-muscovite schist in Kajang area, Selangor” . *Geological Society of Malaysia Warta Geologi*, 21, (1995): 1-8.

Rozanski, K., L. Araguás-Araguás, and R. Gonfiantini. "Isotopic Patterns in Modern Global Precipitation." *Geophysical Monograph Series* 78, (1993): 1-36.

Saleska, Scott R., K. Didan, A. R. Huete, and H. R. da Rocha. "Amazon Forests Green-Up during 2005 Drought." *Science* 318, no. 5850 (2007): 612-612.

Schellekens, J., F. N. Scatena, L. A. Bruijnzeel, and A. J. Wickel. "Modelling Rainfall Interception by a Lowland Tropical Rain Forest in Northeastern Puerto Rico." *Journal of Hydrology* 225, no. 3-4 (1999): 168-184.

Schlesinger, W. H. "Biogeochemistry: An Analysis of Global Change." Academic Press. UK. (1991): 302-303.

Schulte, P., R. van Geldern, Heiko Freitag, A. Karim, P. Negrel, E. Petelet-Giraud, A. Probst, J. Probst, K. Telmer, J. Veizer and J.A.C. Barth "Applications of Stable Water and Carbon Isotopes in Watershed Research: Weathering, Carbon Cycling, and Water Balances." *Earth-Science Reviews* 109, no. 1-2 (2011): 20-31.

Sellers, P. J., R. E. Dickinson, D. A. Randall, A. K. Betts, F. G. Hall, J. A. Berry, G. J. Collatz, A.S. Denning, H.A Mooney, C.A Nobre, N.Sato, C.B. Field, A. Henderson-Sellers. "Modeling the Exchanges of Energy, Water, and Carbon between Continents and the Atmosphere." *Science* 275, no. 5299 (1997): 502-509.

Stauffer, P.H. Cenozoic. In: Gobett D.J. & Hutchinson, C.S. (eds) *Geology of the Malay Peninsula*. Wiley-Interscience, New York, (1973): 143-176

Stevens, B and S. Bony. "Water in the atmosphere." *Physics Today* 66, no. 6 (2013): 29-34.

Stibig, H. J., A. S. Belward, P. S. Roy, U. Rosalina-Wasrin, S. Agrawal, P. K. Joshi, Hildanus, R. Beuchle, S. Fritz, S. Mubareka and C. Giri "A Land-Cover Map for South and Southeast Asia Derived from SPOT-VEGETATION Data." *Journal of Biogeography* 34, no. 4 (2007): 625-637.

Sud, Y. C., G. K. Walker, V. M. Mehta, and William K. -M Lau. "Relative Importance of the Annual Cycles of Sea Surface Temperature and Solar Irradiance for Tropical Circulation and Precipitation: A Climate Model Simulation Study." *Earth Interactions* 6, (2002).

Suhaila, J., S. M. Deni, W. Z. W. Zin, and A. A. Jemain. "Trends in Peninsular Malaysia Rainfall Data during the Southwest Monsoon and Northeast Monsoon Seasons: 1975–2004." *Sains Malaysiana* 39, no. 4 (2010): 533-542.

Suhaila, J., S. M. Deni, W. Z. W. Zin, and A. A. Jemain. "Spatial Patterns and Trends of Daily Rainfall Regime in Peninsular Malaysia during the Southwest and Northeast Monsoons: 1975-2004." *Meteorology and Atmospheric Physics* 110, no. 1-2 (2010): 1-18.

Susan, S., ed. Climate change 2007- the physical science basis: *Working group I contribution to the fourth assessment report of the IPCC*. Vol. 4.Cambridge University Press (2007):129

Svensmark, H. "Influence of Cosmic Rays on Earth's Climate." *Physical Review Letters* 81, no. 22 (1998): 5027-5030.

Syakir, MI., K. Lee, I. D. Clark and J. Veizer “A Reconnaissance Study of Water and Carbon Fluxes in a Tropical Watershed of Peninsular Malaysia: Stable Isotope Constraints”. *Hydrology in a Changing World: Environmental and Human Dimensions. Proceedings of FRIEND-Water 2014, Hanoi, Vietnam*, IAHS Publication 363, (2014)

Taiz. L and E. Zeiger. *Plant Physiology*, 4th ed. Sinamer Associates Inc. (2006):69

Takanashi, S., Yoshiko K., S. Ohkubo, N. Matsuo, M. Tani, and A. R. Nik. "Water and Heat Fluxes Above a Lowland Dipterocarp Forest in Peninsular Malaysia." *Hydrological Processes* 24, no. 4 (2010): 472-480.

Tani, M., A. R. Nik, Y. Yasuda, S. Noguchi, S. A. Shamsuddin, M. M. Sahat, and S. Takanashi. "Long-Term Estimation of Evapotranspiration from a Tropical Rain Forest in Peninsular Malaysia." *Water Resources Systems - Water Availability and Global Change* no. 280 (2003): 267-274.

Telmer, K. and J. Veizer. "Isotopic Constraints on the Transpiration, Evaporation, Energy, and Gross Primary Production Budgets of a Large Boreal Watershed: Ottawa River Basin, Canada." *Global Biogeochemical Cycles* 14, no. 1 (2000): 149-165.

Tinsley, B.A and F. Yu. "Effect of Particle Flux Variations on Clouds and Climate." (2003).

Twining, J., D. Stone, C. Tadros, A. Henderson-Sellers, and A. Williams. "Moisture Isotopes in the Biosphere and Atmosphere (MIBA) in Australia: A priori estimates and preliminary observations of stable water isotopes in soil, plant and vapour for the Tumbarumba Field Campaign." Global and Planetary Change 51, no. 1 (2006): 59-72.

Van Dijk, A. I. J. M. and L. A. Bruijnzeel. "Modelling Rainfall Interception by Vegetation of Variable Density using an Adapted Analytical Model. Part 1. Model Description." *Journal of Hydrology* 247, no. 3 (2001): 230-238.

Veizer, J. "Celestial Climate Driver: A Perspective from Four Billion Years of the Carbon Cycle." *Geoscience Canada* 32, no. 1 (2005): 13-28.

Wasko, C. and A. Sharma. "Effect of Solar Variability on Atmospheric Moisture Storage." *Geophysical Research Letters* 36, (2009): L03703.

Wong, C. I., J. M. Sharp, N. Hauwert, J. Landrum, and K. M. White. "Impact of urban development on physical and chemical hydrogeology." *Elements 8*, no. 6 (2012): 429-434.

Wong, C. L., R. Venneker, S. Uhlenbrook, A. B. M. Jamil, and Y. Zhou. "Variability of Rainfall in Peninsular Malaysia." *Hydrol.Earth Syst.Sci.Discuss* 6, (2009): 5471-5503.

Global Atmosphere Watch (GAW). “Manual for GAW Precipitation Chemistry Programme”. *World Meteorological* Organization (WMO) (2004): 9.

Yin, E. H. *Geological Map of Kuala Lumpur*. Geological Survey of Malaysia. (1976).

Yu, Q. and S. Tremaine. "Observational Constraints on Growth of Massive Black Holes." *Monthly Notices of the Royal Astronomical Society* 335, no. 4 (2002): 965-976.

Yusop, Z., S. Y. Cham, and J. H. Chong. "Throughfall, Stemflow and Interception Loss of Old Rubber Trees." *Jurnal Kejuruteraan Awam* 15, no. 1 (2003): 24-33.

Zhao, L., J. Wang, and H. Zhao. "Solar Cycle Signature in Decadal Variability of Monsoon Precipitation in China." *Journal of the Meteorological Society of Japan* 90, no. 1 (2012): 1-9.

Zheng, D.L., Prince, S.D., Wright, R.(2001) *NPP Multi-biome: Gridded estimates from selected regions worldwide, 1989-2001*. Oak Ridge Natl. Lab. Distrib. Active Archive Cent, Oak Ridge, Tenn, Available at http://www.daac.ornl.gov

Zheng, D., S. Prince, and R. Wright. "Terrestrial Net Primary Production Estimates for 0.5 Grid Cells from Field observations—a Contribution to Global Biogeochemical Modeling." *Global Change Biology* 9, no. 1 (2003): 46-64.

Zhu, C. and F. W. Schwartz. "Hydrogeochemical Processes and Controls on Water Quality and Water Management." *Elements* 7, no. 3 (2011): 169-174.

Appendices

Appendix 1: Langat rainfall data 1980-2011 (Department of Irrigation and Drainage Malaysia)

Year	Jan	Feb	Mar	Apr	May	Jun	Jul	Aug	Sep	Oct	Nov	Dec	Monthly Average	Total
1980	75.00	140.00	269.00	196.50	313.00	160.00	245.50	308.00	311.50	387.00	282.50	258.50	245.54	2946.50
1981	68.00	166.00	97.50	355.00	508.00	26.00	167.00	159.50	299.50	185.00	285.50	179.00	208.00	2496.00
1982	70.00	229.50	189.50	447.50	340.00	287.00	210.50	144.00	139.00	383.00	439.50	107.00	248.88	2986.50
1983	33.00	18.50	125.00	250.50	383.00	176.00	379.30	276.20	347.80	183.80	378.90	133.60	223.80	2685.60
1984	123.00	329.50	252.50									0.00	176.25	705.00
1985	34.60	199.90	100.10	162.50	317.50	32.60	222.50	181.20	176.40	176.70	342.00	215.80	180.15	2161.80
1986	35.50	94.50	219.00	289.00	304.00	76.50	73.50	49.00	197.00	318.00	213.00	209.50	173.21	2078.50
1987	78.50	13.00	7.00	12.50	129.50	4.50	177.50	187.50	504.00	525.50	154.50	228.50	168.54	2022.50
1988	56.00	248.00	115.00	86.50	27.50							97.00	105.00	630.00
1989	90.00	52.00	209.50	256.50	234.50	257.50	225.50	155.00	423.00	473.00	229.00	15.00	218.38	2620.50
1990	34.00	20.50	46.50	56.00	140.50	112.00	114.00	55.50	168.00	203.50	59.50	140.00	95.83	1150.00
1991	17.50	45.50	187.50	204.00	172.50	116.00	22.00	123.00	93.50	155.50	77.00	120.00	111.17	1334.00
1992	41.00	55.00	79.00	113.50	131.50	36.00	90.00	31.00	78.00	74.00	135.50	74.00	78.21	938.50
1993	23.00	59.00	58.50	48.50	112.50	86.50	102.00	303.20	301.20	291.00	402.00	324.10	175.96	2111.50
1994	34.00	55.50			0.00	199.50	29.50	219.50	83.50	310.00	129.50	242.50	130.35	1303.50
1995	99.00	30.50	423.00	228.50	267.50	405.00	80.50	300.00	35.00	374.00	292.50	0.00	211.29	2535.50
1996	63.50	0.00	251.50	373.00	233.50			175.00	148.00	236.00	196.50	318.00	199.50	1995.00
1997	130.00	243.00	285.50	266.50	41.50	123.00	208.00			424.00	274.00	103.00	209.85	2098.50
1999				28.50	272.00	95.00	257.00	220.50	267.00	265.50	376.00	359.00	237.83	2140.50
2000	128.00	243.00	279.00	366.50	175.50	187.50	61.00	192.00	426.00	274.00	268.50	412.00	251.08	3013.00
2001	272.00	140.50	94.00	287.00	200.00	156.50	208.00	90.00	345.50	255.50	135.00	0.00	182.00	2184.00
2002	26.50	8.50	96.00	386.50	243.50	212.00	121.50	257.00	247.50	284.50	429.50	102.00	201.25	2415.00
2003	56.00	178.00	180.50	199.00	48.50	127.00	159.50	151.50	210.00	312.00	347.50	165.50	177.92	2135.00
2004	45.00	85.00	363.50	223.00	181.50	47.50	303.00	53.50	215.50	301.50	508.50	37.50	197.08	2365.00
2005	2.50	244.00	91.00	168.50	367.50	27.00	237.00	273.00	168.50	272.50	212.50	438.00	208.50	2502.00
2006	219.50	97.50	220.00	530.50	233.50	174.50	63.50	185.00	159.00	104.50	38.00	28.50	171.17	2054.00
2007	181.00	128.50	111.00	328.00	100.50	246.50	129.50	215.50	289.50	367.50	321.50	183.50	216.88	2602.50
2008	165.50	174.50	163.50	421.00	114.00	348.50	119.00	205.50	86.50	729.10	243.10	129.00	241.60	2899.20
2009	63.50	192.50	316.50	257.00	109.50	130.50	134.00	269.00	213.00	380.00	284.50	105.50	204.63	2455.50
2010	112.00	54.50	293.00	242.50	102.50	168.50	263.00	340.50	314.50	185.50	298.00	194.00	214.04	2568.50
2011	219.50	168.50	245.50	156.50	319.50	162.50	161.00	287.00	188.00	238.00	214.50		214.59	2360.50
Average														2145

Appendix 2: Record of average total rainfall, Kelantan (Department of Irrigation and Drainage Malaysia)

a. Record of Rainfall in Kelantan Basin base on 13 stations averages

Year	Jan	Feb	Mar	Apr	May	Jun	Jul	Aug	Sep	Oct	Nov	Dec	Monthly Average (m^3/s)	Annual Total Rainfall (mm)
1980	58.33	84.74	64.40	123.71	204.61	155.25	149.04	210.13	184.35	238.90	257.39	241.76	164.38	1972.61
1981	54.44	85.44	64.24	136.60	186.83	66.53	164.21	66.33	175.64	252.21	321.24	256.23	152.49	1829.93
1982	15.75	38.56	79.49	190.91	190.59	158.68	166.61	238.06	188.32	242.70	236.52	456.28	183.54	2202.47
1983	65.00	8.05	54.50	30.08	140.13	112.50	244.81	224.21	206.68	183.80	160.59	820.41	187.56	2250.76
1984	185.30	254.75	173.50	169.15	212.30	143.40	209.09	92.55	210.68	215.00	141.08	388.54	199.61	2395.34
1985	72.46	134.67	284.46	132.33	307.64	44.82	141.67	214.05	292.82	297.88	260.09	207.85	199.23	2390.72
1986	82.41	7.73	89.50	144.30	123.05	118.94	134.06	96.55	292.23	324.36	532.84	328.51	189.54	2274.48
1987	109.81	4.54	131.56	107.01	156.21	191.17	141.92	193.59	244.88	225.40	329.18	549.20	198.71	2384.48
1988	93.55	159.77	92.77	127.18	220.95	183.77	169.78	248.22	271.32	128.77	883.86	212.32	232.69	2792.27
1989	149.93	22.55	107.86	145.82	133.19	171.01	152.77	123.20	189.70	288.10	225.78	144.02	154.49	1853.93
1990	188.56	94.10	45.91	188.92	141.05	85.15	165.46	138.90	204.03	218.73	278.11	274.92	168.65	2023.85
1991	269.15	53.05	78.52	142.00	279.82	105.88	126.51	210.15	187.29	225.14	400.73	492.11	214.20	2570.34
1992	68.65	82.27	42.73	94.17	143.65	239.51	208.05	104.81	149.73	219.81	471.89	343.58	180.74	2168.84
1993	118.38	70.88	193.83	165.73	183.05	215.86	134.50	216.36	320.82	438.84	311.35	663.63	252.77	3033.22
1994	95.38	80.88	270.46	135.50	285.83	274.00	130.33	272.23	326.17	340.63	766.17	208.25	265.48	3185.81
1995	220.36	75.59	97.50	107.59	182.91	255.32	182.90	257.75	202.55	226.59	362.60	322.32	207.83	2493.98
1996	139.77	95.33	56.05	144.95	149.75	201.11	179.65	259.73	215.59	331.27	305.32	504.64	215.26	2583.16
1997	24.21	152.79	69.00	151.63	86.92	178.33	157.20	130.40	143.64	191.97	209.98	371.17	155.60	1867.23
1998	137.17	19.00	39.68	56.80	134.75	127.82	128.90	242.49	212.38	253.11	189.69	446.92	165.73	1988.70
1999	240.55	171.24	152.89	203.04	207.60	189.26	141.55	202.98	165.72	192.35	266.04	343.96	206.43	2477.19
2000	205.22	151.38	204.08	233.08	121.05	127.08	94.21	158.79	251.75	207.75	505.13	291.04	212.55	2550.55
2001	249.08	72.33	215.29	100.96	167.50	112.50	181.42	148.13	255.79	331.31	263.08	433.90	210.94	2531.28
2002	97.63	36.00	74.78	152.78	151.71	171.88	158.83	203.35	210.28	295.98	225.64	267.18	170.50	2046.01
2003	131.89	80.44	170.04	96.17	119.42	178.17	203.42	215.68	184.95	305.13	341.52	467.02	207.82	2493.84
2004	212.79	34.21	184.65	105.66	163.97	66.81	168.61	169.48	278.18	321.74	287.32	342.44	194.65	2335.84
2005	24.64	19.50	98.95	76.16	217.54	129.29	118.29	213.21	209.88	260.50	465.08	530.45	196.96	2363.50
2006	192.29	298.04	81.21	156.29	281.63	161.00	176.00	155.43	250.50	243.09	212.25	331.92	211.64	2539.65
2007	316.75	49.17	108.13	146.77	209.33	147.38	196.25	166.58	221.08	265.46	262.75	607.41	224.75	2697.06
2008	49.21	52.21	63.17	45.13	91.17	108.13	69.67	250.71	156.58	296.46	523.04	383.21	174.06	2088.67
2009	245.92	51.33	261.46	155.33	206.75	174.46	174.58	201.96	197.79	264.75	637.08	315.21	240.55	2886.63
2010	174.08	56.58	119.54	113.50	154.67	225.67	201.00	204.33	243.33	279.92	327.13	291.96	199.31	2391.71
2011	342.14	55.27	291.00	108.41	157.08	227.33	128.95	200.06	153.95	228.64	514.11	176.00	215.24	2582.93
Average													199	2383

b. Record of total average rainfall (mm yr^{-1}) in 13 stations, Kelantan Basin

Year	Blau	Brook	Upper Chiku	Gua Musang	Balai Polis Bertam	Dabong	Ladang Kuala Balah	Lalok	Ladang Lapan Kabu	Lubok Bungor	Kuala Krai	Kg Peringat	Teratak Pulai
1980	1746	1104	357	2481	1495	1792	1459	1676	2095	2061	327	2534	2316
1981				2157	1160	1354	1981	1701	1545	2414	1065	2356	1385
1982	1163	2179		2146	2061	2127	1893	1920	2117	3199	1828	2396	1276
1983	722	744	1670	2027	1279	1985	3076	2263	2622		2523	3127	2960
1984	2200	2084	2197	2763	1691	766	2722	698	2904	3429	2152	2499	2658
1985	1285	1547	1203	2237	2126	2750	2902	2298	2365	3364	2529	3006	2801
1986	1919	749		2479	1638	1542	2799	2999	2267	3134	2294	175	210
1987	1324	857		1377	2470	1105	3523	2139	2193	3457	2308	2285	2062
1988	1474	1990		2548	2490	2895	3464	1056	3032	4238	2899	3530	3138
1989	470	1385		1918	2250	1709	2369	772	1599	2734	1466	2175	2160
1990	2014	1341		2216	646	1783	2432	2123	2088	3379	687	1911	1757
1991	2240	1818		2448	2247	1965	2612	2274	3033	3274	2573	2790	2513
1992	1946	2413		1846	1411	2075	3059	1894	2459	3330	1125	2186	1734
1993	2478	3078	885	3082	2921	2784	1748	3065	3398	3575	3149	3166	2719
1994	2159	4183	3082	2685	2885	1880	3346	2934	2925	4267	2757	4509	3983
1995	2045	2729	2816	2423	2441	2299	2937	2260	875	3593	1766	2667	2595
1996	2726	2547	2569	2421	2490	2259	3023	2649	1802	3633	1551	2922	2888
1997	702	2513	2240	1859	1764	2111	2468	2061	1287	750	1435	2535	1751
1998	1287	1758	1880	1869	2164	2627	2730	1917	2107	190	533	1995	1507
1999	2424	2935	1951	2423	2290	2819	3108	1691	1031	1301	1170	3621	3167
2000	2332	2470	2936	1465	2002	2729	3187	2392	2014	2853	2052	3787	3838
2001	2056	2126	2910	2244	1542	2739	3724	2629	2293	3089	2648	2702	3095
2002	2491	2164	2599	2146	1439	1956	2220	1771	1307	1730	1288	2318	2527
2003	1820	2214	2995	2380	1371	2618	2936	2416	1671	3498	2790	2753	2594
2004	1798	1315	2664	2269	1958	1410	2933	2936	2562	2848	2001	2537	2488
2005	2079	1889	1547	2019	1732	2272	3522	1298	2482	3394	2474	2887	2883
2006	2257	2570	1590	2632	1551	2239	2840	2816	2395	3360	1756	2127	2366
2007	1970	2510	3512	2199	2009	3140	2582	1783	2928	4027	3087	2434	2525
2008	1080	1658	2937	2340	1163	1399	1809	1129	2908	2150	2994	3431	3360
2009	2208	2250	3070	2505	2339	2691	3335	3069	2953	3552	3249	3598	4081
2010	2200	2323	2919	2020	1905	2459	1759	2145	2044	2986	2107	2675	2945
2011	1705	1495	4016	1597	2303	2182	2999	2311	2554	3469	1834	4047	3960
Average	1817	2030	2371	2225	1913	2139	2734	2096	2245	2976	2013	2740	2570

Appendix 2b

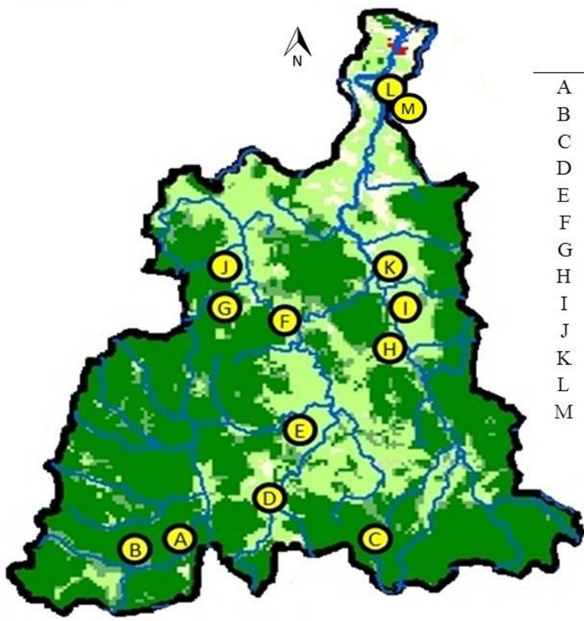

	DID Code	Stations	n	Rainfall (mm)		Remarks
A	4717001	Blau	31	1816.56	± 200	Upstream
B	4614001	Brook	31	2029.98	± 260	Upstream
C	4721001	Upper Chiku	23	2371.32	± 358	Upstream
D	4819027	Gua Musang	32	2225.48	± 128	Upstream
E	5120025	Balai Polis Bertam	32	1913.39	± 182	Upstream
F	5320038	Dabong	32	2139.25	± 198	Upstream
G	5419036	Ladang Kuala Balah	32	2734.08	± 203	Midstream
H	5322044	Lalok	32	2096.27	± 222	Midstream
I	5422046	Ladang Lapan Kabu	32	2245.28	± 217	Midstream
J	5518035	Lubok Bungor	31	2976.49	± 332	Midstream
K	5522047	Kuala Krai	32	2012.83	± 273	Midstream
L	6022001	Kg Peringat	32	2739.69	± 270	Downstream
M	6023072	Teratak Pulai	32	2569.81	± 294	Downstream

Source: Drainage and Irrigation Department of Malaysia (DID)

Appendix 3: Record of river discharge, Langat (Department of Irrigation and Drainage Malaysia)

Dengkil Station (m^3/s)													
Year	Jan	Feb	Mar	Apr	May	Jun	Jul	Aug	Sep	Oct	Nov	Dec	Average
1980	12.20	8.89	25.39	31.06	24.31	24.14	15.97	13.27	15.44	19.62	53.04	41.10	23.70
1981	20.03	36.77	33.66	29.27	73.32	38.02	12.51	9.43	20.79	26.06	25.06	23.16	29.01
1982	11.07	18.98	23.28	16.69					20.32	35.69	98.41	65.42	36.23
1983	23.45	12.33	22.51	25.51	31.84	15.40	18.38	28.88	44.42	18.76	33.43	20.60	24.63
1984	30.20	59.11	37.91	79.63	29.27	25.15	23.08	13.70	17.05	9.84	92.03	81.01	41.50
1985	22.86	36.63	50.45	28.63	41.64	12.46	13.52	7.45	9.67	30.02	59.86	163.90	39.76
1986	35.16	11.82	46.06	69.44	50.83	19.03	12.60	6.70	8.12	18.42	38.93	26.81	28.66
1987	7.66	5.56	5.93	12.98	14.86	10.45	6.83	19.23	28.62	66.23	73.47	50.43	25.19
1988	19.99	46.96		40.36	25.97	16.48	23.16	22.94	81.41	21.93	69.02	32.52	36.43
1989	17.49	19.86	31.93	45.53	36.14	34.44	22.66		73.21	83.69	69.07	43.59	43.42
1990			15.31	14.64	23.65	7.88	9.14	7.95	13.08	30.30	36.26	18.03	17.62
1991	10.24				71.79	14.79	15.87	16.98	25.66	67.58	79.30	73.69	41.77
1992	65.76	49.43	33.44	30.14	38.00	33.20	13.59	20.69				65.95	38.91
1993	27.57	19.18	25.93	44.59	52.13	21.74	17.29	6.38	22.76	44.37	68.83		31.89
1994	21.00	20.25	35.54	39.22	27.84	14.71	5.51	5.81	20.35	23.24	36.80	47.58	24.82
1995	16.26	5.69	33.55	70.56	46.98			29.19	5.80	23.27	50.89	61.62	34.38
1996	32.95	15.76	32.01	26.85	16.06	23.32	27.99	32.68	32.25	39.43	24.41	96.46	33.35
1997	15.84	31.60	54.04	63.52	47.06	31.68	37.66	26.71	32.74	86.34	63.17		44.58
1998	39.99	19.54	35.63	46.17	36.62	35.81	33.40	51.29	9.31	4.17	5.12	9.24	27.19
1999			50.85	42.55	65.32		56.82	15.01	38.06	87.65	30.97		48.40
2000		54.08	73.56	56.73	31.95	27.61	18.28	29.67	38.00	150.29	80.55	59.24	56.36
2001	43.10							6.57	8.86	14.54	28.27	17.58	19.82
2002	8.01	6.65	9.85	26.55	26.21	9.87	9.78	14.78	15.52	13.89	79.80	31.73	21.05
2003	19.61	29.63	29.83	39.06	16.76	13.97	20.51	22.09	22.34	18.68	79.55	64.60	31.39
2004	15.92	13.80	12.65	28.40	15.90	10.16	25.29	9.90	222.75	134.57	110.61	44.56	53.71
2005	7.76	14.73	13.18	23.82	14.95	6.66	15.75	13.22	12.06	23.11	44.16	54.19	20.30
2006	54.88	31.92	35.60	68.98	65.57	48.32	16.96	27.82	30.89	57.84	107.50	41.21	48.96
2007	29.82	24.22	42.17	55.05	31.84	48.76	25.53	25.67	40.50	81.96	61.85	40.85	42.35
2008	30.38	25.85	41.68	82.95	17.94	36.39	23.64	20.24	19.50	49.83	30.28	25.67	33.70
2009	23.01	34.68	80.47	71.09	24.04	19.17	18.27	26.43	33.20	31.93	68.43	44.45	39.60
2010	39.50	23.27	33.31	37.00	55.65	28.90	40.96	49.26	34.46		81.15	47.82	42.84
2011	44.44	31.14	46.55	65.94	62.44	27.47	21.60	41.81	36.41	49.70	67.48	111.16	50.51
Average	25.73	25.30	34.91	43.76	37.23	23.43	20.78	20.73	33.34	45.43	59.60	51.87	35.38

Appendix 4: Record of river discharge, Kelantan (Department of Irrigation and Drainage Malaysia)

Average River discharge (m^3/s) for Tanah Merah Station													
Years	Jan	Feb	Mar	Apr	May	Jun	Jul	Aug	Sep	Oct	Nov	Dec	Average
1980	363.10	288.80	284.50	205.10	288.80	254.80	211.90	454.00	389.00	700.60	695.30	898.80	419.56
1981	411.10	264.80	155.30	254.10	401.50	212.40	225.40	131.40	285.30	446.90	546.30	646.40	331.74
1982	272.20	138.60	117.30	321.40	423.80	443.60	303.20	316.20	409.00	541.90	630.70	1345.20	438.59
1983	503.20	239.80	159.80	99.30	168.40	188.30	274.10	345.10	407.20	369.10	452.90	2631.40	486.55
1984	626.60	859.30	719.70	539.10	634.50	518.20	459.10	359.60	460.70	533.60	438.30	1409.70	629.87
1985	487.50	446.50	843.70	370.90	623.60	355.00	242.30	241.10	507.70	923.40	690.10	777.90	542.48
1986	535.40	232.60	245.00	209.30	157.00	208.70	152.40	123.90	342.80	677.20	751.70	1821.10	454.76
1987	574.20	297.40	271.10	224.90	292.00	287.30	223.90	342.80	433.60	577.40	582.20	1783.10	490.83
1988	410.30	342.10	319.40	253.30	389.70	392.00	400.50	449.30	544.50	366.20	2150.80	1620.20	636.53
1989	769.90	358.60	281.40	290.40	282.00	350.70	322.80	262.80	361.00	544.80	499.60	358.20	390.18
1990	906.00	372.80	173.50	175.70	258.40	203.70	222.60	262.70	359.80	537.60	705.30	1407.70	465.48
1991	595.50	320.20	219.40	203.40		314.10	175.70	216.40	262.00	335.00	745.50	1234.90	420.19
1992	780.20	312.90	235.90	166.40	142.90	285.00	256.00	177.00	181.30	317.50	1262.30	1196.20	442.80
1993	552.10	292.70	364.50	305.00	304.90		372.50	292.50	484.80	903.20	1159.20	2560.30	690.15
1994	663.50	465.00	469.00	329.40	586.50		306.90	436.20	633.50	662.50	2392.90	1031.30	725.15
1995	784.90	417.70	277.60	227.70	256.30	416.70	289.00	569.70	434.80	481.80		1402.50	505.34
1996	619.10	635.00	286.50	325.10	425.50	444.50	501.90	410.10	611.40	797.40	654.10	1099.70	567.53
1997	320.70	340.00	237.80	303.00	252.90	253.80	356.20	251.60	328.30	339.90	631.20	1240.90	404.69
1998	540.60	341.90	162.50	103.30	110.60	229.20	409.60	408.10	532.80	600.60	827.90	1423.30	474.20
1999	1547.80	733.10	498.90	570.60	536.90	426.50	337.30	427.90	457.30	498.20	482.40	962.60	623.29
2000	1100.60	471.20	545.60	581.00	499.40	391.50	253.80	364.00	344.50	495.40	942.80	570.30	546.68
2001	930.30	390.70	363.80	253.80	279.90	261.30	173.20	291.10	305.90	574.50	810.80	1634.20	522.46
2002	595.80	261.30	184.30	153.40	190.50	254.50	171.30	270.90	295.90	472.40	412.90	566.80	319.17
2003	415.80	236.10	171.80	225.70	162.90	168.10	245.80	259.00	248.10	520.80	374.10	1356.30	365.38
2004	502.90	322.40	227.10	136.50	149.00	124.30	125.90	135.60	239.40	615.20	571.60	1081.40	352.61
2005	225.20	155.00	194.00	166.30	169.70	159.00	164.60	178.80	176.10	246.20	651.80	1159.00	303.81
2006	882.20	934.40	251.60	231.60	306.80	311.50	229.30	208.10	303.80	253.80	299.50	558.30	397.58
2007	1084.80	252.10	171.80	218.60	263.50	340.30	248.00	225.60	322.80	361.20	757.00	2853.20	591.58
2008	406.20	304.10	590.20	372.80	403.10	374.90	520.60	594.20	750.50	739.50	929.30	1173.80	596.60
2009	1241.90	331.70	471.60	427.60	420.80	328.00	341.50	298.70	364.10	510.90	1975.50	1080.30	649.38
2010	550.00	297.50	140.10	101.90	101.30	163.10	192.40	222.50	257.60	236.40		1249.60	319.31
2011	869.00	322.80	350.90	316.00		304.40	172.70	153.90	201.20	293.70	793.10		377.77
Average	658.39	374.35	312.05	270.71	316.10	298.85	277.58	302.53	382.40	514.84	827.24	1294.66	483.82

Appendix 5: Record of average Temperature, Relative Humidity and Global Solar Radiation, Langat (Malaysian Meteorological Department)

JABATAN METEOROLOGI MALAYSIA

Records of 24 Hour Mean Temperature

Unit : ° C

Month/ Year	JAN	FEB	MAR	APR	MAY	JUN	JUL	AUG	SEP	OCT	NOV	DEC	ANNUAL
2006	25.3	26.0	26.1	25.4	25.4	25.3	25.6	25.3	25.2	25.1	25.0	25.5	25.44
2007	25.4	25.7	25.7	25.8	26.4	25.7	25.4	25.2	25.4	24.9	24.9	24.9	25.45
2008	25.4	25.4	25.2	25.4	25.8	25.2	25.0	25.2	25.2	25.4	25.3	25.1	25.29
2009	25.2	25.3	25.3	26.1	26.7	26.2	25.7	25.6	25.3	25.6	25.0	25.6	25.63
2010	26.0	26.6	26.8	26.9	27.0	26.0	25.3	25.7	25.5	25.7	25.3	24.7	25.95
2011	24.5	25.8	25.3	25.8	26.0	25.8	25.4	25.4	25.4	25.3	25.1	25.1	25.39
Average													25.53

Records of 24 hour Mean Relative Humidity

Unit : %

Month/ Year	JAN	FEB	MAR	APR	MAY	JUN	JUL	AUG	SEP	OCT	NOV	DEC	ANNUAL
2006	80.2	75.9	78.9	85.0	85.1	84.0	82.9	83.3	83.6	85.0	85.6	80.8	82.5
2007	80.3	76.2	81.2	83.3	82.4	84.3	83.9	82.7	83.0	85.7	85.5	82.2	82.6
2008	79.9	74.3	81.0	85.1	82.9	84.7	83.7	82.5	82.6	84.4	85.9	81.7	82.4
2009	75.5	80.9	84.1	81.5	79.6	81.6	81.1	83.2	83.3	82.5	86.0	79.0	81.5
2010	77.1	76.3	77.9	81.0	82.1	83.6	83.5	82.8	84.1	82.2	84.3	84.9	81.6
2011	82.3	76.2	83.5	83.9	83.1	82.7	81.9	83.9	83.4	83.6	85.4	82.7	82.7
Average													82.22

Records of Mean Daily Global Radiation

Unit : MJm-2

Month/ Year	JAN	FEB	MAR	APR	MAY	JUN	JUL	AUG	SEP	OCT	NOV	DEC	ANNUAL
2006	15.99	19.30	19.51	17.27	15.71	16.35	15.40	16.00	16.88	15.49	17.05	16.17	16.8
2007	15.08	19.90	18.22	18.04	18.44	16.99	15.77	17.31	16.95	15.69	14.92	14.72	16.8
2008	17.59	19.39	17.76	16.99	16.81	16.74	16.46	16.93	17.26	17.79	15.64	15.65	17.1
2009	18.78	19.00	17.78	19.92	19.91	17.97	16.39	16.98	16.24	17.62	13.75	16.57	17.6
2010	18.51	21.45	20.60	19.98	19.07	16.58	15.95	17.31	18.30	17.36	16.10	13.98	17.9
2011	13.11	20.31	16.92	18.23	18.66	17.09	16.17	17.28	16.89	18.21	15.26	13.51	16.8
Average													17.16

Appendix 6: Record of average temperature for Kelantan watershed at Kota Bharu (Malaysian Meteorological Department)

Unit : ° C

Month/ Year	JAN	FEB	MAR	APR	MAY	JUN	JUL	AUG	SEP	OCT	NOV	DEC	ANNUAL
1980	25.70	26.30	27.20	28.00	28.50	27.50	27.00	26.30	26.70	26.70	25.80	25.20	26.74
1981	25.30	26.30	27.10	27.60	27.90	28.00	27.40	27.90	26.90	26.80	26.00	25.40	26.88
1982	25.40	26.10	26.90	27.30	28.20	27.50	26.70	26.70	26.90	26.40	26.40	26.20	26.73
1983	26.10	26.60	27.50	28.30	28.90	28.10	27.20	27.20	26.90	26.70	26.20	25.30	27.08
1984	25.40	25.60	26.30	27.50	27.30	27.00	26.60	26.80	26.10	26.50	26.10	25.60	26.40
1985	25.50	26.40	26.70	27.40	27.30	27.70	26.50	26.30	26.40	26.40	25.90	25.50	26.50
1986	25.30	25.80	26.90	28.20	27.80	27.40	27.50	27.30	26.50	26.50	25.80	26.10	26.76
1987	25.80	25.70	27.70	28.40	28.50	28.10	27.90	27.30	27.00	27.20	26.90	25.90	27.20
1988	26.40	26.80	27.70	28.50	27.80	27.40	26.90	27.00	26.80	26.70	25.80	25.10	26.91
1989	26.00	25.50	26.70	27.80	27.80	27.50	27.30	26.60	26.60	26.50	26.30	26.40	26.75
1990	25.90	27.00	27.20	28.00	28.30	28.00	27.00	27.60	26.90	27.00	27.00	26.50	27.20
1991	26.20	26.50	27.10	28.10	28.40	28.20	27.70	27.10	27.00	26.70	26.10	26.60	27.14
1992	26.10	26.70	27.70	28.70	28.80	28.00	27.40	27.50	27.40	26.90	25.90	26.30	27.28
1993	26.20	25.70	26.50	27.30	28.50	28.30	27.60	27.00	26.70	26.50	26.10	26.10	26.88
1994	26.00	26.50	26.70	27.90	27.60	27.30	27.30	27.00	26.80	26.70	26.00	26.50	26.86
1995	26.50	26.50	27.20	28.40	28.30	28.20	27.40	27.20	27.00	26.90	25.90	25.90	27.12
1996	25.60	26.00	27.10	28.60	28.30	28.10	27.90	27.10	26.90	26.70	26.10	25.30	26.98
1997	25.80	26.50	27.20	27.80	28.90	28.00	27.50	27.50	27.30	27.30	26.30	26.60	27.23
1998	27.70	27.90	28.70	29.30	29.70	28.30	28.00	27.60	27.10	27.30	26.60	26.10	27.86
1999	26.70	26.40	27.50	27.90	27.80	27.50	27.10	27.00	27.10	26.90	26.30	25.30	26.96
2000	26.40	26.50	27.20	28.00	28.60	27.90	28.20	28.00	27.70	27.70	26.50	26.60	27.44
2001	26.50	26.60	27.10	28.40	28.30	28.30	28.30	27.70	27.40	27.20	26.40	26.90	27.43
2002	26.50	26.50	27.50	28.60	28.60	28.40	28.40	27.60	27.40	27.40	26.70	27.40	27.58
2003	26.90	26.90	27.70	28.80	28.50	28.10	27.50	27.80	27.50	26.70	26.70	26.20	27.44
2004	26.80	26.90	28.20	29.00	28.90	28.30	27.60	27.50	27.30	26.70	26.80	26.30	27.53
2005	25.90	27.30	27.70	28.30	28.10	27.60	27.50	27.60	27.50	26.50	26.70	25.60	27.19
2006	26.10	26.80	27.20	28.20	27.50	27.50	27.50	27.60	26.90	27.00	26.50	26.70	27.13
2007	26.20	26.40	27.30	28.10	27.90	28.30	27.70	27.30	27.10	26.70	26.50	26.70	27.18
2008	26.10	26.30	27.10	28.00	27.70	27.60	27.30	27.30	27.40	27.60	26.10	25.60	27.01
2009	25.30	26.70	27.00	27.80	27.70	28.40	27.80	27.70	27.40	26.60	26.10	26.00	27.04
2010	26.20	26.80	27.40	28.70	29.10	28.20	27.70	27.80	27.50	27.30	26.40	25.70	27.40
2011	26.12	26.68	26.52	27.84	28.19	27.83	27.41	27.38	27.11	26.38	26.30	26.17	26.99

Appendix 7: Record of average relative humidity for Kelantan watershed measured at Kota Bharu (Malaysian Meteorological Department)

Unit : %													
Month/ Year	JAN	FEB	MAR	APR	MAY	JUN	JUL	AUG	SEP	OCT	NOV	DEC	ANNUAL
1980	83.6	83.3	82.0	82.2	81.9	85.1	85.5	84.1	84.9	86.3	89.0	87.3	84.6
1981	80.3	82.8	80.5	83.2	84.0	81.3	81.8	79.9	83.4	85.1	87.4	82.2	82.7
1982	79.8	81.3	80.2	83.4	79.7	82.5	83.3	82.2	81.3	84.1	87.1	82.7	82.3
1983	80.6	79.7	79.5	78.5	79.2	80.5	83.7	84.1	84.3	84.3	84.0	84.8	81.9
1984	82.2	83.5	83.6	82.2	82.9	83.1	84.2	85.3	87.1	87.2	88.5	88.0	84.8
1985	81.5	84.4	84.4	83.5	84.9	81.4	81.5	83.5	83.2	84.2	87.9	84.2	83.7
1986	79.8	78.7	79.1	77.3	80.2	80.8	80.3	80.1	83.7	84.9	86.5	81.1	81.0
1987	79.1	78.5	78.2	77.8	76.9	80.4	79.2	81.5	82.8	83.9	84.0	84.8	80.6
1988	81.3	82.8	81.0	80.3	82.2	79.8	83.4	83.3	84.7	82.3	87.5	81.6	82.5
1989	82.4	78.7	79.4	78.5	79.6	77.6	81.0	81.5	82.6	84.0	84.5	77.3	80.6
1990	80.0	77.8	78.5	81.2	80.1	80.6	80.6	80.9	81.5	83.7	81.3	80.3	80.5
1991	83.1	79.4	80.2	79.7	80.3	81.5	80.8	82.3	82.9	83.8	84.5	80.7	81.6
1992	79.2	81.3	78.7	78.3	77.6	81.0	81.0	79.3	79.8	81.0	84.6	81.5	80.3
1993	81.4	80.1	82.1	83.0	78.8	78.0	79.7	81.9	82.1	85.0	87.4	84.3	82.0
1994	80.7	82.2	84.6	81.5	82.0	82.4	83.1	81.6	82.3	84.2	87.4	82.1	82.8
1995	79.5	80.2	80.7	78.4	80.0	80.2	80.4	82.6	83.3	84.7	89.4	83.6	81.9
1996	79.5	78.7	79.2	77.2	78.1	80.3	79.9	81.7	81.5	83.8	87.0	87.7	81.2
1997	79.5	83.0	80.9	82.5	78.4	81.2	82.5	82.9	85.7	85.9	90.1	86.2	83.2
1998	82.1	80.0	77.9	78.0	79.5	80.8	81.0	82.7	85.3	84.7	87.8	88.7	82.4
1999	84.3	84.0	83.2	81.2	82.1	82.1	83.3	83.1	83.4	85.6	87.8	87.5	84.0
2000	81.5	82.6	82.6	82.4	79.3	78.9	80.2	77.6	81.9	81.9	88.2	86.0	81.9
2001	85.3	81.7	84.4	81.4	82.5	79.4	80.1	82.6	82.8	85.0	87.3	82.0	82.9
2002	79.8	80.1	79.8	78.5	82.2	80.9	78.7	80.8	80.8	82.5	87.7	85.6	81.5
2003	79.3	80.1	80.7	78.1	80.7	79.9	82.3	82.0	80.7	85.9	88.1	83.6	81.8
2004	80.4	78.9	78.1	76.5	78.5	79.0	80.6	82.6	82.0	85.7	86.6	82.7	81.0
2005	80.5	78.6	78.2	79.1	77.8	78.8	78.3	77.8	77.3	82.5	81.1	84.7	79.5
2006	78.5	78.2	78.4	75.8	78.8	80.7	80.3	76.3	82.2	82.0	86.6	81.1	79.9
2007	80.3	76.9	79.4	78.1	79.9	78.6	78.7	77.9	79.7	82.6	81.3	78.8	79.4
2008	81.0	76.1	78.6	78.5	79.7	78.5	78.1	77.5	76.8	79.0	85.7	84.1	79.5
2009	79.4	76.9	81.3	80.3	80.7	77.5	77.6	78.7	80.5	85.1	87.5	82.5	80.7
2010	80.7	80.8	77.8	78.4	79.1	76.7	77.8	78.0	78.3	81.0	85.2	84.8	79.9
2011	77.8	75.2	83.3	77.2	77.2	78.0	81.4	80.2	81.4	85.5	86.2	83.8	80.6

Appendix 8: Record of Global Solar Radiation (GSR) for Kelantan watershed at Kota Bharu (Malaysian Meteorological Department)

Records of mean monthly Global Solar Radiation (GSR)													
Unit : MJm^{-2}													
Month/ Year	JAN	FEB	MAR	APR	MAY	JUN	JUL	AUG	SEP	OCT	NOV	DEC	ANNUAL
1980	16.75	17.40	19.43	20.71	19.04	15.77	17.24	17.37	17.90	17.47	12.28	9.71	16.76
1981	16.16	17.14	20.19	19.10	18.33	17.07	16.73	16.89	16.96	16.35	12.25	12.99	16.68
1982	16.41	18.54	19.27	18.09	19.07	16.07	16.59	17.18	17.83	17.15	15.76	11.94	16.99
1983			20.03	17.07			17.77	19.33	19.67	21.14		8.77	17.68
1984	13.05	13.73	18.40	19.89	17.57	16.93	17.62	18.07	18.62	18.06	15.03		17.00
1985	17.37	18.01				16.87	17.37	16.44	17.27	16.54	12.45	11.55	15.99
1986	13.70	18.00	16.92	17.49	16.89	17.11	17.72						16.83
1987							19.51	17.95	18.38	18.07	16.28	10.86	16.84
1988	16.12	17.54	20.01	21.01	17.86	17.83	14.40	14.32	N.A.	16.08	11.16	12.48	16.25
1989	14.93	18.46	19.65	20.02	17.23	18.57	16.73	17.49	18.43	15.26	12.90	14.44	17.01
1990	15.33	17.18		22.04	20.48	19.36		19.87	19.00	19.15	16.19		18.73
1991	15.95	21.21	22.69	23.22	19.79	17.69	16.95	17.39	17.44	17.25	13.85	14.42	18.15
1992	16.40	19.16	22.10		20.22	16.68	18.52	17.77	19.44	17.26	11.56	13.47	17.51
1993	15.72	19.10	19.23	19.28	20.54	19.15	18.90	18.83	19.41	16.07	13.07	11.07	17.53
1994	16.97	18.99	16.43	21.37	19.96	18.79	17.24	18.49	18.76	15.59			18.26
1995	17.15	19.14	23.20	23.99	21.70	21.17	18.63	20.43	17.94	17.53	12.88	13.77	18.96
1996	18.75	20.40	23.74	24.38	20.91	19.59	19.35	19.28	20.03	17.50	16.07	11.58	19.30
1997	19.28	18.80	23.95	22.74	21.04	21.32	18.65	19.86	17.70	20.15	14.31	13.68	19.29
1998	19.49	23.25	23.80	24.17	20.92	19.73	21.29	19.81	18.67	18.37	15.59	12.10	19.77
1999	16.81	18.13	22.91	21.32	21.08	20.31	18.09		20.72	17.93	13.62	10.45	18.31
2000	16.22	19.06	22.00										19.09
2001													
2002	14.61	19.41	21.23	22.04	18.27	17.31	19.80	18.80	19.24	18.91	14.15	15.28	18.25
2003	16.03	19.85	21.14	24.47	17.69	19.77	17.82	19.49	19.52	16.25	14.89	12.48	18.28
2004	17.60	20.08	20.39	23.19	20.33	17.74	20.01	19.65	21.07	16.65	15.29	14.90	18.91
2005	18.01	22.04	21.25	23.60	20.23	19.37	20.35	19.54	19.64	16.43	14.97	10.62	18.84
2006	17.21	17.82	21.79	22.32	19.37	18.96	18.37	20.32	18.60	16.82	15.20	14.03	18.40
2007	13.00	20.25	21.17	22.79	19.64	17.56	17.35	20.13	20.38	15.65	15.95	15.87	18.31
2008	17.10	18.38	20.92	22.15	19.77	20.28	19.49	21.12	18.78	19.64	11.95	11.86	18.45
2009	16.07	21.56	19.03	20.48	19.11	20.53	19.64						19.49
2010													
2011							18.83	19.99	19.52	17.17	15.15	13.18	17.31

Appendix 9: $\delta^{18}O$ and $\delta^{2}H$ values of rainfall collected for Langat watershed from May 2010 to October 2011 at Pongsun

Date	Code ST	$\delta^{18}O$	$\delta^{2}H$
13/05/2010	ILO14 P	-5.84	-39.63
16/05/2010	ILO14 P	-7.30	-56.92
29/05/2010	ILO14 P	-4.27	-35.46
06/06/2010	ILO14 P	-9.10	-65.62
11/06/2010	ILO14 P	-10.91	-82.23
24/06/2010	ILO14 P	-6.32	-41.23
03/07/2010	ILO14 P	-6.26	-47.82
08/07/2010	ILO14 P	-11.46	-78.00
13/07/2010	ILO14 P	-8.52	-58.18
14/08/2010	ILO14 P	-9.63	-71.99
20/08/2010	ILO14 P	-9.61	-68.62
26/08/2010	ILO14 P	-4.34	-31.60
04/09/2010	ILO14 P	-7.81	-52.33
14/09/2010	ILO14 P	-10.45	-74.66
24/09/2010	ILO14 P	-3.89	-14.80
26/09/2010	ILO14 P	-7.58	-59.11
06/10/2010	ILO14 P	-7.59	-46.20
26/10/2010	ILO14 P	-8.50	-56.10
23/12/2010	ILO14 P	-6.37	-39.85
27/12/2010	ILO14 P	-6.41	-38.11
17/01/2011	ILO14 P	-5.60	-32.30
28/01/2011	ILO14 P	-3.66	-15.07
02/02/2011	ILO14 P	-3.93	-27.62
10/04/2011	ILO14 P	-6.25	-43.38
19/04/2011	ILO14 P	-6.86	-43.52
20/04/2011	ILO14 P	-6.17	-48.68
01/05/2011	ILO14 P	-11.14	-80.77
03/05/2011	ILO14 P	-5.14	-30.18
18/05/2011	ILO14 P	-6.31	-42.93
11/06/2011	ILO14 P	-6.90	-39.90
19/06/2011	ILO14 P	-6.97	-40.55
20/06/2011	ILO14 P	-6.87	-39.82
16/08/2011	ILO14 P	-2.55	-18.59
25/08/2011	ILO14 P	-8.91	-62.80
25/08/2011	ILO14 P	-5.64	-39.12
23/09/2011	ILO14 P	-5.62	-38.08
23/10/2011	ILO14 P	-5.61	-38.12

Appendix 10: $\delta^{18}O$ and $\delta^{2}H$ values of waters (river) collected for Langat watershed from May 2010 to December 2011 at Pongsun (ILO14), Kajang (ILO5), Dengkil (ILO3) and Semenyih (SEM, tributary)

Date	Code ST	$\delta^{18}O$	$\delta^{2}H$
13/05/2010	ILO14	-7.1	-49.49
13/05/2010	ILO3	-5.95	-40.57
13/05/2010	ILO3	-5.98	-41.98
13/05/2010	ILO3	-5.99	-43.56
16/05/2010	ILO14	-6.95	-48.16
16/05/2010	ILO3	-6.27	-40.36
16/05/2010	ILO3	-6.21	-41.92
16/05/2010	ILO5	-6.27	-43.58
16/05/2010	SEM	-6.43	-45.61
16/05/2010	SEM	-6.46	-43.87
16/05/2010	SEM	-6.42	-45.09
24/05/2010	ILO14	-6.01	-37.33
30/05/2010	ILO14	-5.68	-41.07
30/05/2010	ILO3	-6.94	-52
30/05/2010	ILO5	-6.87	-45.74
30/05/2010	SEM	-6.62	-50.1
15/06/2010	ILO14	-6.06	-46.93
15/06/2010	ILO3	-6.81	-49.67
15/06/2010	ILO5	-6.8	-48.56
15/06/2010	SEM	-6.43	-45.08
25/06/2010	SEM	-7.19	-46.41
29/06/2010	ILO14	-6.14	-43.85
29/06/2010	ILO3	-7.57	-56.1
29/06/2010	SEM	-7.35	-50.06
11/07/2010	ILO14	-6.06	-43.28
11/07/2010	ILO3	-6.88	-46.52
11/07/2010	ILO5	-6.93	-47.95
11/07/2010	SEM	-7.03	-49.6
25/07/2010	ILO14	-6.26	-45.45
25/07/2010	ILO3	-6.74	-49.48
25/07/2010	ILO5	-6.88	-53.95
25/07/2010	SEM	-6.64	-50.19
07/08/2010	ILO14	-6.11	-46.5
07/08/2010	ILO3	-6.99	-48.4
07/08/2010	ILO5	-6.94	-47.84
07/08/2010	SEM	-6.65	-49.68
21/08/2010	ILO14	-6.34	-45.2
21/08/2010	ILO3	-7.12	-55.66
21/08/2010	ILO5	-7.14	-48.97
21/08/2010	SEM	-7.33	-45.99

Date	Code ST	$\delta^{18}O$	$\delta^{2}H$
07/09/2010	ILO14	-6.66	-46.64
07/09/2010	ILO3	-7.45	-53.38
07/09/2010	ILO5	-7.13	-49.7
07/09/2010	SEM	-7.1	-46.09
25/09/2010	ILO14	-6.6	-50.22
25/09/2010	ILO3	-7.56	-54.12
25/09/2010	ILO5	-7.07	-52.95
26/09/2010	ILO5	-8.6	-62.89
17/10/2010	ILO14	-6.71	-47.28
17/10/2010	ILO3	-6.83	-41.21
17/10/2010	ILO5	-6.95	-46.26
17/10/2010	SEM	-6.97	-42.12
31/10/2010	ILO14	-6.68	-47.54
31/10/2010	ILO3	-6.81	-44.74
31/10/2010	ILO5	-6.89	-45.93
07/11/2010	ILO3	-8.6	-56.89
15/11/2010	ILO14	-7.27	-49.09
15/11/2010	ILO3	-6.3	-43.62
15/11/2010	ILO3	-8.66	-58.57
15/11/2010	ILO5	-7.38	-49.93
15/11/2010	SEM	-8.02	-52.93
30/11/2010	ILO14	-7.29	-48.48
30/11/2010	ILO3	-8.29	-56.72
30/11/2010	ILO5	-7.62	-51.5
30/11/2010	SEM	-8.24	-55.32
05/12/2010	ILO14	-7.35	-49.57
05/12/2010	ILO3	-8.43	-61.43
05/12/2010	ILO5	-7.69	-53.61
05/12/2010	SEM	-8.03	-58.41
19/12/2010	ILO14	-7.36	-48.06
19/12/2010	ILO3	-7.31	-50.55
19/12/2010	ILO5	-7.37	-53.55
19/12/2010	SEM	-7.1	-48.96
09/01/2011	ILO14	-7.39	-46.81
09/01/2011	ILO3	-7.22	-51.24
09/01/2011	ILO5	-7.34	-52.73
09/01/2011	SEM	-7.19	-50.83
22/01/2011	ILO14	-6.88	-49.98
22/01/2011	ILO3	-6.78	-47.75
22/01/2011	ILO5	-7.13	-51.28
22/01/2011	SEM	-7.21	-48.07

Date	Code ST	$\delta^{18}O$	$\delta^{2}H$
12/02/2011	ILO14	-7.11	-50.44
12/02/2011	ILO3	-6.03	-42.7
12/02/2011	ILO5	-6.77	-45.15
12/02/2011	SEM	-6.3	-44.37
26/02/2011	ILO14	-7.21	-50.7
26/02/2011	ILO3	-6	-43.23
26/02/2011	ILO5	-6.82	-50.6
26/02/2011	SEM	-6.16	-39.68
13/03/2011	ILO14	-7.17	-45.8
13/03/2011	ILO3	-6.06	-40.11
13/03/2011	ILO5	-7.08	-48.05
13/03/2011	SEM	-6.35	-40.66
27/03/2011	ILO14	-6.96	-49.8
27/03/2011	ILO3	-6.06	-41.73
27/03/2011	ILO5	-6.83	-45.72
27/03/2011	SEM	-6.3	-42.04
10/04/2011	ILO14	-6.99	-51.88
10/04/2011	ILO3	-5.92	-39.4
10/04/2011	ILO5	-6.66	-45
10/04/2011	SEM	-6.17	-37.61
24/04/2011	ILO14	-6.19	-49.93
24/04/2011	ILO3	-6.45	-50.73
24/04/2011	ILO5	-6.75	-51.79
24/04/2011	SEM	-6.18	-49.05
07/05/2011	ILO14	-6.6	-54.76
07/05/2011	ILO3	-6.64	-49.62
07/05/2011	ILO5	-6.65	-46.69
07/05/2011	SEM	-6.65	-42.76
21/05/2011	ILO14	-6.89	-50.8
21/05/2011	ILO3	-6.82	-47.21
21/05/2011	SEM	-6.26	-47.03
27/05/2011	ILO5	-6.91	-44.19
12/06/2011	ILO14	-6.78	-47.76
12/06/2011	ILO3	-5.91	-36.65
12/06/2011	ILO5	-6.77	-39.72
12/06/2011	SEM	-6.82	-43.26
26/06/2011	ILO14	-6.92	-45.77
26/06/2011	ILO3	-6.86	-42.35
26/06/2011	ILO5	-7.16	-46.15
26/06/2011	SEM	-6.35	-41.08

Date	Code ST	$\delta^{18}O$	$\delta^{2}H$
16/07/2011	ILO14	-6.72	-46.58
16/07/2011	ILO3	-6.07	-42.52
16/07/2011	ILO5	-5.7	-37.28
16/07/2011	SEM	-6.32	-44.23
30/07/2011	ILO14	-6.79	-47.82
30/07/2011	ILO3	-6.22	-40.81
30/07/2011	ILO5	-5.86	-37.61
30/07/2011	SEM	-6.42	-43.3
13/08/2011	ILO14	-6.38	-44.83
13/08/2011	ILO3	-6.16	-43.94
13/08/2011	ILO5	-5.96	-40.37
13/08/2011	SEM	-6.11	-42.74
26/08/2011	ILO14	-6.42	-43.24
26/08/2011	ILO3	-6	-40.9
26/08/2011	ILO5	-5.46	-36.51
26/08/2011	SEM	-6.17	-43.57
13/09/2011	ILO14	-6.4	-44.16
13/09/2011	ILO14	-6.61	-44.13
13/09/2011	ILO3	-5.81	-40.91
13/09/2011	ILO5	-6.53	-43.32
13/09/2011	SEM	-6.35	-41.42
30/09/2011	ILO3	-5.73	-41.14
30/09/2011	ILO5	-6.5	-44.52
30/09/2011	SEM	-6.44	-43.51
16/10/2011	ILO14	-6.52	-45.45
16/10/2011	ILO3	-5.72	-39.39
16/10/2011	ILO5	-6.59	-43.92
16/10/2011	SEM	-6.37	-44.03
29/10/2011	ILO14	-6.97	-46
29/10/2011	ILO3	-6.55	-47
29/10/2011	ILO5	-6.53	-41.59
12/11/2011	ILO14	-6.87	-46.74
12/11/2011	ILO3	-6.38	-43.79
12/11/2011	ILO5	-6.59	-44.06
12/11/2011	SEM	-6.6	-43.54
26/11/2011	ILO14	-6.91	-46.13
26/11/2011	ILO3	-6.42	-45.27
26/11/2011	ILO5	-6.45	-44.68
26/11/2011	SEM	-7.13	-45.12
17/12/2011	ILO14	-6.96	-45.17
17/12/2011	ILO3	-6.45	-45.58
17/12/2011	ILO5	-7.23	-54.06
31/12/2011	ILO14	-6.96	-45.59
31/12/2011	ILO3	-6.36	-42.39
31/12/2011	SEM	-6.48	-43.99

Appendix 11: $\delta^{18}O$ and $\delta^{2}H$ values of groundwater collected for Langat watershed from May 2010 to October 2011 at Pongsun

Date	Code ST	$\delta^{18}O$	$\delta^{2}H$	Date	Code ST	$\delta^{18}O$	$\delta^{2}H$
13/03/2011	GW	-7.13	-47.72	07/09/2010	GW	-7.22	-43.00
27/03/2011	GW	-7.14	-45.65	25/09/2010	GW	-7.23	-42.45
10/04/2011	GW	-7.23	-46.29	13/09/2011	GW	-6.77	-44.61
24/04/2011	GW	-6.41	-51.42	30/09/2011	GW	-6.83	-44.93
30/05/2010	GW	-6.44	-38.58	31/10/2011	GW	-7.22	-45.68
21/05/2011	GW	-7.1	-50.47	17/10/2010	GW	-7.25	-45.82
07/05/2011	GW	-8.18	-64.82	16/10/2011	GW	-6.8	-46.48
15/06/2010	GW	-6.73	-43.10	29/10/2011	GW	-7.22	-47.06
12/06/2011	GW	-7.19	-45.14	15/11/2010	GW	-7.18	-46.83
29/06/2011	GW	-6.84	-39.80	30/11/2010	GW	-7.25	-47.28
26/06/2011	GW	-7.35	-46.35	05/12/2010	GW	-6.97	-47.39
11/07/2010	GW	-6.89	-42.90	19/12/2010	GW	-7.59	-47.81
16/07/2011	GW	-7.24	-49.59	09/01/2011	GW	-7.55	-52.49
30/07/2011	GW	-7.53	-54.10	22/01/2010	GW	-7.04	-48.12
07/08/2011	GW	-6.9	-42.19	12/01/2011	GW	-7.17	-44.70
26/08/2011	GW	-6.9	-45.50	26/02/2011	GW	-7.21	-46.57

Appendix 12: $\delta^{18}O$ and $\delta^{2}H$ values of rainfall for Kelantan watershed from May 2010 to September 2011 collected at Lot 1065 Kg. Bukit Marak, Kota Bharu.

Date	Code ST	$\delta^{18}O$	$\delta^{2}H$	Date	Code ST	$\delta^{18}O$	$\delta^{2}H$
15/05/2010	RN	-8.43	-60.61	11/06/2011	RN	-8.62	-52.24
21/05/2010	RN	-9.89	-72.62	12/06/2011	RN	-4.98	-29.40
04/06/2010	RN	-7.62	-48.17	15/06/2011	RN	-4.56	-30.45
14/07/2010	RN	-7.71	-61.70	18/06/2011	RN	-7.16	-47.19
03/09/2010	RN	-9.63	-66.34	22/06/2011	RN	-4.96	-29.46
25/11/2010	RN	-8.18	-56.42	24/06/2011	RN	-3.92	-22.52
13/03/2011	RN	-7.89	-56.42	25/06/2011	RN	-5.91	-41.28
14/03/2011	RN	-7.92	-58.55	02/07/2011	RN	-7.48	-51.13
18/03/2011	RN	-7.90	-58.88	16/07/2011	RN	-6.96	-46.65
21/03/2011	RN	-7.95	-59.25	06/08/2011	RN	-6.96	-46.05
22/03/2011	RN	-7.93	-58.10	20/08/2011	RN	-6.99	-46.78
04/06/2011	RN	-6.77	-44.38	03/09/2011	RN	-7.65	-54.65
09/06/2011	RN	-8.61	-51.58	17/09/2011	RN	-8.49	-56.43
10/06/2011	RN	-5.74	-37.74				

Appendix 13: $\delta^{18}O$ and $\delta^{2}H$ values of river waters collected at Kelantan watershed from May 2010 to November 2011 at Tanah Merah (TM), Pasir Mas (PM), River View (RV)

Date	Code ST	$\delta^{18}O$	$\delta^{2}H$
21/05/2010	TM	-7.45	-51.77
21/05/2010	TM	-7.38	-49.11
25/05/2010	PM	-7.53	-53.08
25/05/2010	PM	-7.35	-50.91
25/05/2010	PM	-7.51	-49.74
25/05/2010	TM	-6.93	-48.40
25/05/2010	TM	-7.45	-50.32
25/05/2010	TM	-7.45	-48.83
25/05/2010	TM	-7.39	-49.66
12/06/2010	TM	-7.45	-50.60
16/06/2010	PM	-7.39	-50.45
26/06/2010	PM	-7.35	-47.86
26/06/2010	TM	-7.30	-48.37
10/07/2010	PM	-7.18	-47.34
10/07/2010	TM	-7.19	-47.98
24/07/2010	PM	-7.74	-53.87
24/07/2010	TM	-7.62	-54.00
08/08/2010	PM	-7.30	-48.60
08/08/2010	RV	-7.24	-50.75
08/08/2010	TM	-7.26	-52.26
21/08/2010	PM	-7.13	-48.68
21/08/2010	RV	-7.21	-47.69
21/08/2010	TM	-7.27	-50.69
03/09/2010	PM	-6.56	-43.97
03/09/2010	RV	-6.56	-47.36
03/09/2010	TM	-6.50	-43.25
17/09/2010	PM	-6.56	-44.93
17/09/2010	RV	-6.56	-43.81
17/09/2010	TM	-6.53	-45.05
02/10/2010	PM	-10.59	-73.36
02/10/2010	TM	-10.87	-74.98
16/10/2010	PM	-10.61	-74.79
16/10/2010	TM	-10.83	-77.17
06/11/2010	RV	-10.98	-78.08
13/11/2010	RV	-11.01	-79.54
08/01/2011	PM	-7.10	-46.42
08/01/2011	RV	-7.12	-50.17
08/01/2011	TM	-7.12	-47.82
22/01/2011	PM	-7.12	-47.35
22/01/2011	RV	-7.08	-49.31
22/01/2011	TM	-7.08	-44.51
08/02/2011	PM	-7.12	-48.01
08/02/2011	RV	-7.05	-48.50
08/02/2011	TM	-7.10	-49.16
22/02/2011	PM	-7.09	-48.10
22/02/2011	RV	-6.99	-49.41
22/02/2011	TM	-7.08	-45.65
05/03/2011	PM	-7.06	-49.02
05/03/2011	RV	-7.00	-47.51
05/03/2011	TM	-7.11	-47.48
14/03/2011	PM	-7.07	-47.08
14/03/2011	TM	-7.08	-48.90
19/03/2011	RV	-7.05	-48.45
02/04/2011	PM	-6.10	-40.05
02/04/2011	RV	-6.07	-38.73
02/04/2011	TM	-6.10	-37.80
16/04/2011	PM	-6.06	-35.99
16/04/2011	RV	-6.08	-39.30
16/04/2011	TM	-6.12	-38.53
07/05/2011	PM	-6.08	-40.08
07/05/2011	RV	-6.04	-40.28
07/05/2011	TM	-6.04	-38.15
21/05/2011	PM	-6.05	-41.24
21/05/2011	RV	-6.10	-39.64
21/05/2011	TM	-6.07	-39.41
04/06/2011	PM	-7.94	-56.42
04/06/2011	PM	-6.74	-45.76
04/06/2011	RV	-6.70	-45.56
04/06/2011	RV	-6.05	-40.71
04/06/2011	TM	-6.10	-39.71
04/06/2011	TM	-6.76	-45.88
18/06/2011	PM	-6.09	-36.95
18/06/2011	PM	-7.59	-52.86
18/06/2011	RV	-7.56	-52.20
18/06/2011	RV	-6.08	-36.86
18/06/2011	TM	-6.08	-34.50
18/06/2011	TM	-6.76	-44.84
02/07/2011	PM	-7.64	-48.17
02/07/2011	RV	-6.71	-43.26
02/07/2011	TM	-7.64	-52.45
16/07/2011	PM	-6.78	-44.42
16/07/2011	RV	-7.67	-52.94
18/07/2011	TM	-6.82	-43.28
06/08/2011	PM	-7.65	-49.60
06/08/2011	TM	-6.98	-44.92
17/08/2011	RV	-4.90	-24.37
20/08/2011	PM	-7.62	-49.16
20/08/2011	RV	-6.99	-45.66
20/08/2011	TM	-6.74	-42.32
03/09/2011	PM	-7.64	-53.08
03/09/2011	RV	-7.60	-51.86
03/09/2011	TM	-6.99	-44.68
06/09/2011	RV	-7.63	-51.87
17/09/2011	PM	-5.68	-41.29
17/09/2011	TM	-7.67	-53.62
01/10/2011	RV	-8.49	-56.16
01/10/2011	TM	-5.00	-34.11
15/10/2011	PM	-6.22	-43.46
15/10/2011	RV	-4.85	-30.46
15/10/2011	TM	-7.78	-53.56
12/11/2011	PM	-4.88	-32.71
12/11/2011	RV	-7.61	-54.48
12/11/2011	TM	-3.64	-21.73

Appendix 14: $\delta^{18}O$ and $\delta^{2}H$ values of groundwater collected for Kelantan from May 2010 to October 2011 at Lot 1065 Kg. Bukit Marak, Kota Bharu

Date	Code ST	$\delta^{18}O$	$\delta^{2}H$	Date	Code ST	$\delta^{18}O$	$\delta^{2}H$
05/03/2011	GWKB	-7.33	-49.37	21/08/2010	GWKB	-7.05	-52.82
10/03/2011	GWKB	-7.34	-46.22	11/08/2010	GWKB	-6.49	-37.59
02/04/2011	GWKB	-5.62	-40.02	21/08/2010	GWKB	-6.74	-46.78
18/04/2011	GWKB	-5.61	-39.56	06/08/2011	GWKB	-7.21	-47.29
16/04/2011	GWKB	-5.62	-38.00	20/08/2011	GWKB	-7.63	-51.44
23/04/2011	GWKB	-6.27	-43.05	03/09/2010	GWKB	-6.68	-47.48
24/05/2010	GWKB	-6.03	-37.4	17/09/2010	GWKB	-6.84	-45.53
07/05/2011	GWKB	-5.6	-37.92	16/10/2010	GWKB	-6.86	-43.94
21/05/2011	GWKB	-5.62	-41.11	02/10/2010	GWKB	-6.83	-48.28
25/06/2010	GWKB	-6.22	-37.84	01/10/2011	GWKB	-8.23	-57.69
11/06/2010	GWKB	-5.98	-39.43	16/11/2010	GWKB	-6.82	-44.55
04/06/2011	GWKB	-6.78	-43.8	12/11/2011	GWKB	-5.25	-39.60
18/06/2011	GWKB	-6.73	-46.21	08/01/2011	GWKB	-7.35	-47.32
18/06/2011	GWKB	-5.65	-41.63	22/01/2011	GWKB	-7.38	-46.86
??/07/2010	GWKB	-6.9	-49.27	08/02/2011	GWKB	-7.35	-47.98
10/07/2011	GWKB	-6.24	-38.5	22/02/2011	GWKB	-7.32	-48.06
02/07/2011	GWKB	-7.56	-50.71				
18/07/2011	GWKB	-6.75	-45.06				

Appendix 15: Annual Solar Sunspot Number from 1980 to 2011 from Solar Influence Data Analysis Centre (SIDC), Belgium (http://sidc.oma.be/aboutSIDC/)

Sunspot Number (SSN)					
Year	SSN	Year	SSN	Year	SSN
1980	154.60	1990	142.60	2000	119.60
1981	140.50	1991	145.70	2001	111.00
1982	115.90	1992	94.30	2002	104.00
1983	66.60	1993	54.60	2003	63.70
1984	45.90	1994	29.90	2004	40.40
1985	17.90	1995	17.50	2005	29.80
1986	13.40	1996	8.60	2006	15.20
1987	29.20	1997	21.50	2007	7.50
1988	100.20	1998	64.30	2008	2.90
1989	157.60	1999	93.30	2009	3.10
				2010	16.50
				2011	55.70

Appendix 16: Concentrations of major ions (ppm) waters of the Langat watershed (May 2010 to December 2011)

Station		GW						
Sample		Ca	K	Mg	Na	Cl	SO4	NO3
GW	16/05/2010	0.68	1.07	0.21	1.58	1.01	0.79	
GW	16/05/2010	0.64	1.11	0.20	1.49	0.84	0.91	
GW	30/05/2010	0.66	1.13	0.19	1.51	0.93	0.98	
GW	29/06/2010	0.89	1.19	0.25	1.74	1.75	1.33	
GW	11/07/2010	0.77	1.16	0.21	1.62	1.19	0.88	
GW	07/08/2010	0.83	5.28	0.20	1.73			
GW	21/08/2010	0.91	4.39	0.21	1.70			
GW	07/09/2010	0.78	1.15	0.22	1.65			
GW	25/09/2010	0.96	1.60	0.22	1.71			
GW	15/10/2010	0.65	1.06	0.21	1.45	0.95	1.00	
GW	16/10/2010	1.07	1.86	0.32	6.07			
GW	17/10/2010	0.32	0.58	0.07	0.75	1.42	0.75	
GW	02/11/2010	1.07	1.85	0.32	6.05			
GW	15/11/2010	0.50	10.06	0.12	0.84	20.84	0.84	
GW	16/11/2010	1.08	1.85	0.32	6.07			
GW	30/11/2010	0.43	10.18	0.12	0.88	20.39	0.88	
GW	05/12/2010	0.42	10.11	0.12	0.87	20.49	0.86	
GW	19/12/2010	0.32	0.50	0.10	0.71	1.19	0.84	
GW	08/01/2011	1.07	2.04	0.37	6.91			
GW	09/01/2011	0.32	0.51	0.10	0.73	1.16	0.82	
GW	22/01/2011	1.10	2.08	0.38	7.01			
GW	22/01/2011	0.32	0.52	0.10	0.74	1.20	0.84	
GW	26/01/2011	0.48	0.81	0.12	0.78	1.62	0.86	
GW	08/02/2011	1.05	2.01	0.36	6.88			
GW	12/02/2011	0.83	0.57	0.15	0.93	1.33	1.91	0.38
GW	05/03/2011	1.06	2.03	0.37	7.03			
GW	10/03/2011	1.08	2.04	0.36	6.96			
GW	13/03/2011	0.62	0.98	0.17	0.88	1.94	0.93	
GW	27/03/2011	1.26	1.00	0.17	1.04	2.44	2.79	0.58
GW	10/04/2011	0.55	0.93	0.13	0.90	1.93	1.11	
GW	07/05/2011	0.76	209.05	0.24	142.80			
GW	21/05/2011	2.23	1.70	0.43	1.91			
GW	12/06/2011	0.80	1.10	0.27	1.54			
GW	26/06/2011	0.53	1.16	0.23	1.41			
GW	16/07/2011	0.90	1.60	0.23	1.72	12.04	11.83	3.57
GW	30/07/2011	5.79	2.16	0.34	3.13	7.43	14.81	0.87
GW	13/08/2011	1.26	1.70	0.26	1.85	13.53	9.92	4.97
GW	26/08/2011	0.86	1.16	0.29	1.59			
GW	13/09/2011	1.38	2.02	0.24	1.81	10.67	19.45	
GW	30/09/2011	0.91	1.61	0.23	1.71	14.62	10.52	8.57
GW	30/09/2011	2.73	2.58	0.27	2.00	9.27	13.06	10.70
GW	16/10/2011	0.67	2.18	0.21	1.64	9.49	13.39	11.25
GW	29/10/2011	4.67	1.94	0.23	2.58	1.52	1.42	
GW	12/11/2011	5.91	2.14	0.34	3.10	11.26	15.33	16.31
GW	26/11/2011	0.91	1.61	0.24	1.72	14.53	10.27	7.15
GW	17/12/2011	4.43	1.85	0.22	2.48	1.52	1.39	
GW	31/12/2011	5.86	2.03	0.30	3.01	47.12	2.39	1.08

Station		PANGSUN						
Sample		Ca	K	Mg	Na	Cl	SO4	NO3
ILO14	16/05/2010	2.77	2.31	0.88	2.27	7.64	11.03	
ILO14	30/05/2010	2.24	2.19	0.79	2.34	5.11	8.93	
ILO14	29/06/2010	1.94	2.18	0.83	2.30	5.08	10.10	
ILO14	11/07/2010	1.97	2.18	0.84	2.33	7.37	10.33	
ILO14	25/07/2010	2.14	2.17	0.84	2.38	11.09	15.88	
ILO14	07/08/2010	2.18	6.96	0.80	3.82			
ILO14	07/09/2010	1.87	17.35	0.71	1.98			
ILO14	25/09/2010	2.24	20.94	0.80	2.09			
ILO14	15/10/2010	2.27	2.19	0.87	2.25	13.22	15.29	
ILO14	17/10/2010	1.40	1.42	0.41	1.28	3.31	1.21	1.12
ILO14	31/10/2010	1.16	1.31	0.40	1.10	2.84	0.89	
ILO14	15/11/2010	0.47	0.63	0.19	0.51	1.29	0.81	0.27
ILO14	05/12/2010	0.99	1.30	0.38	1.06	1.48	0.93	
ILO14	19/12/2010	1.22	1.03	0.42	1.10	0.74	0.63	0.50
ILO14	09/01/2011	1.16	1.53	0.39	1.94	1.17	0.66	
ILO14	22/01/2011	1.24	1.05	0.43	1.12	0.76	0.66	1.15
ILO14	12/02/2011	1.61	1.58	0.39	1.15	2.48	2.29	0.40
ILO14	26/02/2011	1.03	1.53	0.37	0.96	1.84	0.63	
ILO14	13/03/2011	1.04	1.54	0.38	0.94	1.77	0.57	
ILO14	27/03/2011	1.98	1.70	0.42	1.28	2.84	3.20	0.48
ILO14	10/04/2011	1.15	1.72	0.42	1.07	2.09	0.67	
ILO14	24/04/2011	2.47	2.25	0.97	2.17			
ILO14	07/05/2011	1.81	207.22	0.73	141.37			
ILO14	21/05/2011	1.80	3.14	0.76	1.81			
ILO14	12/06/2011	4.68	3.39	0.89	2.54			
ILO14	26/06/2011	2.09	1.98	0.86	1.88			
ILO14	16/07/2011	2.28	2.20	0.78	2.30	10.99	8.63	7.24
ILO14	30/07/2011	2.25	2.22	0.78	2.33	5.25	10.98	4.65
ILO14	13/08/2011	2.31	2.29	0.78	2.26	32.93	11.93	9.20
ILO14	26/08/2011	2.30	2.22	0.79	2.35	35.15	11.23	6.76
ILO14	13/09/2011	2.94	2.54	0.78	2.41	39.06	12.26	7.95
ILO14	30/09/2011	3.37	2.49	0.76	2.42	9.47	13.36	12.57
ILO14	16/10/2011	2.22	2.18	0.81	2.24	12.41	13.32	8.61
ILO14	29/10/2011	6.63	2.81	0.95	3.86	12.78	14.39	10.27
ILO14	12/11/2011	3.26	2.39	0.92	2.96	9.67	13.70	11.89
ILO14	26/11/2011	4.83	2.65	0.94	3.39	11.08	12.04	9.42
ILO14	17/12/2011	4.98	2.67	0.92	3.49	2.14	3.07	2.50
ILO14	31/12/2011	3.60	2.35	0.92	3.07	0.88	1.14	2.14

Station				KAJANG				
Sample		Ca	K	Mg	Na	Cl	SO4	NO3
ILO5	16/05/2010	16.64	5.07	1.21	13.22			
ILO5	30/05/2010	9.67	2.89	0.59	5.80	4.50	7.75	
ILO5	29/06/2010	9.92	2.67	0.54	4.13	6.18	9.57	
ILO5	11/07/2010	11.80	3.69	0.92	8.25	6.67	9.76	
ILO5	25/07/2010	16.17	4.65	1.16	13.34	10.64	12.90	
ILO5	07/08/2010	11.81	4.33	0.92	9.26			
ILO5	07/09/2010	9.58	19.11	0.81	4.81			
ILO5	25/09/2010	11.22	18.94	0.82	5.45			
ILO5	15/10/2010	15.94	5.10	1.22	14.26	8.79	3.61	
ILO5	17/10/2010	6.32	21.52	0.42	4.10	43.55	10.79	0.55
ILO5	31/10/2010	6.26	21.54	0.41	4.10	45.55	11.04	0.57
ILO5	15/11/2010	4.67	10.02	0.39	3.52	23.01	8.21	3.57
ILO5	30/11/2010	4.24	9.29	0.37	3.04	20.20	7.26	2.64
ILO5	05/12/2010	4.18	8.46	0.37	2.90			
ILO5	19/12/2010	8.36	2.34	0.55	5.21	9.62	67.88	3.97
ILO5	09/01/2011	8.07	2.32	0.54	5.46	9.58	59.85	4.15
ILO5	22/01/2011	8.66	2.08	0.57	5.38	9.46		16.48
ILO5	06/02/2011	5.37	4.34	0.38	3.19	11.36	11.62	3.74
ILO5	12/02/2011	5.79	3.37	0.43	3.22	9.68	13.22	3.52
ILO5	13/03/2011	5.53	4.98	0.35	2.68	11.92	10.80	3.73
ILO5	27/03/2011	5.10	4.50	0.36	3.24	11.60	10.36	3.36
ILO5	07/04/2011	7.52	217.58	0.65	131.27			
ILO5	10/04/2011	6.80	6.22	0.45	3.67	14.87	13.41	4.51
ILO5	24/04/2011	18.23	4.32	1.28	10.97			
ILO5	12/06/2011	13.93	12.26	0.95	6.79			
ILO5	26/06/2011	8.72	35.03	0.77	5.84			
ILO5	16/07/2011	10.80	11.31	0.63	6.53	17.50	10.67	5.62
ILO5	30/07/2011	10.39	11.20	0.58	6.67	7.73	11.67	8.95
ILO5	13/08/2011	9.65	10.04	0.70	6.30	30.23	10.04	11.60
ILO5	26/08/2011	10.82	11.34	0.63	6.55	24.94	9.45	8.71
ILO5	13/09/2011	12.72	13.15	0.83	8.47	29.82	9.65	10.00
ILO5	30/09/2011	11.72	12.11	0.78	7.56	13.34	0.98	
ILO5	16/10/2011	12.86	13.03	0.82	8.38	5.51	6.54	3.53
ILO5	29/10/2011	21.17	5.08	1.25	13.39	4.21	4.79	2.55
ILO5	12/11/2011	12.75	3.80	1.08	8.38	12.13	5.16	
ILO5	26/11/2011	20.47	4.83	1.19	12.92	5.36	6.11	3.70
ILO5	17/12/2011	15.46	3.61	0.93	9.85	7.43	14.81	0.87

Station				SEMENYIH				
Station		Ca	K	Mg	Na	Cl	SO4	NO3
SEM	16/05/2010	5.61	5.48	0.76	5.33			
SEM	16/05/2010	5.53	4.13	0.75	5.51			
SEM	16/05/2010	5.55	9.25	0.75	5.27	10.95	6.05	
SEM	30/05/2010	5.33	4.01	0.64	5.14	5.57	6.56	
SEM	29/06/2010	4.90	3.76	0.65	5.61	4.72	6.87	
SEM	11/07/2010	5.07	3.70	0.70	5.13	4.65	5.60	
SEM	25/07/2010	5.71	3.95	0.81	6.03	5.74	6.68	
SEM	07/08/2010	5.78	4.33	0.79	7.81			
SEM	07/09/2010	6.50	5.61	0.76	11.88			
SEM	25/09/2010	7.47	4.37	0.76	13.41			
SEM	15/10/2010	5.55	3.83	0.73	6.62	6.81	6.59	
SEM	17/10/2010	3.98	7.58	0.37	2.94	19.15	7.99	5.86
SEM	31/10/2010	4.22	8.09	0.44	3.07	18.16	8.15	5.45
SEM	15/11/2010	2.68	2.99	0.32	2.22	7.39	5.88	2.13
SEM	30/11/2010	2.80	1.71	0.32	2.64	4.89	7.22	2.50
SEM	05/12/2010	2.53	2.29	0.31	1.96	6.00	5.79	2.02
SEM	19/12/2010	2.98	13.44	0.35	2.89	28.26	7.22	3.79
SEM	09/01/2011	2.60	12.12	0.32	2.58	25.24	5.98	3.60
SEM	22/01/2011	2.44	9.76	0.33	2.39	20.26	5.24	2.06
SEM	12/02/2011	3.75	1.68	0.35	2.29	4.88	9.74	2.22
SEM	26/02/2011	2.91	1.70	0.32	2.40	4.08	7.27	2.70
SEM	13/03/2011	2.32	1.50	0.28	1.98	3.57	6.07	1.49
SEM	27/03/2011	3.23	1.69	0.33	2.19	4.29	8.44	2.08
SEM	10/04/2011	2.60	1.69	0.32	2.20	3.53	6.76	2.17
SEM	16/07/2011	4.95	4.32	0.62	7.03	0.73	0.51	
SEM	30/07/2011	5.04	4.34	0.62	7.17	1.24	1.58	0.00
SEM	13/08/2011	4.53	9.15	0.60	6.52	1.55	2.40	
SEM	16/08/2011	4.97	4.33	0.62	7.06	0.72	0.68	
SEM	13/09/2011	4.88	34.15	0.61	6.36	49.09	4.94	3.73
SEM	30/09/2011	5.86	24.06	0.65	5.42	6.24	11.22	5.59
SEM	16/10/2011	4.94	34.37	0.64	6.38	10.14	18.74	
SEM	12/11/2011	5.69	3.99	0.70	6.78	0.88	1.14	2.14
SEM	26/11/2011	4.11	3.20	0.54	5.48	4.21	4.79	2.55
SEM	17/12/2011	9.13	3.92	0.88	6.08	6.44	9.36	2.68
SEM	31/12/2011	5.19	4.08	0.70	7.21	5.36	6.11	3.70

Station				DENGKIL				
Sample	Date	Ca	K	Mg	Na	Cl	SO4	NO3
ILO3	16/05/2010	10.58	4.16	1.01	7.54	0.81	0.49	
ILO3	16/05/2010	10.63	4.20	1.02	7.64			
ILO3	16/05/2010	10.68	4.39	1.03	7.69	11.94	15.41	
ILO3	21/05/2010	3.57	2.02	0.35	2.32	6.57	7.27	6.03
ILO3	30/05/2010	6.78	3.05	0.54	3.76	0.89	0.76	
ILO3	29/06/2010	8.50	3.63	0.77	6.32	0.88	0.67	
ILO3	11/07/2010	8.65	3.83	0.86	6.97	0.98	0.72	
ILO3	25/07/2010	12.90	4.80	1.24	11.49	1.05	0.86	
ILO3	07/08/2010	10.63	7.61	1.02	9.69			
ILO3	21/08/2010	8.36	10.37	0.87	5.66			
ILO3	07/09/2010	7.29	7.15	0.77	3.85			
ILO3	25/09/2010	8.26	3.05	0.75	4.74			
ILO3	15/10/2010	11.98	4.27	1.16	9.09	0.88	0.99	
ILO3	17/10/2010	2.59	14.67	0.37	2.15	29.33	5.11	2.51
ILO3	31/10/2010	2.88	19.00	0.35	2.45	37.63	6.36	3.13
ILO3	15/11/2010	3.83	1.56	0.36	2.47	5.76	7.74	2.96
ILO3	30/11/2010	3.46	2.10	0.35	3.03	6.58	8.22	2.56
ILO3	19/12/2010	5.77	1.93	0.51	4.33	8.35	12.25	4.46
ILO3	22/01/2011	5.88	2.02	0.53	4.28	8.45	12.31	1.59
ILO3	12/02/2011	4.26	1.77	0.41	3.62	7.74	9.39	2.57
ILO3	26/02/2011	4.33	1.72	0.37	2.89	9.04	10.14	4.56
ILO3	13/03/2011	3.52	1.50	0.32	2.44	5.95	7.62	4.13

Station				DENGKIL				
Sample	Date	Ca	K	Mg	Na	Cl	SO4	NO3
ILO3	27/03/2011	4.51	1.68	0.37	2.39	5.50	10.18	3.72
ILO3	10/04/2011	4.07	1.80	0.36	2.53	5.73	8.57	4.46
ILO3	24/04/2011	12.30	4.12	1.19	8.75			
ILO3	07/05/2011	9.03	135.99	0.83	94.14			
ILO3	21/05/2011	8.52	3.32	0.76	5.79			
ILO3	12/06/2011	9.39	3.74	0.99	7.84			
ILO3	26/06/2011	9.78	7.95	0.90	7.17			
ILO3	16/07/2011	8.60	3.93	0.76	6.04	9.24	6.83	4.60
ILO3	30/07/2011	8.50	3.99	0.76	6.13	4.97	7.91	2.75
ILO3	13/08/2011	8.45	11.83	0.78	10.03	32.15	6.16	2.32
ILO3	26/08/2011	8.60	3.94	0.77	6.07	23.35	6.90	0.99
ILO3	13/09/2011	11.18	32.87	0.88	9.71	32.07	5.88	1.08
ILO3	30/09/2011	10.71	34.88	0.87	8.54	2.31	2.79	
ILO3	16/10/2011	11.59	38.76	0.91	9.22	2.49	3.13	
ILO3	29/10/2011	14.79	4.52	1.17	10.67	1.52	1.42	
ILO3	09/11/2011	5.44	1.94	0.50	4.10	7.79	11.17	4.87
ILO3	12/11/2011	14.50	4.43	1.15	10.28	6.44	9.36	2.68
ILO3	26/11/2011	14.74	4.50	1.17	10.55	47.12	2.39	1.08
ILO3	17/12/2011	14.85	4.49	1.19	10.42	9.67	13.70	11.89
ILO3	31/12/2011	16.69	5.11	1.34	13.27	11.26	15.33	16.31

Appendix 17: pH and HCO_3 of Langat river water obtained from [*Lee*, *2013*]

Langat											
Time Period	Sample ID	pH	[HCO3] (mol/L)	Time Period	Sample ID	pH	[HCO3] (mol/L)	Time Period	Sample ID	pH	[HCO3] (mol/L)
16/05/2010	GW	7.00	2.89E-04	25/09/2010	ILO5	6.66	1.43E-04	26/02/2011	GW	6.01	1.55E-04
16/05/2010	ILO14		7.36E-11	25/09/2010	SEM	6.42	1.26E-04	26/02/2011	ILO14	6.89	1.99E-04
16/05/2010	ILO3		2.59E-10	17/10/2010	GW	5.92	1.25E-04	26/02/2011	ILO3	6.43	2.88E-04
16/05/2010	ILO3		2.44E-10	17/10/2010	ILO14	6.29	1.28E-04	26/02/2011	ILO5	6.97	4.36E-04
16/05/2010	ILO3		2.65E-10	17/10/2010	ILO3	6.57	1.69E-04	26/02/2011	SEM	6.58	2.21E-04
16/05/2010	ILO5	6.88	7.72E-04	17/10/2010	ILO5	6.83	9.61E-04	13/03/2011	GW	5.98	1.61E-04
16/05/2010	SEM		1.52E-10	17/10/2010	SEM	6.87	3.75E-04	13/03/2011	ILO14	7.33	2.36E-04
16/05/2010	SEM		8.24E-11	31/10/2010	GW	5.97	1.68E-04	13/03/2011	ILO3	7.23	3.54E-04
16/05/2010	SEM		1.55E-10	31/10/2010	ILO14	7.43	2.44E-04	13/03/2011	ILO5	7.01	5.27E-04
30/05/2010	GW		5.39E-11	31/10/2010	ILO3	7.24	3.00E-04	13/03/2011	SEM	7.34	2.74E-04
30/05/2010	ILO14		4.71E-11	31/10/2010	ILO5	7.00	1.38E-03	27/03/2011	GW	6.00	1.67E-04
30/05/2010	ILO3		5.02E-11	31/10/2010	SEM	7.51	4.57E-04	27/03/2011	ILO14	7.89	2.81E-04
30/05/2010	ILO5		9.38E-11	15/11/2010	GW	5.46	1.31E-04	27/03/2011	ILO3	7.63	4.19E-04
30/05/2010	SEM		6.22E-11	15/11/2010	ILO14	6.03	8.36E-05	27/03/2011	ILO5	7.00	5.41E-04
15/06/2010	GW		1.19E-10	15/11/2010	ILO3	6.35	2.52E-04	27/03/2011	SEM	7.91	3.18E-04
15/06/2010	ILO14		3.47E-10	15/11/2010	ILO5	6.59	3.42E-04	10/04/2011	GW	7.01	5.10E-04
15/06/2010	ILO3		2.40E-10	15/11/2010	SEM	6.68	2.68E-04	10/04/2011	ILO14	7.56	2.81E-04
15/06/2010	ILO5		8.86E-11	30/11/2010	GW	5.56	6.43E-05	10/04/2011	ILO3	6.17	2.09E-04
15/06/2010	SEM		1.23E-10	30/11/2010	ILO14	6.19	9.38E-05	10/04/2011	ILO5	7.05	5.97E-04
29/06/2010	GW		1.05E-10	30/11/2010	ILO3	6.31	1.15E-04	10/04/2011	SEM	6.31	1.65E-04
29/06/2010	ILO14		7.12E-11	30/11/2010	ILO5	6.48	3.10E-04	24/04/2011	GW	6.41	1.46E-04
29/06/2010	ILO3		1.31E-10	30/11/2010	SEM	6.53	1.87E-04	24/04/2011	ILO14	6.39	1.54E-04
29/06/2010	ILO5		1.02E-10	05/12/2010	GW	5.91	3.62E-05	24/04/2011	ILO3	6.77	5.56E-04
29/06/2010	SEM		9.32E-11	05/12/2010	ILO14	6.89	1.92E-04	24/04/2011	ILO5	6.78	1.29E-04
11/07/2010	GW		1.21E-10	05/12/2010	ILO3	7.23	2.26E-04	24/04/2011	SEM	6.14	1.11E-04
11/07/2010	ILO14		6.88E-11	05/12/2010	ILO5	7.07	3.42E-04	07/05/2011	GW	7.11	3.67E-04
11/07/2010	ILO3		1.41E-10	05/12/2010	SEM	7.10	2.04E-04	07/05/2011	ILO14	6.67	2.06E-04
11/07/2010	ILO5		2.26E-10	19/12/2010	GW	6.01	1.32E-04	07/05/2011	ILO3	7.03	5.66E-04
11/07/2010	SEM		1.10E-10	19/12/2010	ILO14	6.97	2.36E-04	07/05/2011	ILO5	6.52	5.28E-04
25/07/2010	GW	6.00	1.70E-04	19/12/2010	ILO3	7.13	6.04E-04	07/05/2011	SEM	6.73	2.58E-04
25/07/2010	ILO14	7.12	2.42E-04	19/12/2010	ILO5	6.93	5.06E-04	21/05/2011	GW	7.12	2.41E-04
25/07/2010	ILO3	7.32	8.50E-04	19/12/2010	SEM	7.10	3.34E-04	21/05/2011	ILO14	7.09	1.91E-04
25/07/2010	ILO5	7.13	1.14E-03	09/01/2011	GW	6.52	2.39E-04	21/05/2011	ILO3	6.54	2.24E-04
25/07/2010	SEM			09/01/2011	ILO14	7.30	2.57E-04	21/05/2011	ILO5	7.02	3.21E-04
07/08/2010	GW	5.87	1.42E-05	09/01/2011	ILO3	7.13	5.89E-04	21/05/2011	SEM	6.79	2.52E-04
07/08/2010	ILO14	6.79	4.79E-05	09/01/2011	ILO5	7.24	5.31E-04	12/06/2011	GW	6.34	1.59E-04
07/08/2010	ILO3	6.41	9.46E-05	09/01/2011	SEM	7.10	3.56E-04	12/06/2011	ILO14	6.61	1.17E-04
07/08/2010	ILO5	6.87	1.71E-04	22/01/2011	GW	6.19	0.00E+00	12/06/2011	ILO3	6.27	2.23E-04
07/08/2010	SEM	6.54	6.41E-05	22/01/2011	ILO14	6.26	1.42E-04	12/06/2011	ILO5	6.81	3.67E-04
21/08/2010	GW	5.76	2.93E-05	22/01/2011	ILO3	7.31	5.09E-04	12/06/2011	SEM	6.15	1.13E-04
21/08/2010	ILO14	7.06	7.35E-05	22/01/2011	ILO5	7.36	5.73E-04	26/06/2011	GW	6.14	1.95E-04
21/08/2010	ILO3	6.77	1.00E-04	22/01/2011	SEM	7.17	3.23E-04	26/06/2011	ILO14	6.31	1.55E-04
21/08/2010	ILO5	6.79	1.41E-04	12/02/2011	GW	6.19	2.48E-04	26/06/2011	ILO3	6.27	3.41E-04
21/08/2010	SEM	6.67	7.75E-05	12/02/2011	ILO14	7.23	2.20E-04	26/06/2011	ILO5	6.96	8.02E-04
25/09/2010	GW	5.93	3.36E-05	12/02/2011	ILO3	7.23	5.87E-04	26/06/2011	SEM	6.15	1.56E-04
25/09/2010	ILO14	6.27	3.91E-05	12/02/2011	ILO5	7.15	4.53E-04	16/07/2011	GW	6.01	7.22E-05
25/09/2010	ILO3	6.39	7.20E-05	12/02/2011	SEM	7.10	3.04E-04	16/07/2011	ILO14	6.12	9.10E-05

Langat			
Time Period	Sample ID	pH	[HCO3] (mol/L)
16/07/2011	ILO3	6.35	3.28E-04
16/07/2011	ILO5	6.31	2.10E-04
16/07/2011	SEM	6.19	1.15E-04
30/07/2011	GW	6.66	5.34E-05
30/07/2011	ILO14	7.08	4.65E-05
30/07/2011	ILO3	6.62	6.51E-05
30/07/2011	ILO5	7.22	1.30E-04
30/07/2011	SEM	6.59	5.28E-05
18/08/2011	GW	6.81	1.12E-04
18/08/2011	ILO14	6.83	1.95E-04
18/08/2011	ILO3	7.03	4.07E-04
18/08/2011	ILO5	6.99	3.20E-04
18/08/2011	SEM	6.99	2.49E-04
26/08/2011	GW	6.53	1.39E-04
26/08/2011	ILO14	6.97	1.79E-04
26/08/2011	ILO3	7.27	1.12E-04
26/08/2011	ILO5	7.01	3.21E-04
26/08/2011	SEM	7.40	2.83E-04
07/09/2011	GW	5.89	3.52E-05
07/09/2011	ILO14	6.37	4.19E-05
07/09/2011	ILO3	6.63	8.30E-05
07/09/2011	ILO5	6.71	1.18E-04
07/09/2011	SEM	6.51	1.06E-04
13/09/2011	GW	6.31	7.88E-05
13/09/2011	ILO14	7.00	1.83E-04
13/09/2011	ILO3	7.21	4.84E-04
13/09/2011	ILO5	7.05	4.54E-04
13/09/2011	SEM	7.13	1.80E-04
30/09/2011	GW	6.31	8.25E-05
30/09/2011	ILO14	6.89	1.84E-04
30/09/2011	ILO3	7.21	5.47E-04
30/09/2011	ILO5	7.02	4.40E-04
30/09/2011	SEM	7.11	2.00E-04
16/10/2011	GW	6.19	7.32E-05
16/10/2011	ILO14	6.81	1.45E-04
16/10/2011	ILO3	7.00	6.29E-04
16/10/2011	ILO5	6.99	6.14E-04
16/10/2011	SEM	6.95	2.54E-04
29/10/2011	GW	6.73	2.61E-04
29/10/2011	ILO14	6.70	2.59E-04
29/10/2011	ILO3	6.67	7.41E-04
29/10/2011	ILO5	6.60	1.10E-03
29/10/2011	SEM	6.16	2.08E-04
12/11/2011	GW	6.31	1.67E-04
12/11/2011	ILO14	6.53	2.03E-04
12/11/2011	ILO3	6.75	7.61E-04
12/11/2011	ILO5	6.59	8.46E-04
Time Period	Sample ID	pH	[HCO3] (mol/L)
12/11/2011	SEM	6.90	3.96E-04
26/11/2011	GW	6.37	1.80E-04
26/11/2011	ILO14	6.79	2.53E-04
26/11/2011	ILO3	6.83	8.76E-04
26/11/2011	ILO5	6.51	1.03E-03
26/11/2011	SEM	6.77	2.98E-04
17/12/2011	GW	6.55	1.98E-04
17/12/2011	ILO14	6.72	2.45E-04
17/12/2011	ILO3	6.55	5.35E-04
17/12/2011	ILO5	6.39	5.35E-04
17/12/2011	SEM	6.81	3.72E-04
31/12/2011	GW	6.63	4.63E-04
31/12/2011	ILO14	6.61	2.25E-04
31/12/2011	ILO3	6.83	1.02E-03
31/12/2011	ILO5	6.70	1.19E-03
31/12/2011	SEM	6.67	3.54E-04

Appendix 18: Concentrations of ions (ppm) waters of Kelantan watershed (May 2010 to September 2011)

GROUNDWATER

Date	Sample ID	Ca	K	Mg	Na	NO3	Cl	SO4
11/06/2010	GWKB	1.4	2.8	0.4	9.5		101.0	4.9
25/06/2010	GWKB	1.6	100.1	0.4	8.5		10.5	4.8
11/07/2010	GWKB	1.8	49.8	0.5	12.3		57.5	7.3
23/07/2010	GWKB	1.4	3.0	0.4	10.4		11.8	5.3
11/08/2010	GWKB	1.2	2.2	0.3	8.8		9.9	4.4
21/08/2010	GWKB	1.3	2.3	0.4	10.4		11.1	4.9
03/09/2010	GWKB	0.9	1.3	0.2	6.5	0.2	12.2	5.3
17/09/2010	GWKB	0.8	1.2	0.2	6.3		11.8	4.3
16/10/2010	GWKB	1.1	1.9	0.3	6.1	6.1	3.2	1.0
25/10/2010	GWKB	1.4	2.3	0.4	9.5		9.9	4.9
18/01/2011	GWKB	1.1	2.0	0.4	6.9	6.6	3.7	0.3
22/01/2011	GWKB	1.1	2.1	0.4	7.0	6.6	3.7	0.3
05/03/2011	GWKB	1.1	2.0	0.4	7.0	6.6	3.7	0.3
19/03/2011	GWKB	4.9	1.4	1.2	3.1	1.4	0.8	0.4
02/04/2011	GWKB	2.5	5.3	1.3	8.9	11.0	4.0	0.4
16/04/2011	GWKB	2.5	5.3	1.2	9.0	11.0	3.9	0.4
07/05/2011	GWKB	2.5	5.3	1.3	9.0	11.0	4.0	0.5
21/05/2011	GWKB	2.6	6.3	1.3	9.4	11.8	3.9	0.5
04/06/2011	GWKB	5.5	1.6	1.0	3.4	1.6	0.4	0.1
18/06/2011	GWKB	5.6	1.6	1.0	3.3	1.5	1.2	0.0
02/07/2011	GWKB	3.8	2.0	0.7	1.8	1.8	1.3	0.9
16/07/2011	GWKB	5.7	1.7	1.0	3.4	1.6	1.3	0.0
06/08/2011	GWKB	3.1	2.4	0.7	9.3	7.1	2.3	0.3
20/08/2011	GWKB	3.7	2.0	0.7	2.0	2.0	1.3	0.8
03/09/2011	GWKB	3.9	2.2	0.7	2.6	2.4	1.9	1.5
17/09/2011	GWKB	3.4	6.8	1.2	10.6	12.3	4.8	9.3

RIVER VIEW

Date	Sample ID	Ca	K	Mg	Na	NO3	Cl	SO4
03/09/2010	RV	1.8	0.6	0.5	1.6	0.3	2.4	1.0
17/09/2010	RV	1.8	0.6	0.5	1.5	0.9	2.3	0.9
16/10/2010	RV	2.4	1.9	0.8	1.8	2.3	1.1	
18/01/2011	RV	4.9	1.4	1.2	3.0	1.4	0.9	0.4
22/01/2011	RV	4.9	1.5	1.2	3.1	1.4	0.8	0.4
08/02/2011	RV	1.1	2.0	0.4	6.9	1.3	0.9	0.4
22/02/2011	RV	4.9	1.4	1.2	3.0	1.3	0.9	0.5
05/03/2011	RV	4.9	1.5	1.2	3.1	1.4	0.8	0.5
02/04/2011	RV	7.8	3.2	1.5	6.8	8.6	5.6	
16/04/2011	RV	7.9	3.2	1.5	6.8	8.6	5.6	
07/05/2011	RV	7.8	3.2	1.5	6.9	8.6	5.7	
21/05/2011	RV	7.8	3.2	1.5	6.9	8.6	5.6	0.2
04/06/2011	RV	5.6	1.7	1.0	3.4	1.7	1.3	0.1
18/06/2011	RV	3.7	1.9	0.7	1.7	1.7	1.0	0.9
02/07/2011	RV	5.6	1.6	0.9	3.3	1.5	1.3	0.0
16/07/2011	RV	3.7	1.9	0.7	1.7	1.7	1.3	0.8
06/08/2011	RV	3.8	2.1	0.7	1.9	1.9	1.3	0.9
20/08/2011	RV	2.0	2.8	0.6	15.1	11.2	2.6	
03/09/2011	RV	3.8	2.1	0.7	2.1	2.2	1.3	0.9
17/09/2011	RV	0.4	0.0	0.0	0.1	0.2	0.6	

TANAH MERAH

Date	Sample ID	Ca	K	Mg	Na	NO3	Cl	SO4
12/06/2010	TM	4.8	5.0	1.1	3.1		4.6	1.2
26/06/2010	TM	3.7	2.8	0.8	2.5		2.8	1.9
10/07/2010	TM	5.1	47.9	1.0	2.8		45.3	1.2
24/07/2010	TM	5.3	2.6	1.1	2.9		3.0	1.4
08/08/2010	TM	6.7	3.7	1.1	4.6		4.8	1.4
21/08/2010	TM	5.4	1.5	1.2	2.9		1.7	1.1
03/09/2010	TM	2.1	0.6	0.6	2.1	0.2	4.1	0.9
17/09/2010	TM	2.1	0.6	0.6	2.0	0.3	3.9	0.9
16/10/2010	TM	6.0	4.5	2.0	4.4	7.4	2.3	
25/10/2010	TM	2.6	1.4	0.7	2.3			
25/10/2010	TM	2.6	1.3	0.7	2.2			
25/10/2010	TM	4.6	9.8	1.1	3.1			
25/10/2010	TM	2.7	2.6	1.3	4.2			
18/01/2011	TM	4.9	1.4	1.2	3.0	1.3	0.8	0.4
22/01/2011	TM	4.9	1.4	1.2	3.0	1.4	0.9	0.5
08/02/2011	TM	4.9	1.4	1.2	3.0			
22/02/2011	TM	5.0	1.4	1.2	3.0	1.2	0.8	0.5
05/03/2011	TM	4.9	1.4	1.2	3.0	1.3	0.9	0.5
19/03/2011	TM	4.8	1.3	1.2	3.0	1.3	0.8	0.4
02/04/2011	TM	7.7	3.1	1.5	6.7	8.5	5.6	0.2
16/04/2011	TM	7.9	3.2	1.5	6.9	8.6	5.6	0.2
07/05/2011	TM	7.8	3.2	1.5	6.9	8.8	5.6	
21/05/2011	TM	7.9	3.3	1.5	7.1	9.1	5.6	0.3
04/06/2011	TM	7.8	3.2	1.6	7.0	8.8	5.6	0.3
18/06/2011	TM	5.6	1.6	1.0	3.4	1.5	1.3	0.0
02/07/2011	TM	3.8	2.0	0.7	1.9	1.8	1.3	0.9
16/07/2011	TM	5.7	1.7	1.0	3.7	1.9	1.3	0.1
06/08/2011	TM	2.0	2.8	0.6	15.0	11.2	2.6	0.0
20/08/2011	TM	5.7	1.7	1.0	3.4	1.6	1.2	0.0
03/09/2011	TM	2.0	2.8	0.6	15.0	11.1	2.6	0.0
17/09/2011	TM	3.8	2.1	0.7	2.0	1.9	1.3	0.9

PASIR MAS

Date	Sample ID	Ca	K	Mg	Na	NO3	Cl	SO4
12/06/2010	PM	4.6	3.2	1.0	3.2		3.4	1.2
26/06/2010	PM	3.9	5.1	0.9	2.1		4.7	2.0
10/07/2010	PM	5.5	86.0	1.1	2.5		82.7	1.5
24/07/2010	PM	4.8	3.3	1.0	3.0		4.0	1.5
08/08/2010	PM	5.4	1.8	1.0	2.4		1.9	1.3
21/08/2010	PM	5.2	1.5	1.2	3.2		2.3	1.3
03/09/2010	PM	1.8	0.7	0.5	1.5	1.0	2.4	0.9
17/09/2010	PM	1.8	0.7	0.5	1.5	1.0	2.4	0.9
16/10/2010	PM	2.7	2.1	0.8	2.4	3.4	1.2	
25/10/2010	PM	4.0	2.4	1.0	3.0			
25/10/2010	PM	4.2	2.3	1.0	3.3		2.6	1.5
25/10/2010	PM	4.1	8.8	1.0	3.0			
25/10/2010	PM	4.6	3.3	1.1	3.2			
25/10/2010	PM	4.7	2.7	1.1	3.4		2.4	1.4
18/01/2011	PM	4.9	1.4	1.2	3.1	1.4	0.8	0.3
22/01/2011	PM	4.9	1.4	1.2	3.0	1.4	0.9	0.4
08/02/2011	PM	4.9	1.4	1.2	3.0	1.3	0.8	0.3
22/02/2011	PM	4.9	1.4	1.2	3.0	1.2	0.8	0.4
05/03/2011	PM	5.0	1.4	1.2	3.0	1.3	0.8	0.4
19/03/2011	PM	4.9	1.4	1.2	3.1	1.4	0.8	0.4
02/04/2011	PM	7.8	3.1	1.5	6.8	8.5	5.6	0.2
16/04/2011	PM	7.8	3.2	1.5	6.9	8.7	5.7	0.2
21/05/2011	PM	7.8	3.1	1.5	6.8	8.6	5.7	0.2
04/06/2011	PM		0.1	0.0	0.3	0.5	0.2	0.3
18/06/2011	PM	3.8	2.3	0.7	2.5	2.7	1.3	1.0
02/07/2011	PM	3.7	1.9	0.7	1.8	1.7	1.3	0.9
16/07/2011	PM	5.9	1.8	1.1	3.7	2.1	1.2	0.5
06/08/2011	PM	3.7	1.9	0.7	1.7	1.6	1.2	0.8
20/08/2011	PM	3.8	2.2	0.7	2.2	2.3	1.3	0.9
03/09/2011	PM	3.8	1.9	0.7	1.8	1.9	1.3	0.8
17/09/2011	PM	3.3	6.9	1.2	10.7	12.3	4.6	4.8

Appendix 19: pH and HCO_3 of Kelantan river water obtained from [*Lee, 2013*]

Kelantan											
Time Period	Sample ID	pH	[HCO3] (mol/L)	Time Period	Sample ID	pH	[HCO3] (mol/L)	Time Period	Sample ID	pH	[HCO3] (mol/L)
25/05/2010	GWKB	7.05	0.000998	02/10/2010	TM	7.05	0.000707	07/05/2011	TM	6.77	0.000533
25/05/2010	PM	7.05	0.000230	16/10/2010	GWKB	7.05	0.001066	07/05/2011	RV	6.77	0.000540
25/05/2010	PM	7.05	0.000230	16/10/2010	PM	7.05	0.000362	21/05/2011	GWKB	6.77	0.001013
25/05/2010	PM	7.05	0.000212	16/10/2010	TM	7.05	0.000667	21/05/2011	PM	6.77	0.000517
25/05/2010	PM	7.05	0.000233	08/01/2011	GWKB	6.77	0.000990	21/05/2011	TM	6.77	0.000497
25/05/2010	PM	7.05	0.000232	08/01/2011	PM	6.77	0.000287	21/05/2011	RV	6.77	0.000508
25/05/2010	PM	7.05	0.000217	08/01/2011	TM	6.77	0.000278	04/06/2011	GWKB	6.77	0.000849
25/05/2010	TM	7.05	0.000148	08/01/2011	RV	6.77	0.000294	04/06/2011	PM	6.77	0.000508
25/05/2010	TM	7.00	0.000169	22/01/2011	GWKB	6.77	0.001235	04/06/2011	TM	6.77	0.000513
25/05/2010	TM	6.60	0.000133	22/01/2011	PM	6.77	0.000286	04/06/2011	RV	6.77	0.000523
11/06/2010	GWKB	7.05	0.001213	22/01/2011	TM	6.77	0.000290	18/06/2011	GWKB	6.77	0.000834
12/06/2010	PM	7.05	0.000259	22/01/2011	RV	6.77	0.000286	18/06/2011	PM	6.77	0.000536
12/06/2010	TM	7.05	0.000311	08/02/2011	GWKB	6.77	0.001164	18/06/2011	TM	6.77	0.000483
26/06/2010	GWKB	7.05	0.001235	08/02/2011	PM	6.77	0.000285	18/06/2011	RV	6.77	0.000492
26/06/2010	PM	7.05	0.000196	08/02/2011	TM	6.77	0.000292	02/07/2011	GWKB	6.77	0.000843
26/06/2010	TM	7.05	0.000281	08/02/2011	RV	6.77	0.000286	02/07/2011	PM	6.77	0.000890
10/07/2010	PM	7.05	0.000122	22/02/2011	GWKB	6.77	0.001183	02/07/2011	TM	6.77	0.000782
10/07/2010	TM	7.05	0.000103	22/02/2011	PM	6.77	0.000300	02/07/2011	RV	6.77	0.001711
11/07/2010	GWKB	7.05	0.000346	22/02/2011	TM	6.77	0.000288	16/07/2011	GWKB	6.77	0.001542
23/07/2010	GWKB	7.05	0.000316	22/02/2011	RV	6.77	0.000297	16/07/2011	PM	6.77	0.000189
24/07/2010	PM	7.05	0.000092	05/03/2011	GWKB	6.77	0.001320	16/07/2011	TM	6.77	0.000187
24/07/2010	TM	7.05	0.000073	05/03/2011	PM	6.77	0.000280	16/07/2011	RV	6.77	0.001661
08/08/2010	PM	7.05	0.000104	05/03/2011	TM	6.77	0.000292	06/08/2011	GWKB	6.77	0.000077
08/08/2010	TM	7.05	0.000141	05/03/2011	RV	6.77	0.000474	06/08/2011	PM	6.77	0.000076
08/08/2010	RV	7.05	0.000112	19/03/2011	GWKB	6.77	0.001138	06/08/2011	TM	6.77	0.000191
11/08/2010	GWKB	7.05	0.000334	19/03/2011	PM	6.77	0.000289	06/08/2011	RV	6.77	0.000191
21/08/2010	GWKB	7.05	0.000327	19/03/2011	TM	6.77	0.000292	20/08/2011	GWKB	6.77	0.000071
21/08/2010	PM	7.05	0.000098	19/03/2011	RV	6.77	0.000299	20/08/2011	PM	6.77	0.000238
21/08/2010	TM	7.05	0.000102	02/04/2011	GWKB	6.77	0.000931	20/08/2011	TM	6.77	0.000071
21/08/2010	RV	7.05	0.000147	02/04/2011	PM	6.77	0.000503	20/08/2011	RV	6.77	0.000059
03/09/2010	GWKB	7.05	0.001329	02/04/2011	TM	6.77	0.000505	03/09/2011	GWKB	6.77	0.000182
03/09/2010	PM	7.05	0.000360	02/04/2011	RV	6.77	0.000549	03/09/2011	PM	6.77	0.000182
03/09/2010	TM	7.05	0.000372	16/04/2011	GWKB	6.77	0.000832	03/09/2011	TM	6.77	0.000183
17/09/2010	GWKB	7.05	0.001377	16/04/2011	PM	6.77	0.000542	03/09/2011	RV	6.77	0.000185
17/09/2010	PM	7.05	0.000336	16/04/2011	TM	6.77	0.000478	17/09/2011	GWKB	6.77	0.000184
17/09/2010	TM	7.05	0.000379	16/04/2011	RV	6.77	0.000547	17/09/2011	PM	6.77	0.001602
02/10/2010	GWKB	7.05	0.001180	07/05/2011	GWKB	6.77	0.000866	17/09/2011	TM	6.77	0.000190
02/10/2010	PM	7.05	0.000374	07/05/2011	PM	6.77	0.000489	17/09/2011	RV	6.77	0.000180

Appendix 20: PCA Scores for Langat River

PCA Scores

No	Stations	Comp.1	Comp.2	Comp.3
1	Pongsun	2.6	-0.1	-1.3
2	Pongsun	2.4	0.1	-1.2
3	Pongsun	2.2	0.0	-1.2
4	Pongsun	0.0	-0.7	2.5
5	Pongsun	0.0	-0.2	1.9
6	Pongsun	-0.3	-0.3	2.4
7	Pongsun	-0.2	-2.1	2.3
8	Pongsun	2.4	0.1	-1.2
9	Pongsun	0.0	-1.6	1.7
10	Pongsun	3.3	0.2	-1.2
11	Pongsun	-0.5	-2.2	2.2
12	Pongsun	-0.6	-1.7	1.4
13	Pongsun	2.6	0.1	-1.5
14	Pongsun	0.5	-0.5	-1.3
15	Pongsun	1.0	-0.4	-1.6
	n	15	15	15
	n-Positive	11	5	7
	n-Negative	4	10	8
	Score impact	0.73	0.33	0.47
		0.27	0.67	0.53
		1.00	1.00	1.00

No	Stations	Comp.1	Comp.2	Comp.3
16	Kajang	0.3	-0.4	0.4
17	Kajang	0.2	-0.7	0.4
18	Kajang	0.4	-0.2	0.3
19	Kajang	0.4	-0.2	0.1
20	Kajang	0.1	-0.5	1.1
21	Kajang	-1.7	-0.2	2.0
22	Kajang	-1.7	0.2	1.1
23	Kajang	-3.0	0.3	1.0
24	Kajang	-1.8	3.3	0.2
25	Kajang	-0.9	3.1	1.1
26	Kajang	-2.7	0.5	-2.0
27	Kajang	0.4	0.9	0.6
28	Kajang	0.8	0.9	0.3
29	Kajang	-2.3	0.2	-2.6
30	Kajang	-4.7	-0.5	-3.1
31	Kajang	-2.9	-0.9	-1.2
	n	16	16	16
	n-Positive	7	8	12
	n-Negative	9	8	4
	Score impact	0.44	0.50	0.75
		0.56	0.50	0.25
		1.00	1.00	1.00

PCA Scores

No	Stations	Comp.1	Comp.2	Comp.3
32	Dengkil	-0.1	-0.6	-0.4
33	Dengkil	0.5	-0.4	-0.5
34	Dengkil	0.9	-0.7	0.4
35	Dengkil	1.3	-0.6	-0.1
36	Dengkil	0.9	-0.8	0.0
37	Dengkil	1.2	-0.8	0.2
38	Dengkil	1.6	-0.8	0.6
39	Dengkil	-1.3	-0.3	-1.2
40	Dengkil	-1.4	1.4	-0.1
41	Dengkil	-2.8	3.5	-0.3
42	Dengkil	1.0	2.0	0.6
43	Dengkil	0.2	2.7	0.9
44	Dengkil	1.4	-0.5	-0.2
45	Dengkil	1.5	-0.5	0.0
46	Dengkil	-0.3	-0.8	-0.2
47	Dengkil	-3.4	-0.7	-2.1
48	Dengkil	-2.8	1.5	-1.2
49	Dengkil	-0.3	-0.9	0.1
50	Dengkil	-4.1	-2.1	0.5
51	Dengkil	-6.1	-2.5	0.6
	n	20	20	20
	n-Positive	10	5	9
	n-Negative	10	15	11
	Score impact	0.50	0.25	0.45
		0.50	0.75	0.55
		1.00	1.00	1.00

No	Stations	Comp.1	Comp.2	Comp.3
65	Semenyih	0.36	-0.07	-1.89
70	Semenyih	-0.25	-0.42	-0.90
66	Semenyih	0.84	-0.26	-0.90
69	Semenyih	-1.00	-0.70	-0.81
56	Semenyih	2.01	-0.23	-0.60
63	Semenyih	1.57	0.02	-0.54
67	Semenyih	1.94	-0.15	-0.39
64	Semenyih	1.57	-0.39	-0.35
58	Semenyih	1.91	-0.42	-0.32
57	Semenyih	1.51	-0.48	-0.29
55	Semenyih	1.69	-0.48	-0.24
54	Semenyih	1.33	-0.59	-0.09
53	Semenyih	1.33	1.21	0.08
52	Semenyih	0.95	1.42	0.61
62	Semenyih	0.40	0.28	0.66
68	Semenyih	0.65	1.51	0.92
61	Semenyih	0.75	0.22	0.96
60	Semenyih	-0.69	0.75	1.10
59	Semenyih	-1.12	4.27	1.61
	n	19	19	19
	n-Positive	15	8	7
	n-Negative	4	11	12
	Score impact	0.79	0.42	0.37
		0.21	0.58	0.63
		1.00	1.00	1.00

Appendix 21: PCA Scores for Kelantan River

No	Station	Comp.1	Comp.2	Comp.3	No	Station	Comp.1	Comp.2	Comp.3	No	Station	Comp.1	Comp.2	Comp.3
						PCA Scores								
1	Pasir Mas	0.75	-0.81	-0.24	19	Tanah Merah	0.78	-0.79	-0.15	50	River View	-1.77	2.90	-2.47
2	Pasir Mas	0.79	-0.71	-0.18	20	Tanah Merah	0.73	-0.73	-0.11	41	River View	1.59	1.97	-0.74
3	Pasir Mas	0.83	-0.80	-0.25	21	Tanah Merah	0.78	-0.74	-0.13	52	River View	2.26	1.15	-0.16
4	Pasir Mas	0.83	-0.75	-0.14	22	Tanah Merah	1.19	-1.14	-0.52	40	River View	0.72	-0.71	-0.14
5	Pasir Mas	0.78	-0.76	-0.22	23	Tanah Merah	0.80	-0.67	-0.09	39	River View	0.76	-0.72	-0.13
6	Pasir Mas	0.79	-0.68	-0.16	24	Tanah Merah	0.84	-0.89	0.18	42	River View	0.79	-0.72	-0.11
7	Pasir Mas	-3.34	-1.03	-0.02	25	Tanah Merah	-3.32	-1.03	-0.06	45	River View	0.56	-0.89	-0.09
8	Pasir Mas	-3.44	-1.04	0.05	26	Tanah Merah	-3.43	-1.07	0.04	51	River View	2.29	1.20	-0.05
9	Pasir Mas	-3.40	-1.06	0.01	27	Tanah Merah	-3.43	-1.17	-0.28	44	River View	-3.41	-1.05	-0.01
10	Pasir Mas	0.78	0.90	0.30	28	Tanah Merah	-3.54	-0.78	-0.51	49	River View	1.10	0.69	0.22
11	Pasir Mas	1.21	0.68	0.09	29	Tanah Merah	-3.47	-1.00	-0.04	43	River View	0.71	-0.79	0.23
12	Pasir Mas	0.27	-0.52	-0.44	30	Tanah Merah	0.61	-0.91	-0.54	46	River View	1.28	0.49	0.81
13	Pasir Mas	1.25	0.58	0.26	31	Tanah Merah	1.15	0.73	0.28	47	River View	0.53	-1.82	1.92
14	Pasir Mas	1.00	0.81	0.04	32	Tanah Merah	0.49	-0.64	-0.86	48	River View	1.05	-0.46	2.78
15	Pasir Mas	2.19	1.22	-0.08	33	Tanah Merah	-1.74	2.90	-2.44					
16	Pasir Mas	1.02	-0.40	2.64	34	Tanah Merah	0.63	-0.65	-0.88					
17	Pasir Mas	-4.75	5.31	4.16	35	Tanah Merah	1.69	0.99	-0.16					
18	Pasir Mas	2.20	1.09	0.22	36	Tanah Merah	1.73	0.94	-0.12					
					37	Tanah Merah	-1.76	2.79	-2.23					
					38	Tanah Merah	1.08	0.55	0.53					
	n	18	18	18		*n*	20	20	20		*n*	14	14	14
	n-Positive	14.00	7.00	9.00		*n-Positive*	13.00	6.00	4.00		*n-Positive*	12.00	6.00	5.00
	n-Negative	4.00	11.00	9.00		*n-Negative*	7.00	14.00	16.00		*n-Negative*	2.00	8.00	9.00
	Score impact	0.78	0.39	0.50		*Score impact*	0.65	0.30	0.20		*Score impact*	0.86	0.43	0.36
		0.22	0.61	0.50			0.35	0.70	0.80			0.14	0.57	0.64
		1.00	1.00	1.00			1.00	1.00	1.00			1.00	1.00	1.00